Assessment of Geothermal Energy Extracted from Upper Carbonate Aquifer beneath the City of Winnipeg

by

Sylvia Hindri Susanto

A Thesis submitted to the Faculty of Graduate Studies of

The University of Manitoba

in partial fulfilment of the requirements for the degree of

MASTER OF SCIENCE

Department of Civil Engineering

University of Manitoba

Winnipeg

Abstract

The Upper Carbonate aquifer beneath the City of Winnipeg has been utilized as a heat source and sinks since the 1940s. The majority of open loop geothermal systems in Winnipeg extract groundwater from the Upper Carbonate aquifer, run the groundwater through a heat exchanger and return the thermal wastewater back into the aquifer. Injection of thermal wastewater creates thermal plume surrounding the injection well and thermal feedback which causing groundwater temperature increase in the production well. The first objective of this study was to provide information and resources on the current usage and impacts of the geothermal systems for engineers, scientists and the public in general. The analysis was carried out by developing maps, such as location and utilization of geothermal systems, the rate of groundwater being diverted, the quantity of groundwater diverted annually, the locations of production and recharge wells, the depths of casing and open hole for production wells, and the estimated heat balance. Assessment indicated up to 80% of the estimated heat was injected into the aquifer by extracting groundwater up to 100% of the permissible quantity. Analytical approaches were applied to estimate the thermal breakthrough time, the abstraction temperature, and thermal plume caused by heat injection. The results were in good agreement with recorded data and numerical analysis. Therefore, these approaches should be included in initial stage development of geothermal system to assess the sustainability of the system and the potential thermal interference in an urban area.

The second objective was to study the impact of an open loop geothermal system with multiple wells on groundwater temperature by developing a 3D numerical model of the Upper Carbonate aquifer in the southwestern part of Winnipeg. The model was developed using hydrogeological

maps, provincial observation wells, geothermal system wells, and earlier research on the carbonate bedrock aquifer. Three steps of calibration were performed: constant hydraulic head, pumping test, and heat transport. Result indicated that extracting groundwater using all supply wells produced low entering water temperature. Long term simulation showed that higher groundwater flow increased thermal plume size, while high temperature created higher temperature zone within the thermal plume.

Acknowledgments

I would like to express my deepest gratitude to my advisor Dr. Hartmut Holländer for giving me the opportunity to conduct research under his supervision. I am grateful for his guidance, understanding and encouragement throughout my study. I highly appreciate the knowledge and skills that I have learnt from his guidance.

I would like to thank my advisory committee members: Dr. Scott Ormiston and Dr. James Blatz for their support and valuable comments.

I would like to thank Manitoba Sustainable Development personnel: Kylene Wiseman, Rob Matthews, and Christopher McCombe for providing me access to groundwater use license data base; Dr. Graham Phipps and Ronald Hempel for providing groundwater level and temperature data; also Trevor Cielen for helping me converting the paper data into pdf files.

I would like to thank IKEA Properties Limited personnel: Jason Lehman and Mark Mostowy for providing groundwater use and temperature data.

I also would like to express my gratitude to Rob Sinclair of KGS Group for providing information on IKEA geothermal system and his help in connecting me to IKEA's personnel.

Finally, I thank my family Dan, Gaby and Emma Susanto for their love, understanding and support throughout my study.

Dedication

I dedicate this thesis to my best friend, my husband and my home: Dan Susanto, who has been vital in helping me to be a better person I am today. He has always been a permanent source of enthusiasm and support during my research. His silly jokes about groundwater, encouragements, loves, and critiques have immensely impact on my work ethic and perseverance that I need in completing this thesis.

Life has more imagination than We carry in our dream (Christopher Columbus)

Contributions of Authors

Susanto, S. and Holländer, H. M. (in preparation). Geothermal Energy Extracted from Upper Carbonate Aquifer beneath a Major City in the Canadian Prairie.

Hydrogeology Journal.

a. Susanto, S.: Suggested, developed and implemented the methodology, paper writing and correction.
b. Holländer, H. M.: Suggested and supervised the research and assisted with the editing of the paper.

Susanto, S. and Holländer, H. M. (in preparation). Modelling the effect of Open Loop Geothermal System with Multiple Wells on Upper Carbonate Aquifer.

Hydrogeology Journal.

a. Susanto, S.: Suggested, developed and implemented the methodology, model simulation, paper writing and correction.
b. Sinclair, R.: Contributed to the data and the editing of the paper
c. Holländer, H. M.: Suggested and supervised the research and assisted with the editing of the paper.

Table of Contents

List of Tables

List of Figures

List of Parameters

b	L	effective aquifer thickness
c_i	$L^2 T^{-2}K^{-1}$	groundwater heat capacity
c_p	$L^2 T^{-2}K^{-1}$	specific heat capacity
c_s	$L^2 T^{-2}K^{-1}$	heat capacity of solid phase
c_w	$L^2 T^{-2}K^{-1}$	heat capacity of fluid
D	L	spacing of production well and recharge well
H	$M^{-2} L^2T^{-3}$	heat source/sink
h	L	hydraulic head
i	-	hydraulic gradient
K	MT^{-1}	hydraulic conductivity
m_i	M	groundwater mass
n	-	total porosity
n_e	-	effective porosity
Q	L^3T^{-1}	groundwater flow rate
Q_c	ML^2T^{-2}	heat transfer for cooling
Q_h	ML^2T^{-2}	heat transfer for heating
Q_{inj}	L^3T^{-1}	Injected groundwater flow rate
Q_t	ML^2T^{-2}	heat transfer
q_{cond}	ML^2T^{-2}	heat transfer rate required for cooling
q_{evap}	ML^2T^{-2}	heat transfer rate required for heating
R	-	Retardation factor
S_S	L^{-1}	specific storage
T	K	temperature
T_0	K	undisturbed groundwater temperature
T_{abs}	K	abstracted groundwater temperature
T_{inj}	K	injected groundwater temperature
T_R	L^2T^{-1}	transmissivity
ΔT	K	temperature difference
ΔT_{inj}	K	temperature difference between T_{inj} and T_0
t	T	time
V	L^3	Groundwater volume
v_D	LT^{-1}	Darcy velocity
v_e	LT^{-1}	Effective velocity
x	L	x-coordinate
y	L	y-coordinate
α_L	L	longitudinal dispersivity

α_T	L	transverse dispersivity
λ	$MLT^{-3}K^{-1}$	thermal conductivity of porous medium
λ_s	$MLT^{-3}K^{-1}$	thermal conductivity of solid matrix
λ_w	$MLT^{-3}K^{-1}$	thermal conductivity of fluid
ρ	ML^{-3}	density
ρ_s	ML^{-3}	density of solid phase
ρ_w	ML^{-3}	density of fluid phase
ρc	$ML^{-1}T^{-2}K^{-1}$	volumetric heat capacity of aquifer
$\rho_s c_s$	$ML^{-1}T^{-2}K^{-1}$	volumetric heat capacity of solid phase
$\rho_w c_w$	$ML^{-1}T^{-2}K^{-1}$	volumetric heat capacity of fluid phase

List of Abbreviations

ASHP	air source heat pump
d	day
dam	decameter
$EFLC_c$	equivalent full load hour for cooling
$EFLC_h$	equivalent full load hour for heating
EWT	entering water temperature
GCHP	ground-coupled heat pump
GS	geothermal system
GSHP	ground source heat pump
GWHP	groundwater heat pump
J	joule
kJ	kilojoule
LWT	leaving water temperature
m	meter
RMSE	root mean squared error
R^2	coefficient of determination
s	seconds
SD	Manitoba Sustainable Development
SWHP	surface water heat pump
W	watt
3D	three dimensional

1 Introduction

Among the renewable energy systems, the ground-source heat pump (GSHP) system is increasingly popular to generate heating and cooling in residential and commercial buildings (Lund and Boyd 2016). Included in ground-source heat pumps are surface-water heat pumps (SWHP), ground-coupled heat pumps (GCHP), and groundwater heat pumps (GWHP) (Kavanaugh and Rafferty 2014). These systems use surface water, soil, or groundwater as a heat source or sink. GWHP, built as open loop geothermal systems usually consist of one production well and one recharge well. The systems extract groundwater, pass it through a heat exchanger and return the thermal wastewater back into the aquifer. Due to groundwater temperature that remain constant, open loop geothermal systems offer greater energy efficiency and energy savings compare to air source heat pump (ASHP) systems (Milenić et al. 2010). Compared to closed loop geothermal systems, open loop systems have better thermodynamic performance because the systems use groundwater directly instead of a heat exchange fluid, lower initial cost due to simple design and lower drilling requirement, and low operating cost (Mustafa Omer 2008; Self et al. 2013). For larger energy demands, open loop systems require smaller area of installation compared to closed loop systems (Park et al. 2018). By using direct use of groundwater, the efficiency of a geothermal system depends on the hydrogeological and thermal properties of the aquifer (Nam and Ooka 2010; Casasso and Sethi 2015; Park et al. 2015).

All groundwater in Manitoba belongs to the Provincial Crown and is monitored by Manitoba Sustainable Development (SD) who administers groundwater permits (Matthews 2003). Open loop geothermal systems have been used within the City of Winnipeg since the 1940s (Render 1970) with little planning during the initial stage of development. The systems extract groundwater from the Upper Carbonate aquifer, run the water through a heat exchanger

and direct the thermal wastewater back to the aquifer, the City of Winnipeg sewer system, Assiniboine River or Red River. The purposes of injecting the thermal wastewater back into aquifer are to prevent hydraulic head loss and reduce stress on the City of Winnipeg sewer system (Render 1981; Render 1983; Betcher 1995). Thermal wastewater injection into the aquifer beneath the City of Winnipeg caused increase in groundwater temperature which has been reportedly occurring in several geothermal system locations. At these locations, the groundwater temperature is several degrees Celsius greater than in the surrounding rural areas of the City of Winnipeg.

In August 2002 and August 2007, Ferguson and Woodbury conducted groundwater temperature measurements in 40 monitoring wells within the City of Winnipeg and the surrounding area. The result indicated that groundwater temperature change ranging from -0.1°C to 0.25°C during the five years. The maximum temperature change occurred near the city centre, within a few hundred meters of sites where wastewater from a geothermal system was injected into the aquifer. This change could be attributed to changes in pumping at production wells and injection of wastewater into the aquifer (Ferguson and Woodbury 2004, 2005, 2007). The increase of groundwater temperature makes the current practice of open loop geothermal system unsustainable; therefore some plans to prevent the increase in temperature should be included in early development (Ferguson 2004).

The objectives of this study were to provide useful information and resources on the current usage and impacts of the geothermal systems for engineers, scientists and public in general, by developing maps on geothermal energy extracted from the Upper Carbonate aquifer; and to study the impact of a geothermal system with multiple wells on groundwater temperature by developing 3D numerical model of Upper Carbonate aquifer. The study was performed in two

separate studies which are presented in this thesis as two papers that are in preparation. The first paper titled “Geothermal Energy Extracted from Upper Carbonate Aquifer beneath a Major City in the Canadian Prairie” discusses the development and analysis of geothermal energy maps. The second paper titled “Modelling the effect of Open Loop Geothermal System with Multiple Wells on Upper Carbonate Aquifer” discusses the development and analysis of a three dimensional (3D) model of the Upper Carbonate aquifer beneath the City of Winnipeg.

.

2 Geothermal Energy Extracted from Upper Carbonate Aquifer beneath a Major City in the Canadian Prairie

Abstract

Since the 1940s, open loop geothermal systems have been utilized within the City of Winnipeg to generate heating and cooling by extracting groundwater from the Upper Carbonate aquifer. The majority of the systems inject thermal wastewater back into the aquifer causing the increase in groundwater temperature at several locations. Injection of thermal wastewater creates a thermal plume surrounding the injection well. Depending on the extraction rate and spacing between production and recharge wells, injection thermal wastewater also creates thermal feedback causing groundwater temperature increase in the production well. This study develops maps for geothermal energy extracted from the Upper Carbonate aquifer such as location and utilization of geothermal energy systems, the rate of groundwater being diverted, the quantity of groundwater diverted annually, the locations of production and recharge wells, the depths of casing and open hole for production wells, and the estimated heat balance. The maps and their data are used to analyze the impact of open loop geothermal systems on groundwater temperature. The allowable groundwater that can be extracted is 32,650 dam^3/yr with an estimated heat discharge of $470x10^9$ kJ/yr and a heat demand of $116x10^9$ kJ/yr. The available data of both cooling and combined systems indicate heat discharge up to 80% of the estimated value with groundwater extraction up to 100% of the permissible quantity. Thus, there is a surplus of heat being discharged into the aquifer. This has local impacts on the groundwater temperatures, such as temperature increased to more than 12°C in western Winnipeg. Other areas of the City are also impacted and the groundwater temperature will rapidly increase without any mitigation such as using winter chilling systems. Performing thermogeological risk assessment

should be included in the initial stage of development for a geothermal system to assess the sustainability of the system and the potential thermal interference in an urban area. Analytical approaches to estimate thermal breakthrough time, future abstraction temperature and thermal plume are applied on some of the geothermal systems. The results are in good agreement with recorded data and numerical analysis. The applied analytical approaches prove to be useful candidates for risk assessment.

2.1 Introduction

With the increase in energy cost, a Groundwater Heat Pump (GWHP) provides an alternative in reducing the cost on heating and cooling. The pump exchanges heat from groundwater to the building during winter. In summer, the pump transfers heat from the building to groundwater. Groundwater temperature is relatively constant throughout the year making the aquifer ideal as a heat source or sink. During the heat transfer process, groundwater is run through a heat exchanger and then returned back into the aquifer without any additional pollutant except the temperature difference. The groundwater temperature differences may cause an abnormal effect on groundwater temperature for example groundwater temperature increased beyond 25°C at different aquifers beneath some European cities due to the intensive use of groundwater for cooling purposes (Guimerá et al. 2007).

Utilization of open loop geothermal systems have been reportedly increasing (Lund and Boyd 2016), especially in urban areas. The majority of open loop systems (62%) in central London, UK, have been utilized for combined heating and cooling, while 36% for cooling only (Fry 2009; Abesser 2010). This indicates that the Chalk aquifer beneath central London receives more warm water through injection. The study on a shallow unconsolidated urban groundwater

body in the City of Basel, Switzerland, indicated that open loop geothermal systems for cooling purpose were the major thermal input to the aquifer. In summer time, groundwater downstream of geothermal systems would reach its annual maximum temperature (Epting et al. 2013). In undisturbed regions, groundwater temperature is expected to correspond to the mean annual air temperature. In the City of Basel area, groundwater temperature is between 16 to 18°C, while mean annual air temperature is 10°C (Epting et al. 2017; Epting et al. 2018). Currently, 73 open loop geothermal systems extract groundwater from urban alluvial aquifer beneath the City of Zaragoza, Spain. In total, the systems use 188 wells, consisting 112 production wells and 76 recharge wells (Muela Maya et al. 2018). Groundwater temperature measurement within the City of Zaragoza indicates 41°C while the mean annual air temperature is 15.5°C (Epting et al. 2017).

The Upper Carbonate Aquifer beneath the City of Winnipeg has been used as heat source and sink since the 1940s. Undisturbed groundwater temperature beneath the City of Winnipeg is around 6°C. A groundwater temperature increase has been reported occurring in several geothermal locations. Ferguson and Woodbury (2006) indicated groundwater temperatures of 12°C and 16°C at the production wells of two buildings that extract large quantities of groundwater for cooling purposes. In the western part of Winnipeg, the temperature measurement at the production well of a cooling system belonging to an aerospace manufacturing company, indicated 1.4°C increase after the system was operated for 3 to 4 years (Sinclair 2003). About one kilometer from this geothermal system, a packaging company reported groundwater temperature at 6.7°C when the geothermal cooling system started its operation in 1977. The temperature increased to 8.9°C after 8 years of operation. This system had to be modified into a heating and cooling system to prevent a further increase of temperature, which resulted in a temperature dropped to 8.3°C (Lucas 1994). However, an

increase between 8.8 to 9.2°C was observed in 1995. Several kilometers from these geothermal systems, the groundwater temperature measured at production wells of a hotel cooling system, indicated a gradual increase from 8.2°C in 1984 to 14.2°C in 1999 (Wolowich 1999). In the southwestern part of Winnipeg, an egg products company cooling system observed a temperature increase of 2 to 3°C between 1998 and 2000 (Wiecek 2001a). At a plastic fabrication company in eastern Winnipeg, groundwater temperature measured at observation wells indicated 7.2°C in 1998, 12.7°C in 2003 and 14°C in 2009 (Oleksiuk 2009).

The increase of groundwater temperature affects physical, biological and chemical properties of groundwater (Hähnlein et al. 2013); such as local thermal anomalies in the subsurface and groundwater (Palmer et al. 1992; Ferguson and Woodbury 2006; Banks 2009), groundwater dependent organisms and ecosystems (Hancock et al. 2009), mixing processes in groundwater (Bonte et al. 2011), organic compound mobilization from sediment (Brons et al. 1991), oxygen saturation and gas solubility (Danielopol et al. 2003), and dissolution of silicate minerals (Arning et al. 2006). To prevent substantial disturbance of natural conditions, good management of groundwater use for energy source or sink is needed. Preventing groundwater temperature increase should be included in the early design stage of an open loop geothermal system (Ferguson 2004) for the sustainable use of groundwater as a source of energy, and maintaining the efficiency of geothermal system itself.

Most urban areas have no static regulation to manage the thermal resources of aquifer (Banks 2009; Fry 2009) due to local differences in geology, hydrogeology and technical requirements (Hähnlein et al. 2013). Haehnlein et al. (2010) compiled the international status of the use of shallow geothermal energy. The study showed that countries such as Netherlands, Denmark and Germany embedded the regulation for groundwater temperature management in

national laws; in Canada the regulation was managed provincially; Switzerland and France set temperature difference between extraction and injection at 3°C and 11°C respectively; while most countries had no regulation (Haehnlein et al. 2010). In London, UK, protection of groundwater beneath central London was the responsibility of the Environmental Agency but the agency had no responsibility to manage the thermal resources of aquifer (Fry 2009). In Winnipeg, groundwater use is being managed by Manitoba Sustainable Development. The groundwater use license specifies the maximum flow rate and quantity of groundwater that can be diverted from the Upper Carbonate Aquifer. The license also limits injection water temperature between 1.5 to 12°C (Matthews 2003).

The main purpose of this study is to provide information and resources on the current usage and impacts of the geothermal systems for engineers, scientists and public in general which can be useful during initial stage development of open loop geothermal system. The analysis was carried out by developing maps and applying analytical approach on geothermal energy systems. The analysis was carried out for the City of Winnipeg, MB, Canada.

2.2 Methods

2.2.1 **Area of Study**

The carbonate bedrock of the Red River Formation in the Winnipeg area (Figure 2.1) contains three aquifers: Upper Carbonate Aquifer, Middle Carbonate Aquifer and Lower Carbonate Aquifer. The carbonate bedrock is characterized by Paleozoic carbonate formations with a thickness ranging from 76 to 230 m and is overlain by Pleistocene drift with a maximum thickness of 60 m (Baracos et al. 1983). The major aquifer beneath the City of Winnipeg is the Upper Carbonate aquifer that occurs in the top 15 to 30 m of the dolomitic limestone and

dolomite of the Red River Formation. The aquifer is semi-confined by the surficial deposits on top and the slightly pervious carbonate rock below. Its permeability is characterized by a network of fracture openings, joints and bedding planes. The transmissivity ranges from 25 to 2500 m^2/d, and the storativity varies from $1x10^{-6}$ to $1x10^{-3}$. The Middle Carbonate aquifer has been found in western Winnipeg at 90 m depth from bedrock surface. At this location, the carbonate bedrock is impermeable between depths of 60 to 90 m. The transmissivity is ranging from 250 to 1250 m^2/d and storativity is in the range of $1x10^{-5}$ to $1x10^{-4}$. The Lower Carbonate aquifer is located at the bottom 15 m of the carbonate bedrock with the estimated transmissivity less than 62 m^2/d (Baracos et al. 1983).

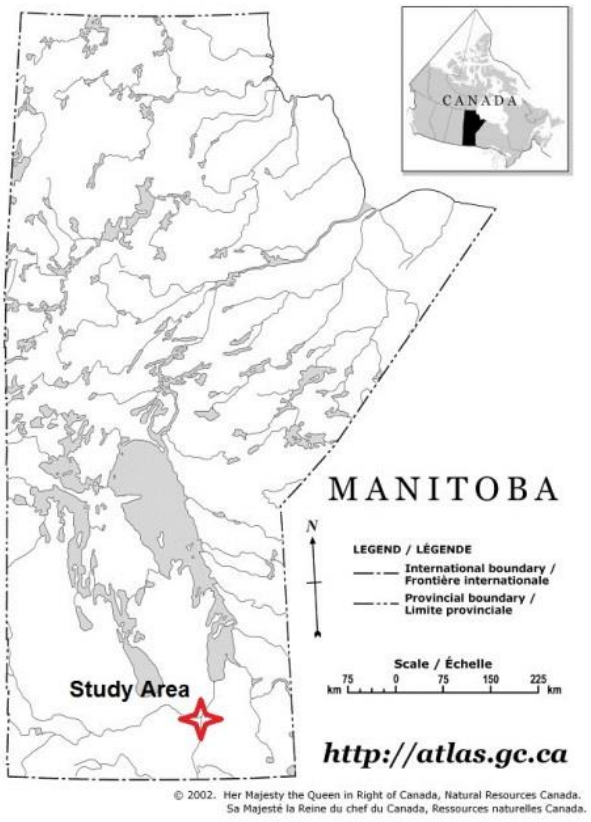

Figure 2.1 Location of the City of Winnipeg in Manitoba, Canada

Beneath the City of Winnipeg, groundwater flows from Northwest, Southwest and East towards the city centre. The potentiometric surface is different in winter and summer caused by the pumping (Figure 2.2). In winter, the lowest potentiometric surface occurs in the city centre, east and northeast area. In summer, the lowest potentiometric surface occurs in the east area.

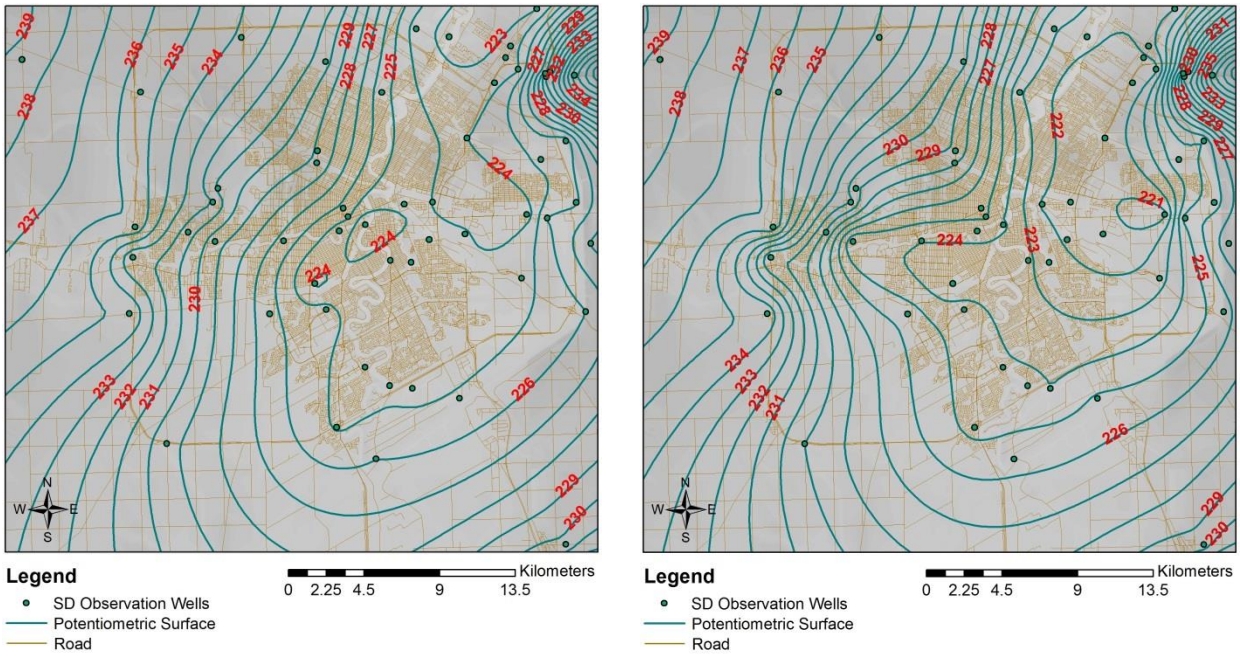

Figure 2.2 Potentiometric surface on January 15, 2012 (Left) and July 15, 2012 (Right).

The Upper Carbonate aquifer beneath the City of Winnipeg was the source of water for municipal and industrial water since the early development of the City of Winnipeg until 1919. The excessive groundwater withdrawals during that period caused the water level to decline about 12 m below ground. Since then, the groundwater was abandoned because of excessive natural hardness and sulphate and used mainly for commercial and industrial cooling due to its constant low temperature of 3.9 to 6.1°C (Render 1970). The practice during that time was to direct the wastewater to the City of Winnipeg sewer system which causing an excessive amount of strain. Application of the groundwater sewage tax by the City of Winnipeg in 1940 encouraged the recharge of groundwater back into the aquifer. More supply-recharge wells were

developed since 1960 for air cooling systems of apartments and hotels. These systems usually extract a large volume of groundwater and increase groundwater temperature to a few degrees prior discharging it back into the aquifer (Render 1970).

Groundwater temperature measurements were conducted at 50 locations within the City of Winnipeg area between May 2000 and August 2002. Measurements at 20 m depth from the ground surface indicated a temperature range between 5.4°C and 14.3°C. The lowest temperature was located in the rural area surrounding Winnipeg area and the highest was near the centre of Winnipeg (Ferguson and Woodbury 2004). Between August 2002 and August 2007, groundwater temperature at 40 locations recorded an increase ranging from 0.05°C to 0.25°C. The largest increase was observed in an industrial area nearby the location where warm wastewater from the cooling process was injected into the aquifer (Ferguson and Woodbury 2005, 2007). Although the aquifer has the ability to absorb heat from the injected wastewater, this heat may cause an increase in groundwater temperature at production wells which will affect the efficiency of the geothermal system (Ferguson 2004). Some implementation has been applied to prevent or delay groundwater temperature increase such as the application of combined cooling and heating system, regulation of the temperature of return water to aquifer must not exceed 12°C, and installation of winter chilling system.

2.2.2 **Data**

Data of open loop geothermal systems were collected from Manitoba Sustainable Development, consisting licenses for groundwater use, consultant reports and records of groundwater use. These documents contained Universal Transverse Mercator coordinates (Zone 14N) of the geothermal system, purpose of groundwater usage, maximum rate at which groundwater can be diverted, maximum allowable groundwater diverted annually, allowable

return water temperature, approximate location of supply wells and return wells, drilling record, pumping test record, monthly water usage and monthly temperature measurement at production wells. The licenses also showed the approximate locations of production and recharge wells. More accurate locations of these wells were obtained by comparing the locations with drilling records and consultant records and were verified using satellite images from Google Maps, and site visits.

There were 87 geothermal systems being utilized within the City of Winnipeg and surrounding area. Manitoba Sustainable Development requires geothermal users to record monthly water usage, entering groundwater temperature and leaving water temperature. Unfortunately, despite these requirements, only 48 users recorded the monthly water usage. Among these 48 users, only 25 users recorded the monthly groundwater temperature measurement. In most geothermal system locations presented in this study, the geothermal system are identified as GS as prefix followed by two digits number (Figure 2.3) to protect the privacy of the owner.

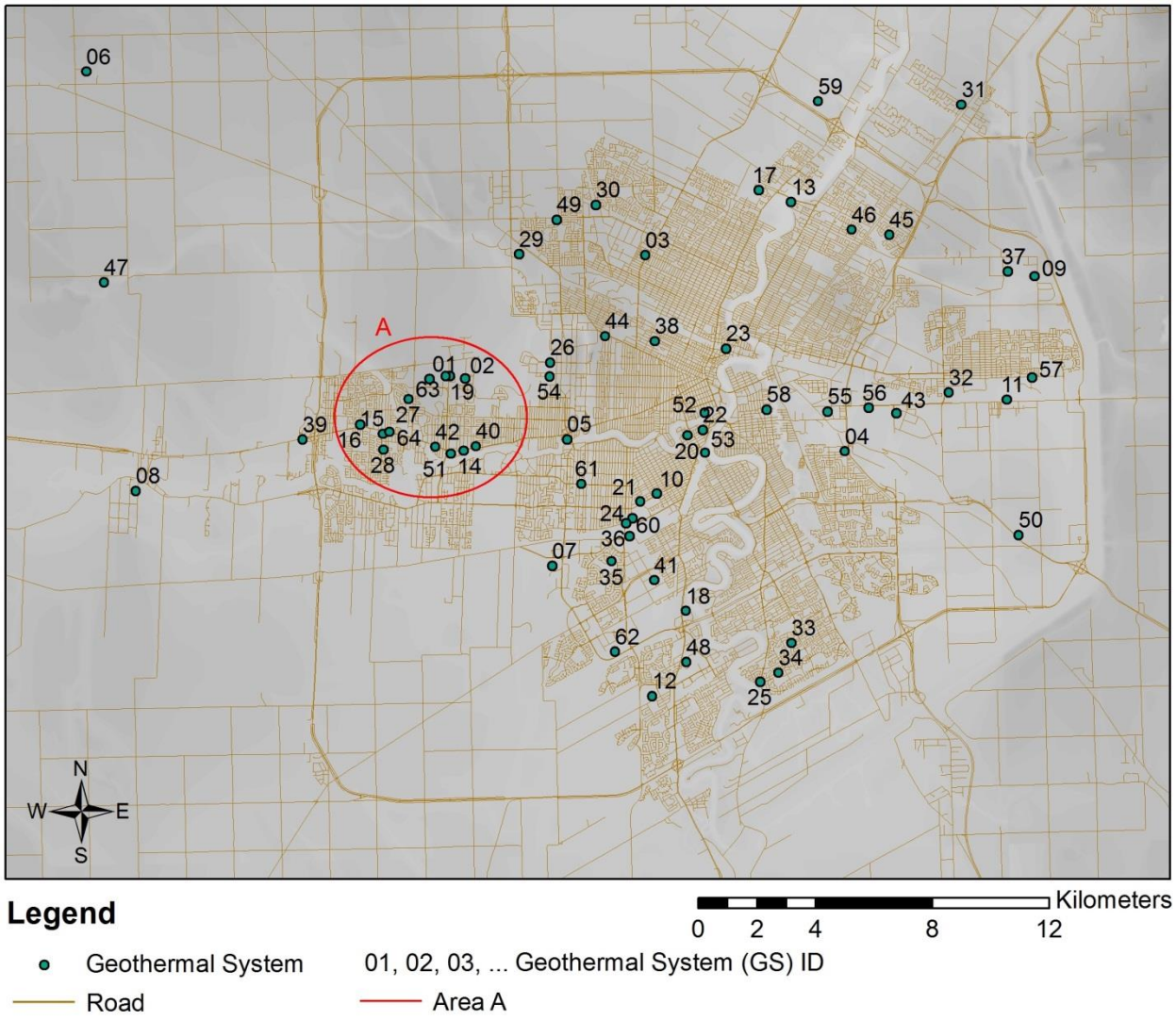

Figure 2.3 Geothermal Systems Identification

2.2.2.1 Geothermal Energy Resources Maps

Geothermal energy resources maps consisting of six maps were developed using ArcGIS 10.4.1 (Inc. 1999-2016). The maps show the location of geothermal systems and how the systems are being utilized, maximum rate of groundwater that can be diverted by each geothermal system, maximum quantity of groundwater that can be diverted by each geothermal system, locations of production wells and recharge wells, depth of open hole for production wells, and depth of casing for production wells.

Location and Utilization of Geothermal Systems

There were 48 systems for cooling purposes and 39 systems for heating and cooling purposes within the City of Winnipeg and surrounding area in 2015 (Figure 2.4). Most of the systems were located in western and southwestern parts of Winnipeg, in the proximity of the Assiniboine River and Red River. In the southwestern part of Winnipeg, the majority of the systems were for heating and cooling purpose. Southwestern Winnipeg is a newer development area for residential and commercial therefore suitable for the application of an open loop geothermal system for both heating and cooling to prevent groundwater temperature increase in this area.

On the western part of Winnipeg, the majority of geothermal systems were for cooling systems which were developed in the 1970's. Area A (Figure 2.3) shows the concentration of geothermal systems for industrial, commercial and residential buildings. This concentration of geothermal systems and cooling purpose of the majority of the systems elevated the groundwater temperature in the area. In this area, groundwater temperature measured in 2007 was above 8°C (Ferguson 2007). In 2014, GS01 recorded groundwater temperature at a production well between 10.5 to 11.8°C. To prevent a further temperature increase, GS02 modified their geothermal system to include a well water cool down system (Lear 1987). Using this system, G02 pumped a larger volume of groundwater than necessary for about 6 months of the year. The system used air units to cool the groundwater after being heated in the cooling process, prior returning the groundwater back into the aquifer. Using this additional system, GS02 not only used the groundwater for industrial cooling purpose but also for fresh air heating and cooling. This additional system was able to decrease the groundwater temperature from 8.9°C to 8.3°C (Lucas 1994). A newer report (Bielus 2005) indicated that GS02 extracted the groundwater only for industrial cooling purpose.

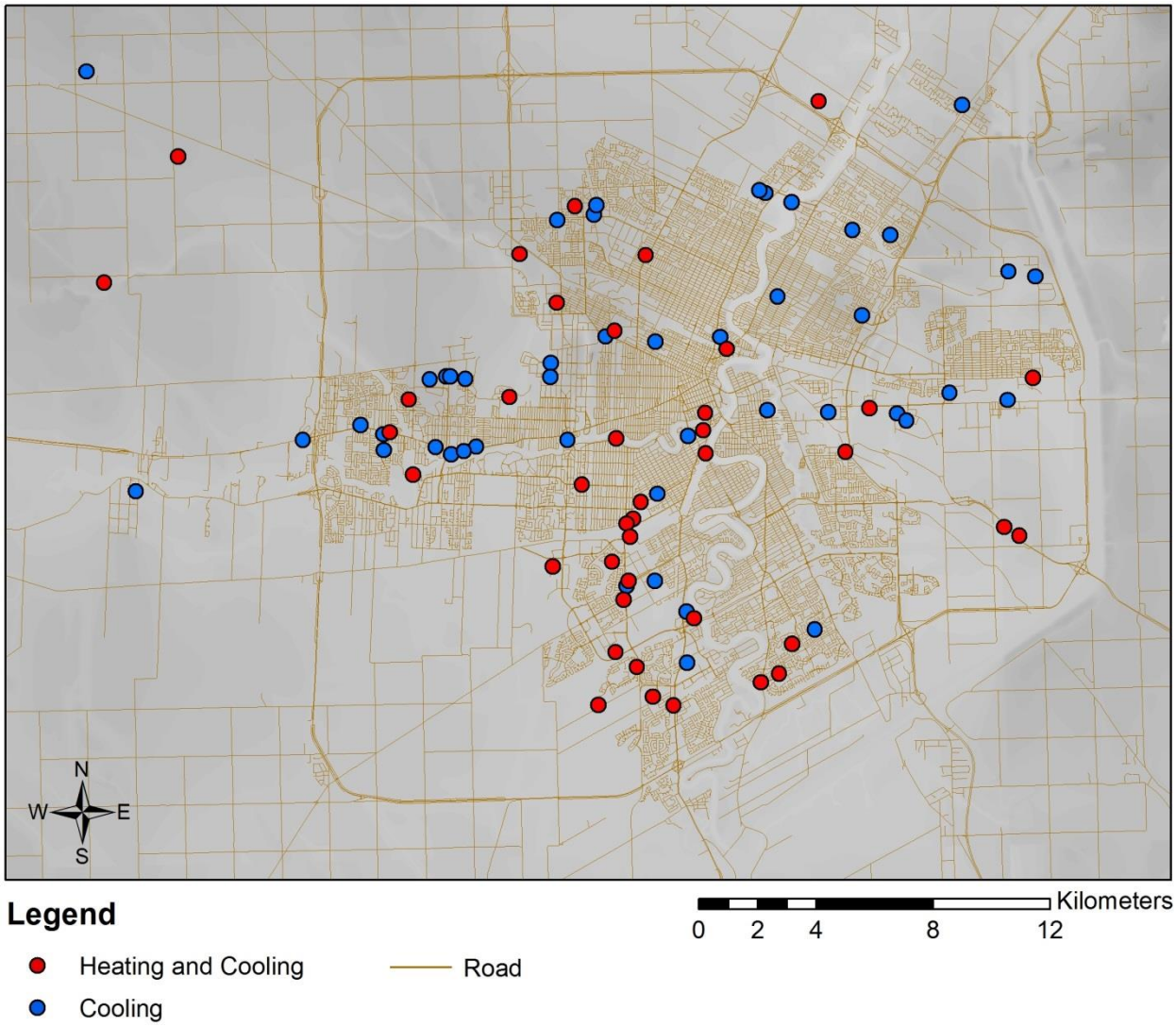

Figure 2.4 Location and utilization of open loop geothermal systems in the City of Winnipeg and its vicinity.

Quantity of Groundwater

Manitoba Sustainable Development permitted 32,650 dam^3 per year of groundwater extraction from the Upper Carbonate Aquifer for heating and cooling purposes (Figure 2.5). GS06 (Figure 2.3) held the highest volume at 5,923 dam^3, while GS08 located in Headingly, was allowed the lowest volume of 4.6 dam^3. Both systems were located in the northwest area outside the perimeter of Winnipeg.

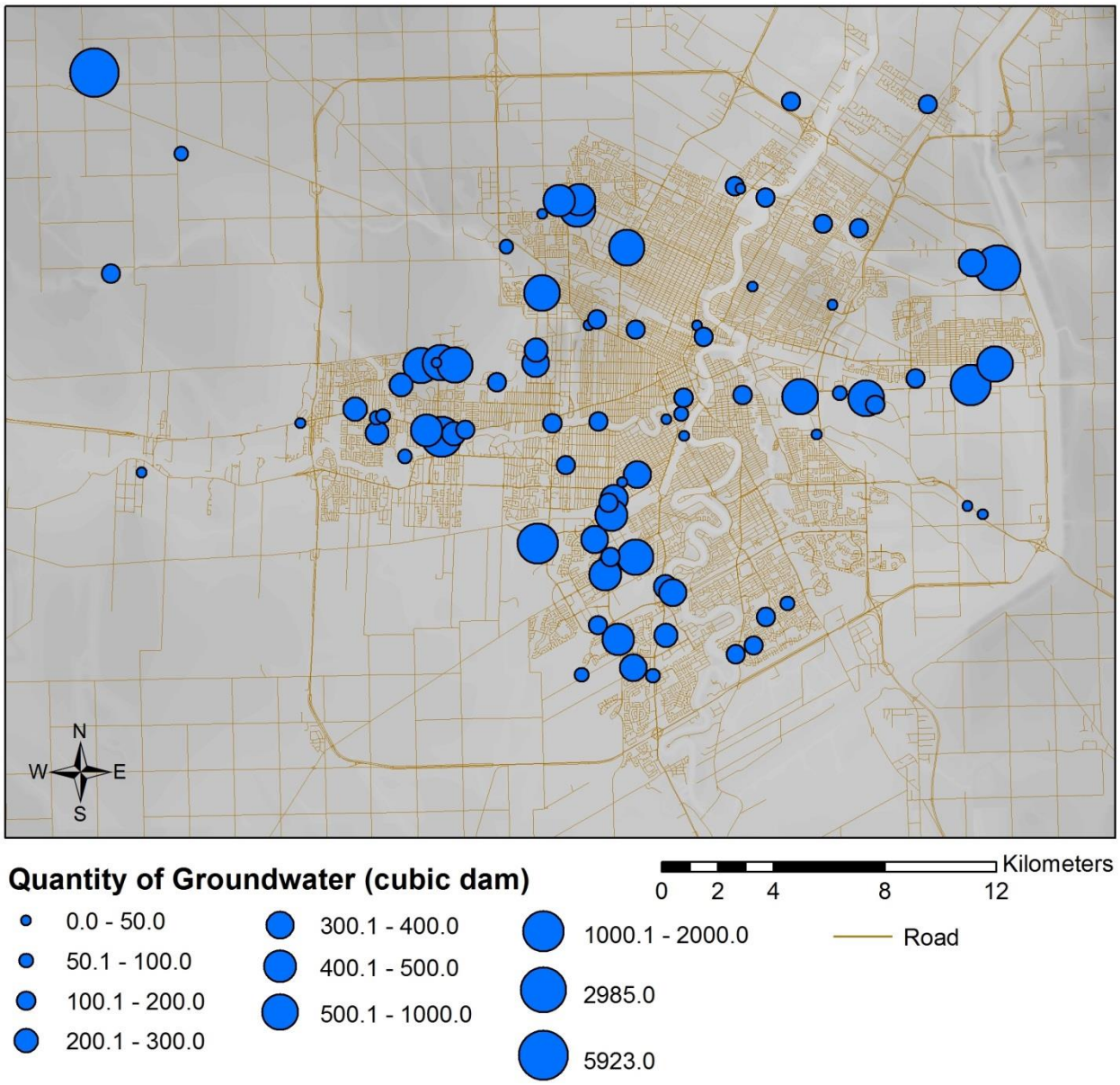

Figure 2.5 Maximum quantity of groundwater that can be diverted from upper carbonate aquifer.

GS06 was permitted to divert up to 5,923 dam^3 of groundwater every year. Although its geothermal system was licensed for cooling purpose, GS06 was permitted to extract groundwater volume twice than the required, because GS06 added a winter chilling system as part of its geothermal system. During the winter season, the geothermal system pumped equal or more quantity of the groundwater that was diverted during the summer season, run the groundwater

through the chilling system and lower groundwater temperature using cold winter air prior injecting the water back into the aquifer (Sinclair 2003).

GS09 held the second highest volume of groundwater extraction per year at 2,985 dam^3 with a maximum rate of 0.095 m^3/s. The company operated the geothermal system all seasons for the industrial cooling purpose. GS07 was permitted to divert groundwater up to 1,642 dam^3 per year, being the third highest volume. This quantity of groundwater was much less than GS09, considering the peak pumping rate for GS07 at 0.113 m^3/s. This condition occurs because GS07 was designed for heating and cooling purpose. The geothermal system required less quantity of water for heating than for cooling, beside the fact that geothermal system ran under peak pumping rate only for short period of time (Burns and Sinclair 2012b).

Groundwater Pumping Rate

The maximum pumping rate of groundwater that can be diverted from the aquifer (Figure 2.6) for each geothermal system is usually used only for short term to accommodate peak heating and cooling requirement. The system requires a lower pumping rate if not operated at the peak load. GS03 (Figure 2.3) operated the geothermal system for heating and cooling with a peak pumping rate of 0.3 m^3/s. This was the highest pumping rate licensed by Manitoba Sustainable Development. GS04 extracted up to $7.6x10^{-4}$ m^3/s groundwater from the upper carbonate aquifer, which was the lowest rate compared to the other geothermal systems. The system also runs for heating and cooling.

GS05 operated a geothermal system for cooling purpose and was permitted to extract groundwater up to 0.228 m^3/s, which was the second highest pumping rate. However the system did not return the wastewater back into the aquifer. GS06 operated the geothermal system with the third highest pumping rate of 0.19 m^3/s. The geothermal system was for cooling purpose in

summer. The system also runs in winter with the purpose to lower groundwater temperature that was increased during the cooling period, by using cold winter air. Therefore, the system may run the maximum pumping rate during summer and winter season.

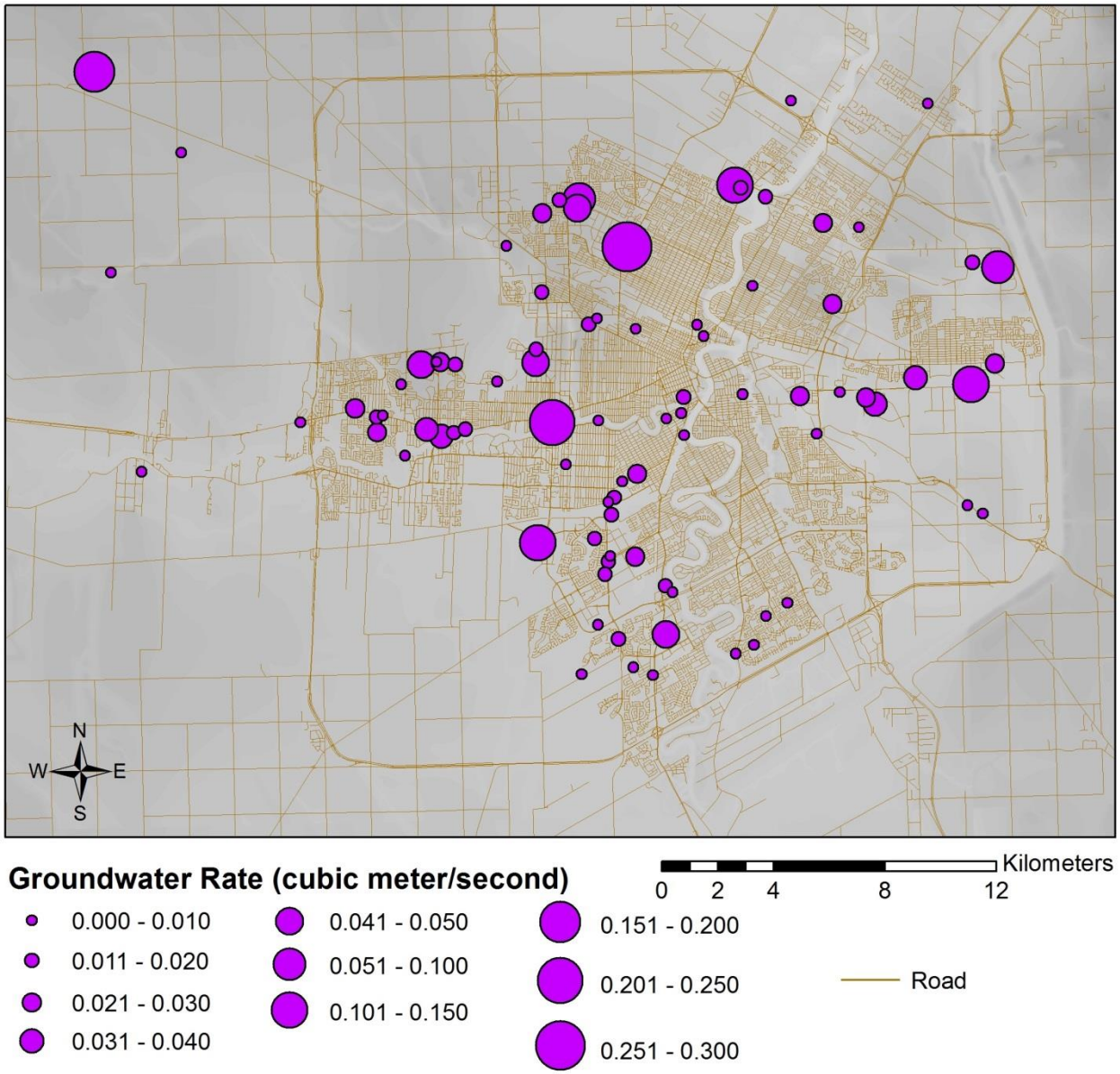

Figure 2.6 Maximum pumping rate of groundwater that can be diverted from Upper Carbonate Aquifer.

GS07 was permitted to extract groundwater up to 0.113 m^3/s, which was the fourth highest pumping rate. The geothermal system was designed for heating and cooling purpose. During

normal heating and cooling demand, the system extracted groundwater at a rate between 0.032 m^3/s to 0.088 m^3/s (Burns and Sinclair 2012b).

GS03 operated a geothermal system with the highest peak pumping rate, but the system was permitted to extract groundwater only up to 946 dam^3 per year (Figure 2.5), which is less than GS07. Although both geothermal systems were designed for heating and cooling purpose, GS03 accommodated residential building, while GS07 commercial building. These conditions affected the heating and cooling loads, which defined the peak pumping rate and the quantity of groundwater. As a residential building, building for GS03 had more windows compared to building for GS07. During normal summer temperature, the residents were more likely to open the windows and let the fresh air flowing within building. Therefore, the building requires less groundwater for cooling. During the hottest days in summer, the residents preferred to close the windows and ran the cooling system, causing higher peak pumping rate. While the lower peak pumping rate of GS07 indicated that the building had better insulation design.

Production and Recharge Wells

The number of production wells for each geothermal system depends on the specific capacity of each production well and the maximum groundwater pumping rate. Pumping test on the production well determines its specific capacity to meet the maximum groundwater pumping rate required for peak demand. The maximum groundwater rate during peak demand also determines the number of recharge wells required for each geothermal system. Conducting injection test on recharge wells identifies their capability to adequately handle the maximum rate.

Majority of geothermal systems were a withdrawal-injection doublet consisting one production well to withdraw groundwater from the Upper Carbonate aquifer and one recharge well to inject groundwater back into the aquifer (Figure 2.7). GS07 (Figure 2.3) operated a

geothermal system with the highest number of required wells, consisting of 4 production wells and 8 recharge wells. A geothermal system with the second highest number of well was operated by GS06, consisting of 4 production wells and 7 recharge wells. GS02 operated a geothermal system with 3 production wells and 4 recharge wells. GS10 required 2 production wells and 4 recharge wells. GS11 operated a geothermal system that required 5 wells, 2 production wells and 3 recharge wells.

There were 8 geothermal systems within the city limits that required 4 wells including GS03. Most of the systems consisted of 2 production wells and 2 recharge wells, except GS09 and GS12. GS09 operated a geothermal system that required 1 production well and 3 recharge wells. Although GS12 was designed for maximum groundwater pumping rate of 0.010 m^3/s, almost one tenth of GS09 maximum rate, GS12 required 3 production wells and 1 recharge wells. This condition occurred because aquifer thickness below GS09 area is shallower than aquifer below GS12 area. Usually, shallow productive water bearing fractures in fractured-bedrock aquifer have higher transmissivity (Risser 2010). As shown in the drilling report, production well at GS09 was cased until 18 m depth with open hole depth of 45 m, which indicates aquifer thickness approximately 27 m. Pumping test performed at GS09 production well indicated aquifer transmissivity of 1240 m^2/d (Wiecek 2001b). Aquifer thickness at GS12 is approximately 57 m based on the depth of casing and borehole at three production wells. Pumping test performed at the production wells indicated transmissivity range from 87 to 99 m^2/d (Bell and Friesen 2008b).

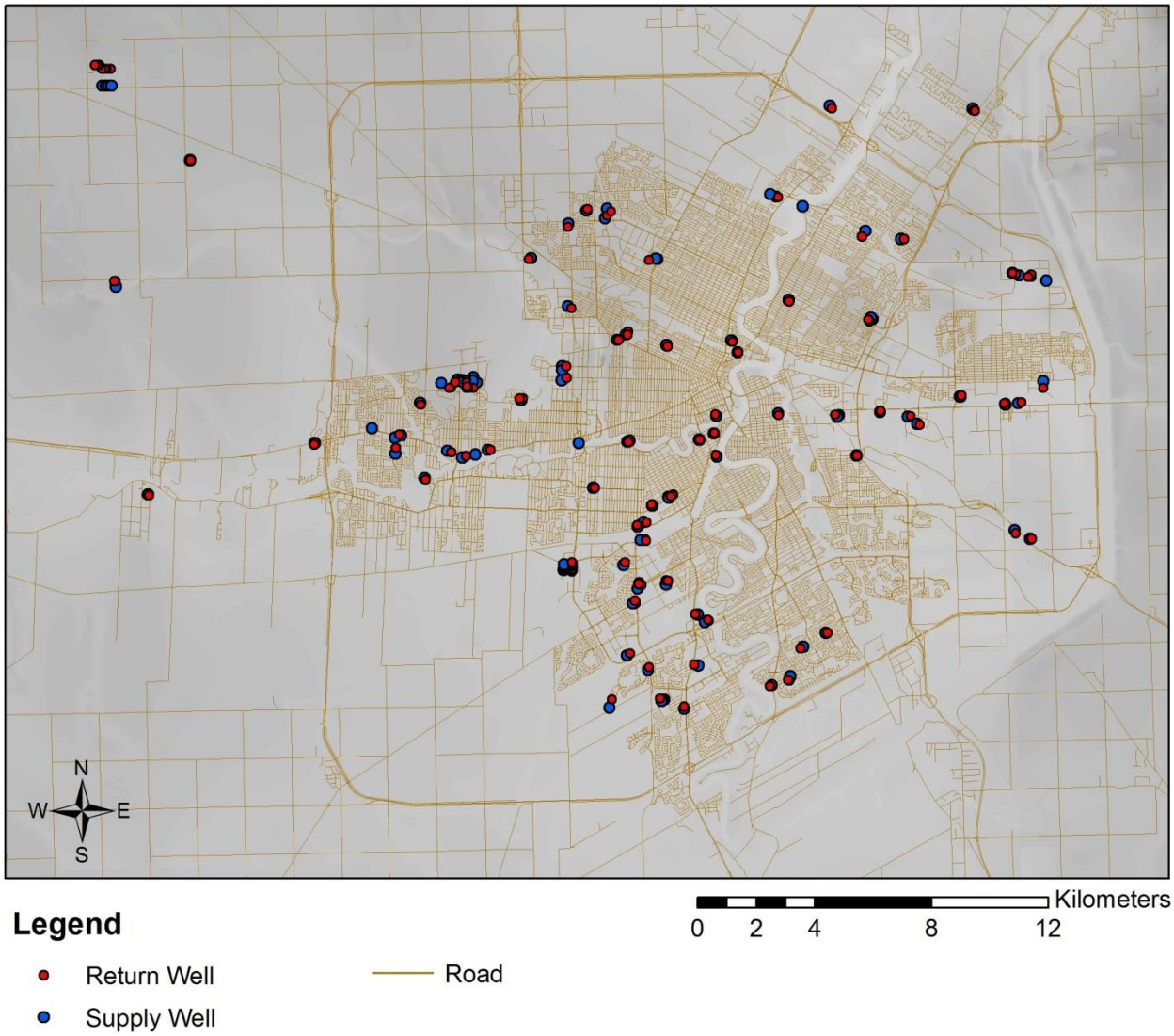

Figure 2.7 Production wells and recharge wells for each geothermal system.

Within the City limit, there were seven buildings that direct their thermal wastewater to the river or the City of Winnipeg sewer system. These buildings operated geothermal systems for cooling purpose only. Six of these geothermal systems used only one well. GS13 directed its wastewater to the Red River, while GS14 and GS05 directed their waste water to the Assiniboine River. GS15, GS16, and GS17 directed their thermal wastewater to the city land drainage sewer system which then discharged into the Assiniboine River and the Red River. Although GS18 also

discharged its wastewater into the city storm sewer, this geothermal system required two wells, one production well and one recharge well. Unlike the other geothermal systems, GS18 runs for cooling in all seasons. During summer from June 1st to November 15th, the system discharges its wastewater into the city sewer system. In winter, the system injects thermal wastewater into the aquifer because the City of Winnipeg prohibits discharging wastewater into the sewer system when ice is already formed on the river.

The spacing between recharge and production well plays an important role on groundwater temperature entering the production well. Recharge well should be located at an optimum distance from the production well to prevent wastewater flow from recharge well into a production well. The location should also be designed to ensure any flow between the wells is sufficiently low. When the flow between the wells is sufficiently low, it takes longer time for the wastewater to reach the production well; therefore, when the wastewater reaches the production well, the temperature of the wastewater is almost equal to the aquifer temperature. Factors that affecting optimum spacing are the maximum cooling or heating load, duration of maximum load, well capacities, groundwater gradient, groundwater flow velocity, groundwater temperature, aquifer transmissibility, aquifer thickness, and effective porosity (USEPA 1999). Researches were performed to provide guidelines for minimum spacing between a production well and recharge well. Kavanaugh and Rafferty (2014) described a method developed by Kazmann and Whitehead (1980) in designing minimum wells spacing for the unconsolidated aquifer. They suggested a minimum of 30 m for well spacing depending on the aquifer thickness, porosity, system average flow rate, and the period of duration of the dominant load. Clyde and Madabhushi (1983) suggested a distance of 15 to 22 m between a production well and a recharge well, with consideration of locating the recharge well on a lower gradient from the production

well, and both recharge well and production well are on a line parallel to the groundwater flow direction. These minimum spaces were developed based on porous medium aquifer which may not be applicable for fractured bedrock aquifer such as the Upper Carbonate aquifer.

Recharge wells at GS06 (Figure 2.3) were located about 580 m from production wells which are the farthest spacing. GS07 spaced its recharge wells 300 m from production wells. Within area A, the distances were 224 m at GS02, 123.5 m at GS19, and 101.5 m at GS01. Some geothermal systems had their recharge wells less than 30 m from production wells, such as GS04, GS20, GS21, and GS22. There were no reports indicated that these wells need to be relocated due to temperature increase at the supply well.

Some open loop geothermal users had to relocate their recharge well such as GS01, GS24, GS25 and GS26. Production wells and recharge wells at a manufacturing plant (GS01) were relocated to accommodate the expansion of geothermal system which required more groundwater (Wolowich and Tamburi 1987). The long term care building (GS24) relocated its production well due to the expansion of geothermal system from cooling purpose to a combined heating and cooling system, the poor condition of wells and the increase of groundwater temperature at production well (Bell 2004). A personal care home (GS25) relocated its recharge well due to the poor condition of existing well and the increase of groundwater temperature at its production well (Bell 2014). At GS26, temperature increase at production well occurred because the well was located downstream of recharge well; therefore the role of the wells were exchanged (Tamburi et al. 1987).

Casing Depth and Open Hole Depth of Production Wells

Construction of geothermal wells in the City of Winnipeg typically consists of solid casing through the surficial deposits continued by open hole in the carbonate bedrock. The open hole

must be deep enough to intersect water bearing fractures in order to meet the groundwater flow rate required. The casing must extend to a minimum of six meters below the ground surface unless the borehole is shallower (Development 2017). The majority of casing depths of production wells in the City of Winnipeg were between 15 m to 20 m, and the minimum casing depth was 9.75 m (Figure 2.9).

Pervious fracture zones at GS06 were found at three main carbonate bedrock zones: Lower Stonewall Formation at the depth of 21 m, Stoney Mountain Foundation at various depths between 24 m to 42.7 m, and Red River Formation where the increase water seepage was noted below 61 m (Sinclair 2003). The production wells were drilled to 88 m below grade and cased to the depth of 15 m.

In the western part of Winnipeg, the upper fracture bedrock zone is not present due to the presence of the Amaranth Formation approximately at the depth of 27 m below grade. In this area, groundwater was available in deeper fracture zones of the Stony Mountain Formation or Red River Formation (Bell 2012a). At GS01, major water bearing fractures were found at 40 m and 58 m below grade (Waedt 1988); production well was drilled to a depth of 72.2 m and cased to a depth of 38.7 m. At GS02, water bearing fracture zones were found in the limestone bedrock at depths of 34.4 m, 51.8 m to 53.3 m, and 54.8 m to 60.9 m (Bielus 2005), the open hole of production wells depth ranging from 106.7 m to 112.8 m with casing depth ranging 25.6 m to 36.27 m. At GS27, water bearing fractures were encountered at the depth of 30.5 m with additional fracturing at 70 m to 73 m below grade (Bell and Friesen 2011); the production well was drilled to 85.3 m depth and cased to a depth of 29.9 m. At GS28, main water bearing zone was found at the horizontal bedrock fractures between 29 m and 76 m depth (Wolowich 1990); the production well was drilled to 129.5 m depth below grade and cased to the depth of 30.5 m.

Not far from area A, GS26 has the deepest production well at 159.3 m; the well was cased to 14 m depth from grade.

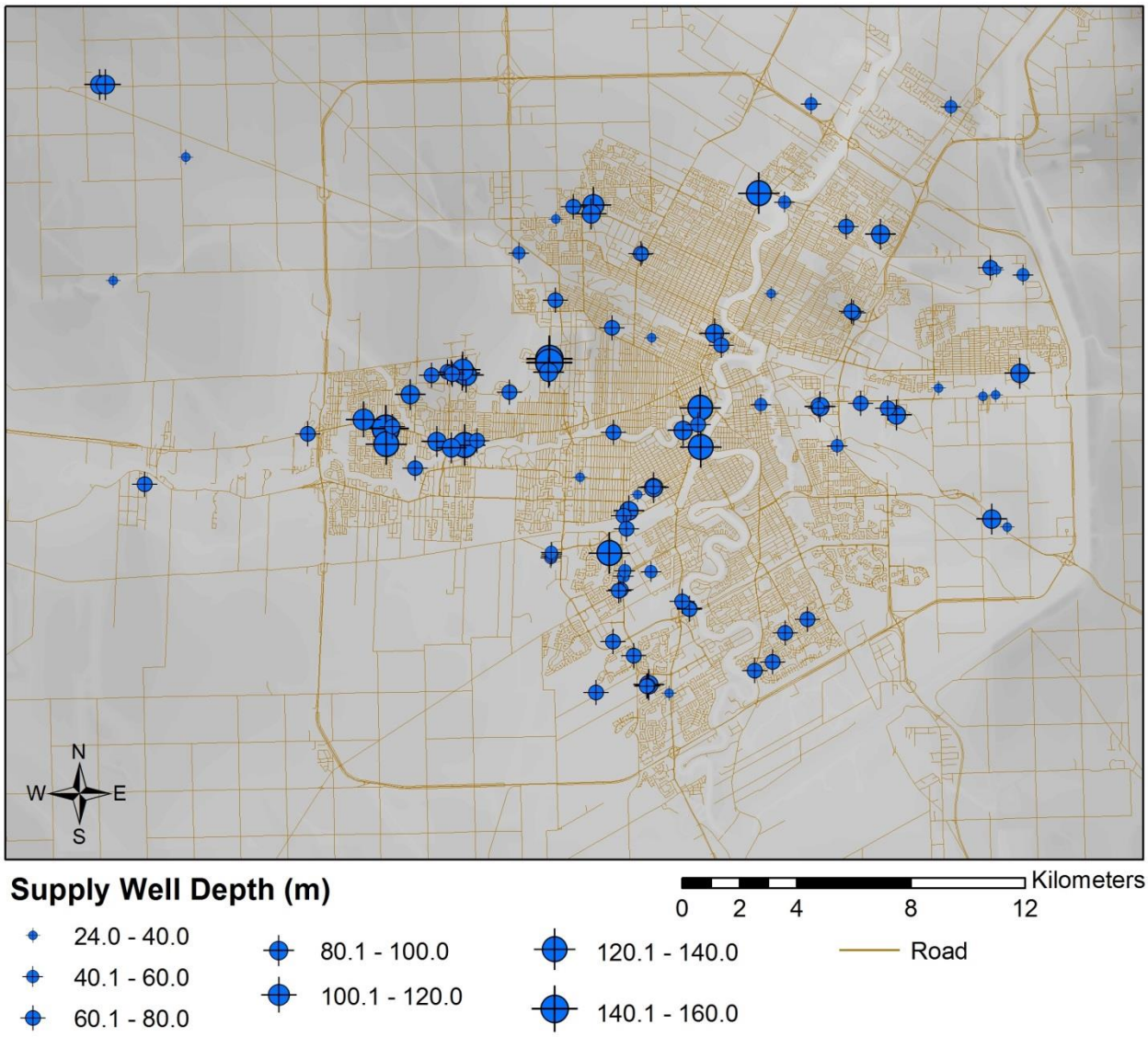

Figure 2.8 Open hole depth of each production well.

In the northwestern part of Winnipeg, at GS29, water bearing fracture was found below 22.6 m depth, the production well was drilled to a depth of 44.2 m and cased to a depth of 23.5 m below grade (Sinclair 2006). While at GS30, water bearing fractures were found at 15.8 m to

17.4 m and 19.8 m to 24.4 m depth below grade (Wiecek 2004); the production well was drilled to 109.7 m depth and cased to 18.9 m depth below grade.

In the northeastern part of Winnipeg, at GS31, the production well was drilled to 42.7 m depth and cased to 14 m depth below grade, the well intersected water bearing fracture between 15 m to 16.8 m depth (Wolowich et al. 1987c). At GS45, water bearing fractures were found at 26, 40, and 79 m depth below grade (Development 2003). Close to the City perimeter, at GS09, major water bearing fractures were found between 18 to 20 m depth, with smaller fractures between 16 to 17 m depth and 22 m depth below grade (Development 2009).

In the eastern part of Winnipeg, the majority of groundwater at GS11 was encountered between 17.7 m to 26 m depth below grade, on the east side of property water bearing fractures were found at depth 18.6 m and 21.6 m. The production wells were drilled to 36.6 m depth and cased to 18.3 m and 16.7 m below grade (Burns and Sinclair 2012a). At GS32, the production well was drilled to a depth of 27.4 m which intersected a major water bearing fracture at a depth of 18.3 m below grade, with minor fractures at 18 m and between 24 and 26 m depth below grade. The well was cased to 17.8 m depth from ground surface (Sinclair 2009). The production well of GS55 was cased to 18 m with open hole depth 95 m below grade. The water bearing fractures were found between 61 to 85 m below grade (Development 2012).

Close to the city centre, the production well at GS58 was drilled to 42.7 m and cased to 29.6 m below grade. Major water bearing fractures were found at 38 m depth (Bell 2011). At GS20, the production well was drilled to 98 m and cased to 15 m. Water bearing fractures were found at depth of 29, 49, and 96 m (Bell 2012b). At production well 1 of GS10, two water bearing zones were encountered, a fracture zone between 35.1 and 36.6 m below ground surface and a very porous limestone at 64 m below ground surface. The production well was drilled to

79.3 m depth and cased to 24.7 m below ground surface. At production well 2, water bearing fractures were encountered between 34.4 and 38.1 m below ground surface. The well was drilled to 91.5 m depth and cased to a depth of 24.1 m (Sinclair 2008).

In the southwestern part of Winnipeg, the majority of groundwater at GS07 was encountered in fracture between 36.3 and 47.3 m below grade. The production well were drilled to 51.8 m depth and cased to 30.2 m or 32.8 m depth below grade (Burns and Sinclair 2012b). At GS35, major water bearing fractures was intercepted at 17, 25, 38, and 58 m depth; the production well was drilled to 61 m depth and cased to 16.8 m below grade (Wolowich et al. 1987a). Around GS41, water bearing fractures were found at depths 17.7 m, 29.3 m, and between 33.5 to 36.6 m (Wiecek 2001a).

In the southeastern part of Winnipeg, at GS33, major water bearing fractures were encountered from 15 to 16.8 m depth, and 55 m to 55.5 m depth, production well was drilled to 61 m depth and was cased to a depth of 15.8 m (Wolowich et al. 1987b). At GS34, major water bearing fractures were encountered at 20 m and 26 m below surface, the production well was drilled to 61 m depth and was cased to 19.5 m depth (Wolowich et al. 1987).

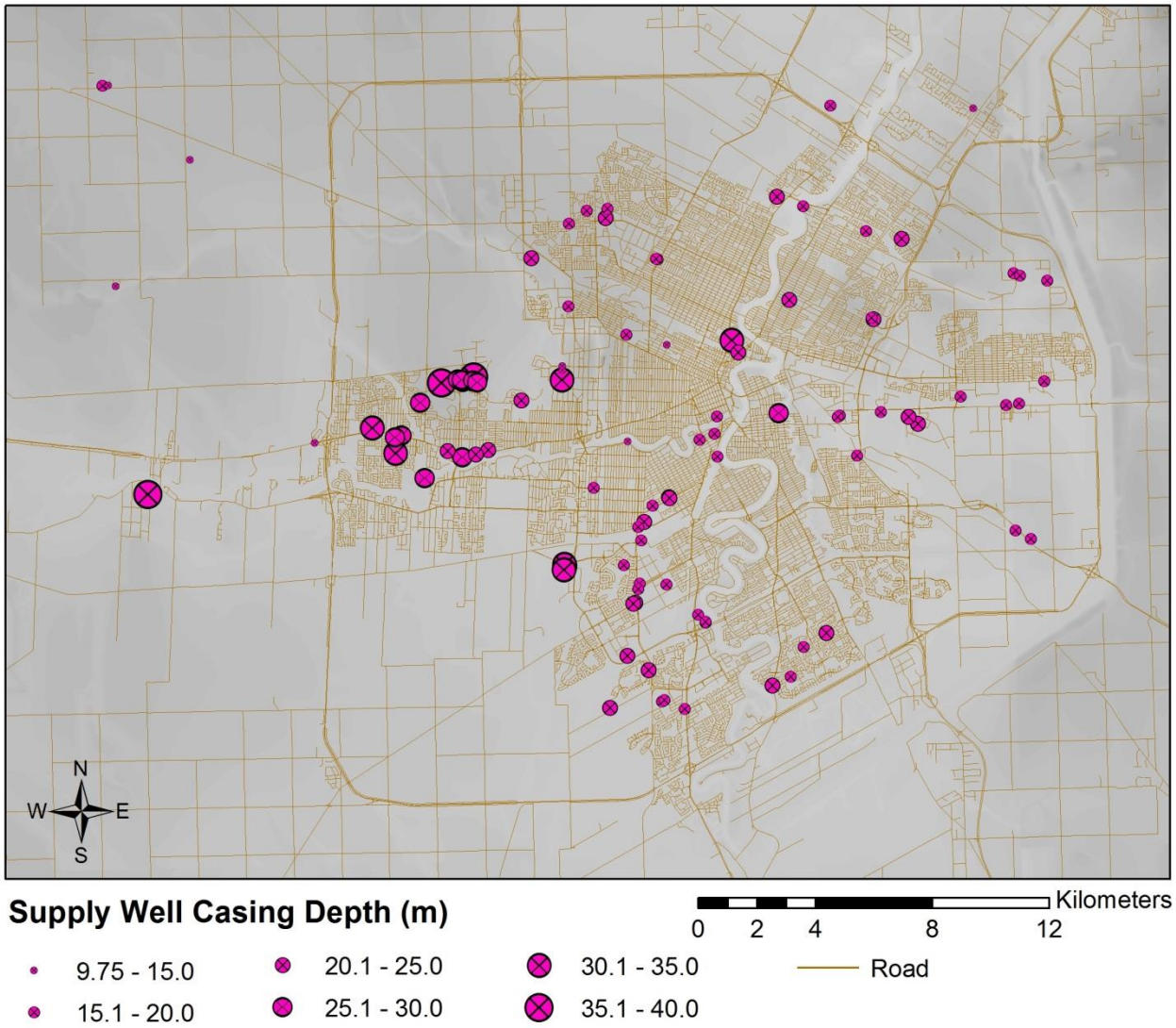

Figure 2.9 Casing depth of each production well.

Some production wells with depth more than 120 m below grade were cased at shallower depth than the wells with shallower open hole depth (Figures 2.8 and 2.9), such as production wells at GS26, GS52, and GS53 (Figure 2.2). At GS26, a production well was drilled to 159.3 m depth and cased to 14.3 m depth. At GS52, production well was drilled to 128 m depth and cased to 15.2 m depth. While at GS53, a production well was drilled to 121.9 m depth and cased to 15.8 m depth. There are no records about the depth of water bearing fractures at these locations. The possibility is that these locations contain more than one major water-bearing fracture zone,

such as recorded at GS02. In contrary, the production wells at GS07 and GS54 were cased deeper than the production wells with more than 120 m depth. Production wells at GS07 were drilled to 51.8 m depth with casing depth varied from 30.2 m to 32.8 m below grade. While at GS54, the production well was drilled to 92 m and cased to 33.5 m depth. There is no record why this was performed at GS54, but at GS07, the casings were purposely designed to extend into production zone because the upper 15 m of carbonate bedrock contained very few fractures therefore produce only limited water. By extending the casing into the production zone, GS07 was able to install the submersible pumps deeper into the production wells. Installing the pump deeper into the production well will prevent cavitation should the reduction of groundwater potentiometric surface occur in the future (Burns and Sinclair 2012b).

2.2.2.2 Actual Groundwater Usage

Among 87 geothermal systems only 48 users record the groundwater quantity extracted and injected, but only 23 sets of these records that were used for the analysis (Figure 2.10). From these 23 geothermal users, three systems extracted more groundwater than the allowable quantity, eight systems extracted groundwater between 80 to 100% of the allowable quantity, seven systems extracted groundwater 50 to 79% of the allowable quantity, and five systems extracted groundwater less than 50% of the allowable quantity. To support this study, comprehensive data from geothermal systems belonging to Hydro Power Station (GS06) and Furniture Retail Store (GS07) were used to perform further analysis.

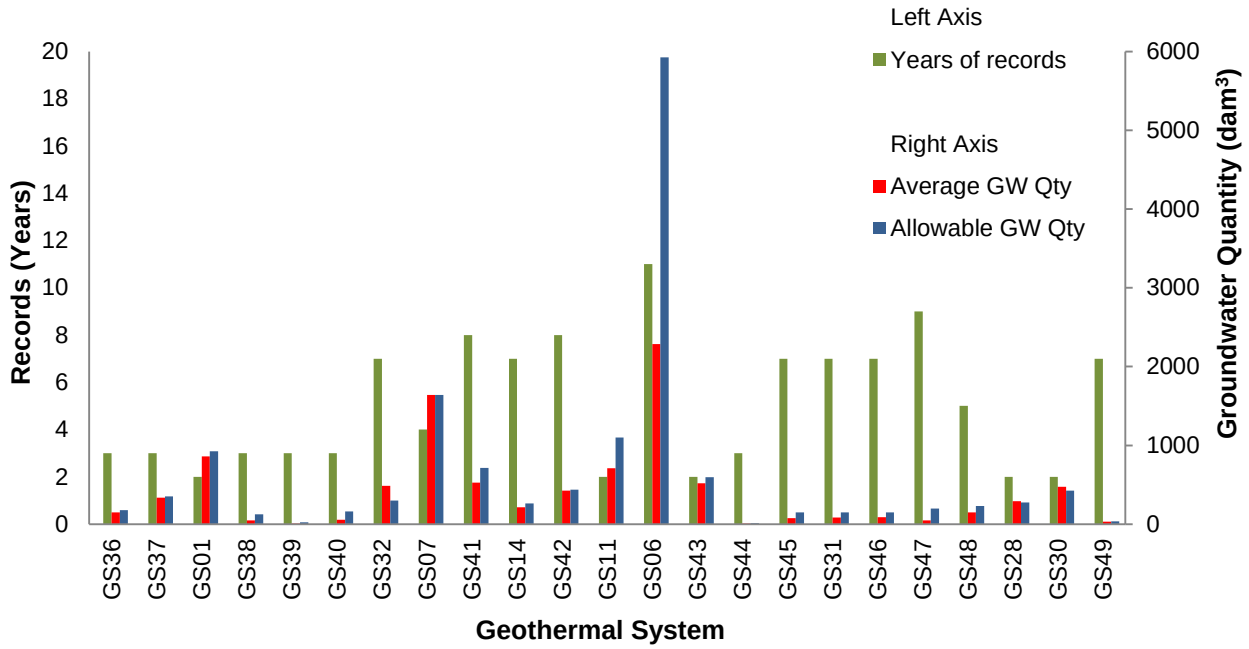

Figure 2.10 Average recorded groundwater usage compared to allowable annual groundwater usage.

GS06 (Figure 2.3) is located near the village of Rosser, northwest of Winnipeg. The station converts DC power from Hydro Power Stations in northern Manitoba to AC power for consumer use in southern Manitoba and for export in neighbouring Manitoba. The geothermal system has been utilized since April 2004 for space cooling purpose. The groundwater cooling system used four production wells and seven recharge wells. During the summer cooling period from May to October, the system extracts groundwater, runs the groundwater through the heat exchanger and returns the groundwater back to the aquifer. In winter chilling period, the system extracts groundwater and runs the groundwater through winter chilling system before returning the groundwater back into the aquifer. In winter chilling system, groundwater is directed to a plate and frame heat exchanger where the groundwater temperature is lowered using cold winter air. The purpose of winter chilling system is to thermally balance the heat load from summer cooling period (Burns and Mann 2006).

During 2004 to 2014 (Figure 2.11), the highest quantity of groundwater extraction occurred in 2010 at 2,887 dam^3, 75% of groundwater was used for space cooling and 25% for winter chilling. The low groundwater quantity for winter chilling occurred because of warmer winter in 2010. The winter chilling system ran at higher pumping rates on colder days to maximize groundwater chilling efficiency. In warmer winter days, the system ran at lower pumping rates because groundwater chilling was no longer efficient (Thiessen et al. 2011). This was also the year when the lowest average temperature change occurred at 1.3°C.

The highest average temperature change occurred in 2007 at 3°C, with a peak value at 8.4°C in September (Mann 2008). During this year, the system used 56% of the groundwater quantity for space cooling and 44% for winter chilling. The highest groundwater use for space cooling occurred in 2009 at 2,219 dam^3 which was 81% of total groundwater extracted in that year. In 2009, the system used only 19% of the groundwater extracted for winter chilling, this occurred mainly because winter chilling system was shut down from mid-November until mid-January of the following year (Thiessen and Mann 2010).

In 2013 and 2014, the system was able to somewhat equalize the groundwater quantity and temperature change for summer cooling and winter chilling. In 2013, 53% of total groundwater quantity was used for summer cooling and 47% for winter chilling. The average temperature difference for summer cooling was 2°C while the average temperature difference for winter chilling was -1.7°C. In 2014, the system used 54% of total groundwater for summer cooling and 46% for winter chilling. As the previous year, the average temperature difference for summer cooling was 2°C and for winter chilling was -1.8°C.

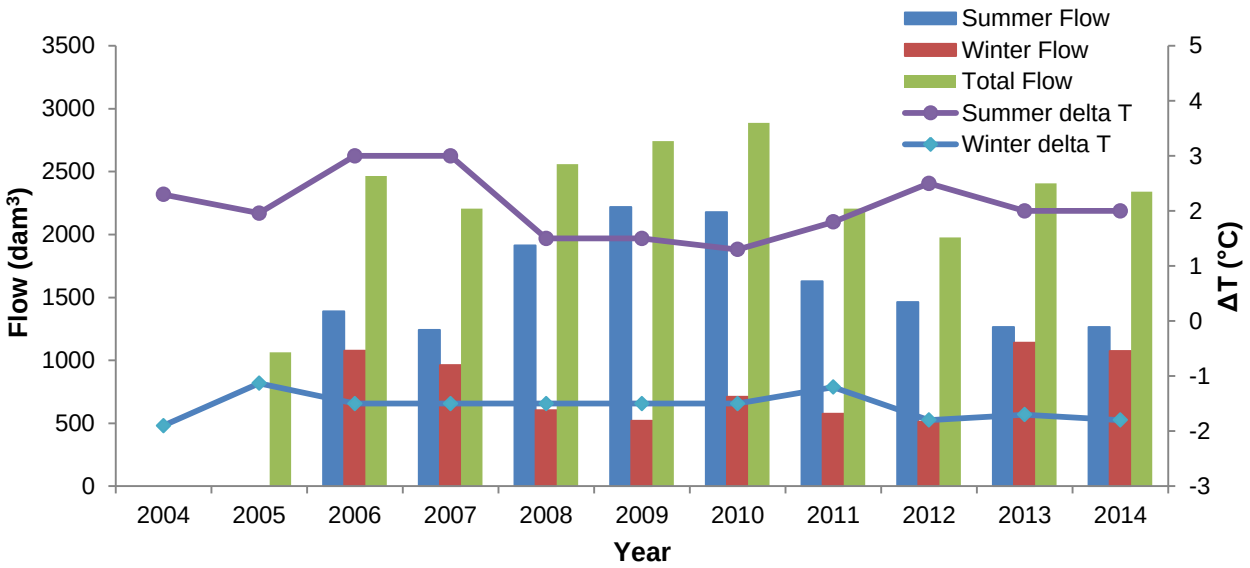

Figure 2.11 Recorded annual groundwater usage at GS06. Positive temperature change (ΔT) indicates the system runs for space cooling while negative ΔT indicates the system runs for winter chilling.

GS07 (Figure 2.2) is located in the southwestern part of Winnipeg. The store uses a geothermal system for heating and cooling with four production wells and eight recharge wells. Although the system has been operated since November 2012, groundwater temperature and quantity were not recorded until early 2013 and early 2014.

Records of groundwater quantity, groundwater temperature at the production well and recharge well from January 2013 to September 2017 (Figure 2.12) indicated that groundwater temperature measured at the production well showed an increase every year. Average temperature measured was 6.7°C in 2013, 6.73°C in 2014, 6.75°C in 2015, 6.81°C in 2016, and 7.06°C in 2017. By the end of 2016, GS07 already extracted groundwater at an average of 2,033 dam^3 per year which was 391 dam^3 more than the allowable quantity. Significant average temperature change occurred in 2017 at 3.82°C which was more than the system was originally set at 3°C temperature difference. From January to September 2017, GS07 extracted only 748 dam^3 of groundwater that was only about 45% of the allowable quantity. This indicated that in

order to extract groundwater less than the allowable quantity, the geothermal system must increase the temperature change to more than 3°C. The annual groundwater temperature increase was 0.03°C to 0.11°C from 2013 to 2016, but significant increase of 0.25°C occurred in 2017.

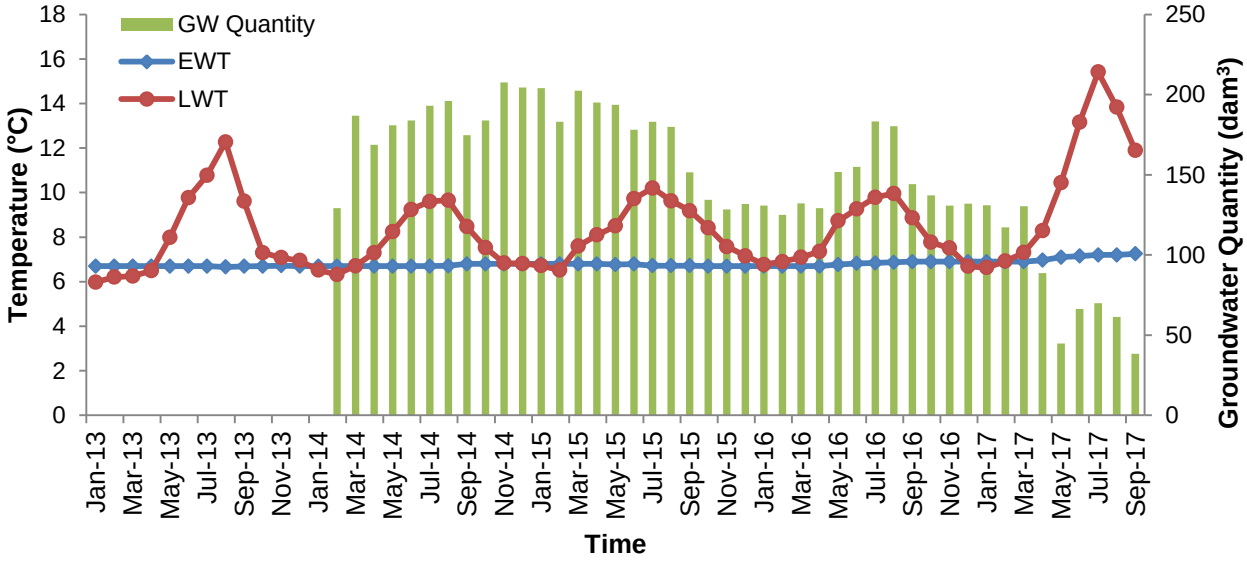

Figure 2.12 Recorded annual groundwater usage at GS07.

2.2.2.3 Groundwater Temperature Map

Temperature data were obtained from 16 observation wells managed by Manitoba Sustainable Development (SD) and groundwater usage records from 28 geothermal systems (Figure 2.13). Ideally development of undisturbed groundwater temperature should be based on the measurement at observation wells located upstream of geothermal system production well. The temperature map (Figure 2.13) was developed to show the temperature at production wells reported by geothermal users for the purpose of this study. Groundwater temperature at SD observation wells mostly were measured at the depth of few meters below the top of aquifer (Ferguson and Woodbury 2004). Groundwater temperature at geothermal system wells were either measured at production wells or before entering the heat exchanger. Groundwater temperature before entering the heat exchanger generally is the average groundwater temperature

in the aquifer. These differences in measurement depth have little effect on the temperature map because the records indicated that temperature variation in the Upper Carbonate aquifer was between 0.1 to 0.3°C (Ferguson 2004; Ferguson and Woodbury 2004).

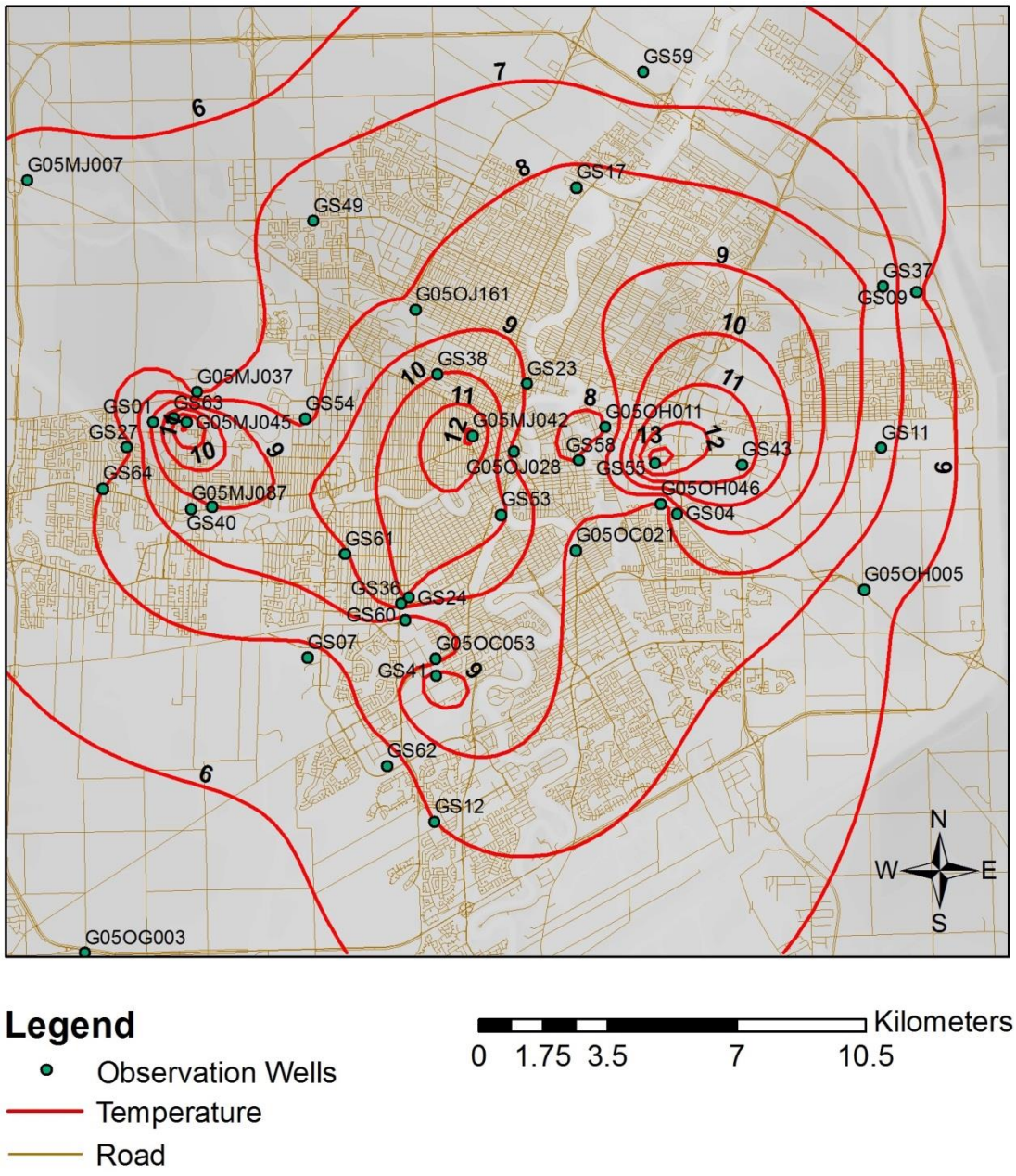

Figure 2.13 Average groundwater temperature in 2014 measured at SD observation wells and geothermal system supply wells.

Groundwater temperatures at SD observation well G05MJ045 (Figure 2.13) were recorded ranging from 7.4°C to 9.1°C from 1999 to 2004 (Bielus 2005). At this observation well, groundwater temperature reached 13.3°C in August 2014, an increase of more than 4°C. At SD observation well G05MJ042 (Figure 2.13), average groundwater temperature was increasing from 12.2°C in 2012 to 12.5°C in 2014. At this observation well, temperature measurement in August 2002 was between 8 to 9°C and measurement in August 2007 was 9°C (Ferguson and Woodbury 2004, 2007). The other 14 observation wells indicated temperature within the recorded temperature in 2002 and 2007 (Ferguson and Woodbury 2004, 2007).

The temperature record at geothermal systems may not represent the temperature at the neighbouring area especially upstream of the geothermal systems, due to thermal breakthrough and thermal plume. Newer geothermal systems such as GS08, GS64, GS11, GS12, GS62, GS07, GS61, GS53, GS23, GS58, and GS04 had recorded temperatures that were similar to the undisturbed groundwater temperature because thermal feedback had not occurred. In western part of Winnipeg, GS01 and GS63 recorded temperature between 10 to 11°C, both geothermal systems are located upstream of SD observation well G05MJ045. GS54 and GS49 recorded temperature that were within the recorded temperature in August 2002 and 2007 (Ferguson and Woodbury 2004, 2007). GS24 and GS36 were in the same neighbourhood separated about 265 m, both geothermal systems had similar average groundwater temperature at their production wells, about 10°C. Upstream of GS24 and GS36 was GS61 which recorded temperature 8.9°C. Downstream these three geothermal systems was a new system, GS53, which reported temperature at 10.25°C in its production well. These conditions indicated groundwater temperature in this neighbourhood had increased between 1 to 2°C from temperature in 2002 and 2007.

2.2.3 **Heat Balance Calculation**

Annual groundwater heat balance was estimated based on the allowable groundwater quantity shown in Figure 2.5. The total heat transferred by each geothermal system was calculated using:

$$Q_t = c_p \, \rho \, \Delta T \, V \qquad \text{Eq. 2.1}$$

Where Q_t is the heat transfer (kJ), c_p is the specific heat capacity of water (4.1868 kJ/kg.°C), ρ is the density (999.35 kg/m^3), ΔT is the temperature change (5°C), and V is the groundwater volume (m^3).

Heat transfer (Q_t) can be expressed by:

$$Q_t = Q_c + Q_h \qquad \text{Eq. 2.2}$$

With Q_c is heat transfer for cooling (kJ), Q_h is heat transfer for heating (kJ).

Heat transfer for cooling or heating was calculated using:

$$Q_c = q_{cond} \times EFLC_c \qquad \text{Eq. 2.3}$$

$$Q_h = q_{evap} \times EFLC_h \qquad \text{Eq. 2.4}$$

With q_{cond} and q_{evap} are the heat transfer rate (heat transfer per hour) required for cooling and heating; while $EFLC_c$ and $EFLC_h$ are Equivalent Full Load Hour for cooling and heating respectfully (hours).

The following assumptions were applied in estimating heat balance:

- Cooling mode rejected 80% more heat per hour than in heating mode (Kavanaugh 2008).

- Temperature difference between entering water temperature (EWT) and leaving water temperature (LWT) was 5°C (9°F). The temperature difference was regulated by Manitoba Sustainable Development (Matthews 2003).
- Equivalent Full Load Hour for cooling ($EFLC_c$) was 500 hours and Equivalent Full Load Hour for heating ($EFLC_h$) was 1250 hours. Manitoba Hydro guideline for commercial building geothermal system suggested $EFLC_c$ between 400 to 600 hours and $EFLC_h$ between 1000 to 1500 hours (Manitoba Hydro 2016).

2.2.4 **Thermal Breakthrough and Thermal Plume Calculation**

When the wastewater is injected back into the aquifer, a proportion of wastewater will flow back to the production well. Depending how far the distance between recharge well and production well, the wastewater eventually will reach the production well causing the increase of abstraction water temperature. After thermal breakthrough occurs, abstraction water temperature will continue to rise over time until the system become unsustainable. Thermal breakthrough time can be estimated using the following formulas (Banks 2009):

$$t_{the} = \pi b \frac{\rho c L^2}{3\rho_w c_w Q} \quad \text{for } i = 0 \qquad \text{Eq. 2.5}$$

$$t_{the} = \frac{\rho c L}{\rho_w c_w K i}\left[1 + \frac{4\alpha}{\sqrt{-1-4\alpha}} \tan^{-1}\left(\frac{1}{\sqrt{-1-4\alpha}}\right)\right] \text{ for } i < 0 \qquad \text{Eq. 2.6}$$

$$\alpha = \frac{Q}{2\pi T_r i L} \qquad \text{Eq. 2.7}$$

With t_{the} is thermal breakthrough time (d), b is effective aquifer thickness (m), L is spacing between supply well and recharge well (m), Q is abstracted groundwater flow rate (m^3/d), T_r is transmissivity (m^2/d), K is hydraulic conductivity (m/d), i is regional natural hydraulic gradient,

ρc is volumetric heat capacity of saturated aquifer (J/m^3.°C), and $\rho_w c_w$ is volumetric heat capacity of water (J/m^3.°C).

Temperature increase at production well following the thermal breakthrough can be estimated using the following formula (Banks 2009; Lippmann and Tsang 1980):

$$\frac{T_{abs}-T_{inj}}{T_0-T_{inj}} = 0.338 \exp\left(-0.0023 \frac{t}{t_{the}}\right) + 0.337 \exp\left(-0.1093 \frac{t}{t_{the}}\right) + 1.368 \exp\left(-1.3343 \frac{t}{t_{the}}\right)$$

Eq. 2.8

With T_0 is undisturbed groundwater temperature (°C), T_{abs} is temperature of abstracted groundwater (°C), T_{inj} is temperature of injected groundwater (°C), t is time since geothermal system started (d).

The above formulas are applicable with assumptions (Banks 2009): groundwater flow is laminar and Darcian, the aquifer is homogeneous, hydrodynamic dispersion and conductive thermal diffusion are not considered, instantaneous thermal equilibration between groundwater and aquifer matrix, negligible conductive heat losses into overlying and underlying strata, and the location of recharge well is immediately downstream of production well. Banks (2009) also indicated that the analytical solutions may not be able to solve more complex design such as: the location of recharge well is not directly drown-gradient of production well, combined heating and cooling system, varied injection temperature, multiple wells, heterogeneous aquifer, and different elevation between abstraction and injection.

Pophillat et al. (2018) studied and compared analytical solutions for predicting thermal plumes: radial heat transport model (Guimerá et al. 2007; Gelhar and Collins 1971), linear advective heat transport model (Bauer et al. 2009; Kinzelbach 1992), and planar advective heat transport model (Domenico and Robbins 1985; Hähnlein et al. 2010). The result showed that the linear advective heat transport model was able to define the thermal impact up-gradient of

recharge well. Although this model underestimated the width of the plume, this method was able to predict the length of thermal plume down-gradient of recharge well similar to the result from 3D numerical model using FEFLOW. The method describes heat propagation of injected water with assumptions that the heat source is a vertical line with continuous injection and the groundwater flow is 2D and transient with high background flow (higher than 1 m/d):

$$\Delta T(x,y,t) = \frac{Q_{inj}\Delta T_{inj}}{4n_e b v_s \sqrt{\pi \alpha_T}} \exp\left(\frac{x-r'}{2\alpha_L}\right) \frac{1}{\sqrt{r'}} \operatorname{erfc}\left(\frac{r'-v_s t/R}{2\sqrt{v_s \alpha_L t/R}}\right) \quad \text{Eq. 2.9}$$

$$r' = \sqrt{x^2 + y^2 \frac{\alpha_L}{\alpha_T}} \quad \text{Eq. 3.0}$$

$$R = \frac{\rho c}{n_e \rho_w c_w} \quad \text{Eq. 3.1}$$

With ΔT temperature difference between calculated temperature and undisturbed temperature (°C), x and y are x-coordinate (m) and y-coordinate (m), t is time (d), Q_{inj} is injection rate (m^3/d), ΔT_{inj} is temperature difference between injected and undisturbed temperature (°C), n_e is effective porosity, v_s is seepage velocity (m/d), α_L is longitudinal dispersivity (m), α_T is transverse dispersivity (m), and *R* is thermal retardation factor. The method produce 10% error compare to exact solution when $r'/(2\alpha_L) > 1$, and 1% error when $r'/(2\alpha_L) > 10$ (Kinzelbach 1992).

Calibrated carbonate bedrock thermal properties from the numerical analysis in chapter 3 were applied on all the geothermal systems in concern:

- Volumetric heat capacity of saturated aquifer = 3,251 kJ/m^3.°C
- Volumetric heat capacity of groundwater = 4,216 kJ/m^3.°C
- Porosity = 0.1 and effective porosity (heat) = 0.05
- Longitudinal dispersivity = 1.5 m and transverse dispersivity = 0.15 m

The results from analytical approaches were evaluated by calculating the relative errors (RE) between analytical and recorded data or result from numerical analysis. The abstraction temperature result was compared to the temperature recorded by the geothermal system, while temperature breakthrough time and thermal plume size were compared to the results from numerical analysis. The acceptance criteria used by (Pophillat et al. 2018) were adopted: the result is considered good when $|RE| < 10\%$, the result is considered satisfactory when $10\% < |RE| < 30\%$, the result is weak when $30\% < |RE| < 50\%$, and when $|RE| > 50\%$ the result is unacceptable.

2.3 Results

Every year, an estimated more than 470×10^9 kJ of heat was injected into the Upper Carbonate aquifer and 116×10^9 kJ of heat was extracted from the aquifer (Figure 2.14). The highest estimated heat transfer into the aquifer occurred at GS09 where the geothermal system rejected heat more than 62×10^9 kJ. At GS06, both injection and extraction were estimated at about 62×10^9 kJ which applied during cooling season and winter chilling. At GS07, geothermal system rejected an estimated of 14×10^9 kJ in summer and extracted an estimated of 20×10^9 kJ in winter. GS18 only returned groundwater back into aquifer during winter. Its system ran for cooling all year long. Estimated heat this system injected into aquifer was 0.9×10^9 kJ annually. GS08 injected an estimated at 0.1×10^9 kJ annually which was the lowest heat transfer.

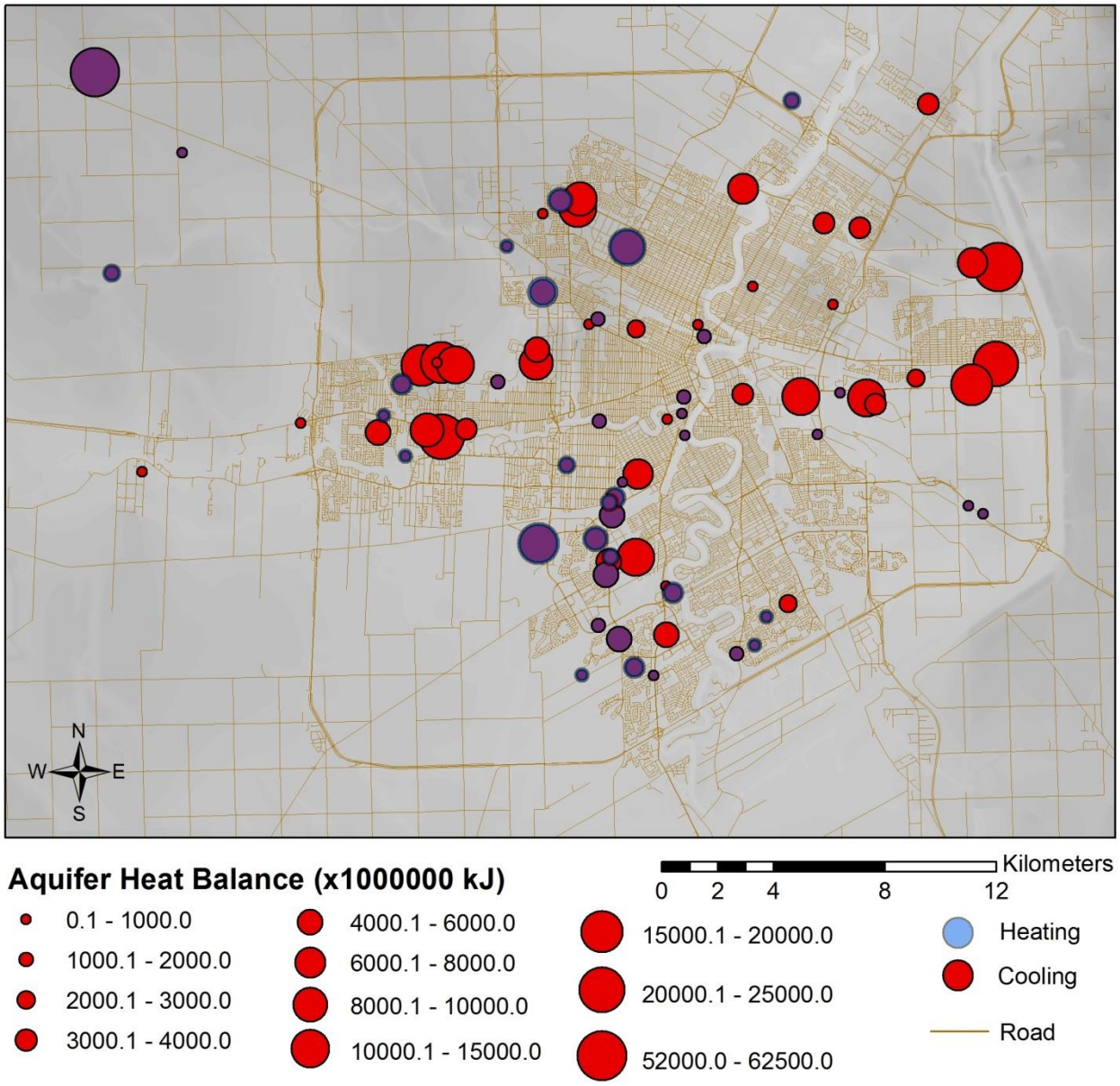

Figure 2.14 Estimated Annual Groundwater Heat Balance.

Calculation of the actual heat balance was performed on 9 geothermal systems, seven systems were evaluated using the average value of groundwater quantity and temperature difference (Figure 2.15) and two systems using the comprehensive data recorded. Four systems, GS37, GS01, GS41 and GS43, are geothermal system for industrial cooling that run for the whole year. Two geothermal systems provide air cooling for office buildings; GS44 operates

from June to August and GS38 from May to October. The other geothermal system, GS49 provides air cooling for school building from May to September.

Geothermal systems for industrial cooling returned the groundwater to the aquifer with temperature difference between 3°C to 4°C. The geothermal systems for air cooling of office buildings returned the groundwater with temperature difference between 2°C to 3°C. The geothermal system for school building, GS49, discharged groundwater back into the aquifer with 4°C temperature difference.

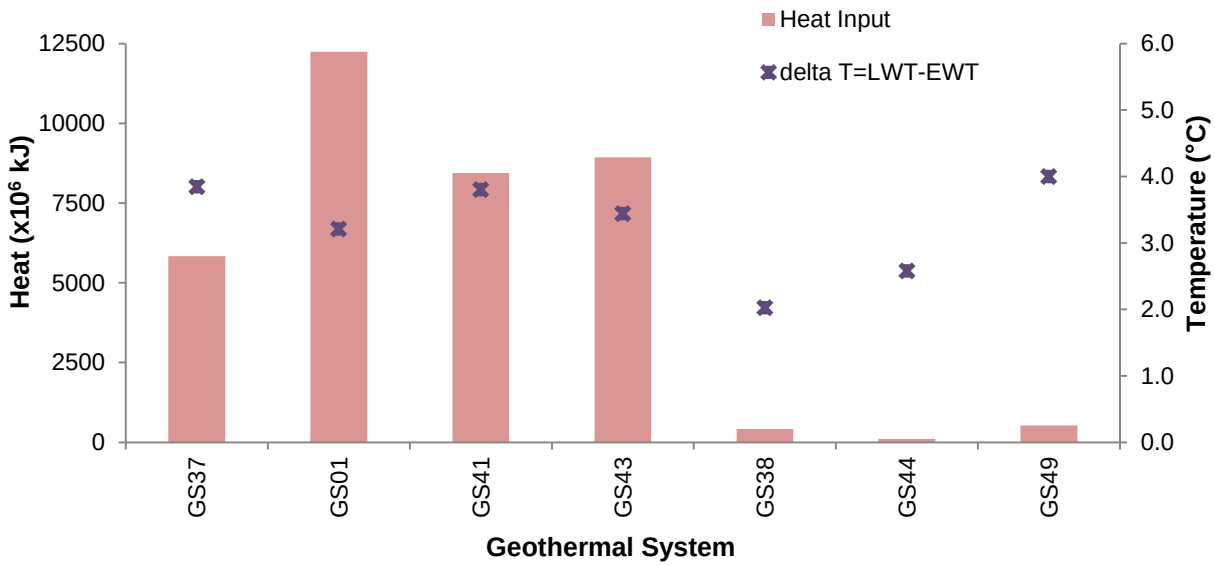

Figure 2.15 Calculated average annual heat injected into groundwater at 7 geothermal locations.

From 2004 to 2014, the Upper Carbonate aquifer beneath GS06 received heat input more than 7.8×10^9 kJ annually with a peak of 13.7×10^9 kJ in 2012 (Figure 2.16). Heat input into aquifer was significantly reduced to 4.1×10^9 kJ in 2013 and 3.5×10^9 kJ in 2014. The temperature measured at production well was approximately 0.8°C higher than in 2004 (Lindell and Mann 2015). Therefore, the average groundwater temperature increase was less than 0.1°C per year by using winter chilling.

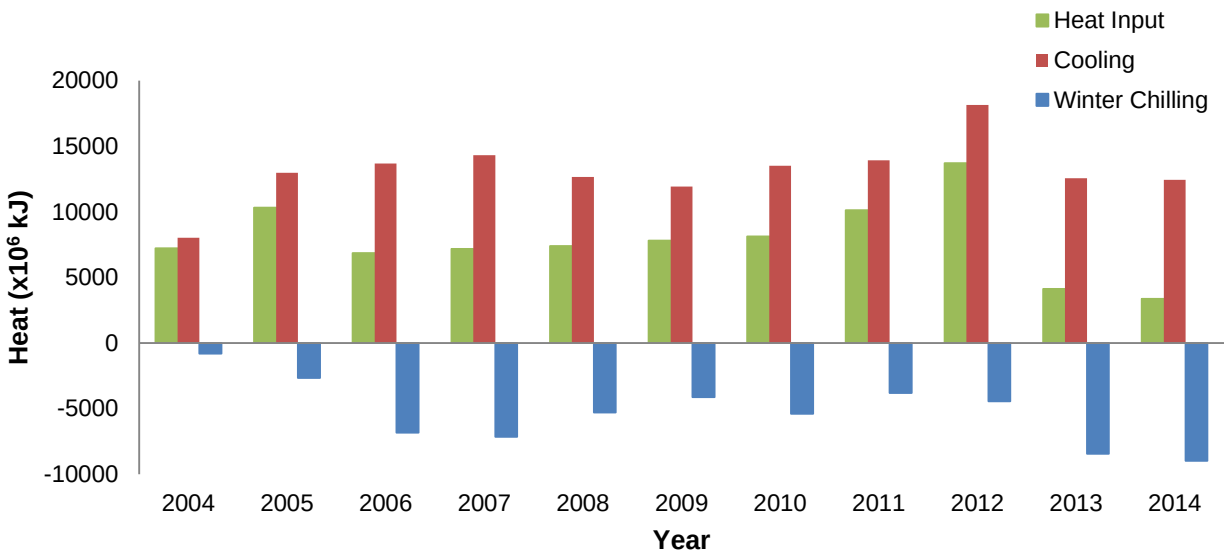

Figure 2.16 Calculated annual groundwater heat balance at GS06.

From January 2013 to September 2017, the Upper Carbonate aquifer beneath GS07 received more heat from cooling than released it (Figure 2.17). In 2014, GS07 injected 9.9×10^9 kJ into the aquifer, heat injection increased to 13.2×10^9 kJ in 2015, then reduced to 10×10^9 kJ in 2016. The heat injection increased again in 2017 to 7.7×10^9 kJ considering that only the data from January to September 2017 were available. In any given year, the highest temperature change occurred in either July or August. Records indicated 5.6°C in July 2013, 2.95°C in August 2014, 3.5°C in July 2015, and 3.1°C in August 2016. From June 2017 to August 2017, temperature change was recorded at 6.0°C, 8.2°C, and 6.6°C; while groundwater temperature injected to aquifer was recorded at 13.2°C, 15.4°C, and 13.8°C. These values were higher than the maximum value set by Manitoba Sustainable Development with temperature change at 5°C and return groundwater temperature at 12°C (Matthews 2003).

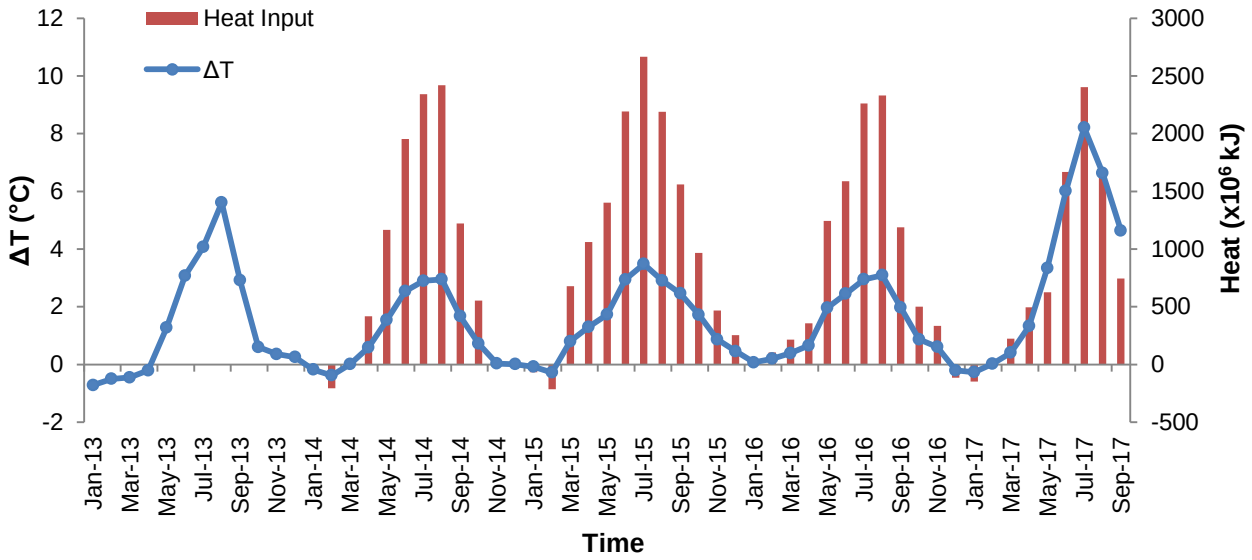

Figure 2.17 Groundwater heat balance at GS07.

Analytical solutions to estimate the thermal breakthrough time and thermal plume size down-gradient of recharge well were performed on 13 geothermal systems (Table 2.1). The ability of analytical solutions on Upper Carbonate aquifer was tested on GS07 which has better data required and numerical analysis result (Chapter 3). However, GS07 is a combined heating and cooling system with multiple wells. Analysis was performed on production well PW-3 and recharge well RW-8 with 1308 m^3/d abstraction rate, and 603 m^3/d injection rate. For effective aquifer thickness in equation 2.9, major fracture zone found in the well was used. Abstraction temperature from the analytical approach produced 0.6% higher than the observed temperature. The analytical approach estimated 559 days for thermal breakthrough time while the numerical analysis recorded 518 days (Figure 2.18 A), an 7.9% relative error. The numerical analysis produced 236 m distance of 7°C isotherm down-gradient RW-8. The analytical approach produced thermal plume that was 2.1% smaller for 7°C isotherm compared to the result from numerical analysis (Table 2.1). Applying the analytical approach on GS09, GS37 and GS41

produced abstraction temperature with 2.8%, -1.5% and -1.9% relative errors respectively. These three geothermal systems are for industrial cooling.

A

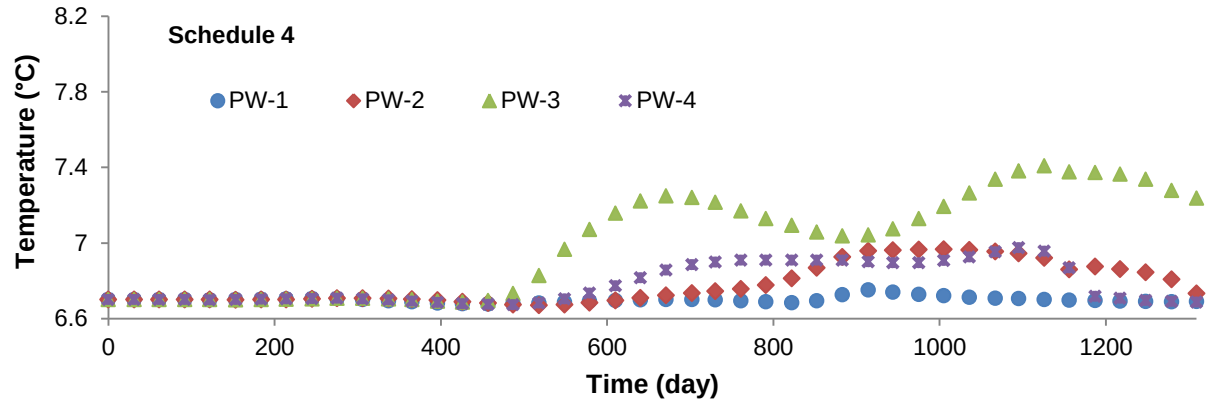

B

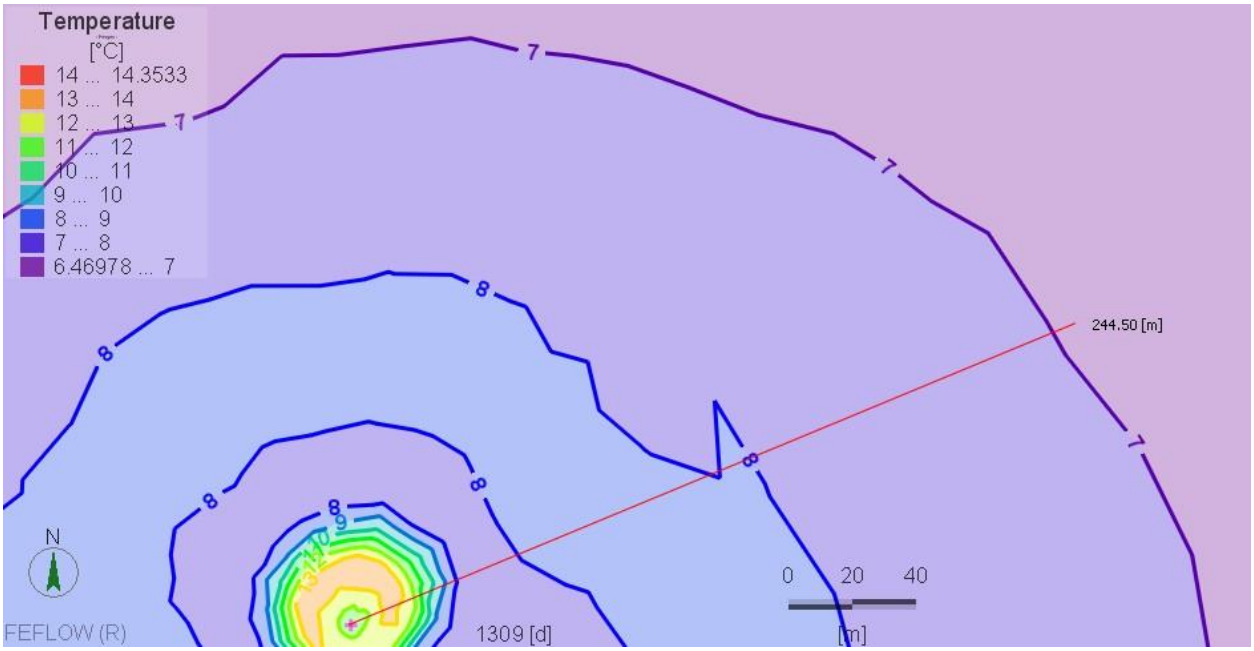

Figure 2.18 Thermal breakthrough time at PW-3 (A); Thermal plume size downstream RW-8 (B).

Table 2.1 Thermal breakthrough time and thermal plume size on natural groundwater flow direction.

Geothermal System		L	b	Q	T	i	t_{the}	t	ΔT_{inj}	T_0	T_{abt}	T_R	v_s	x[(a)]	RE[(b)]
Upstream	Downstream	(m)	(m)	(m^3/d)	(m^2/d)		(d)	(d)	(°C)	(°C)	(°C)	(°C)	(m/d)	(m)	(%)
GS07		287	11	1308	1341.3	0.00305	559	1309	1.72	6.7	7.29	7.25	2.06	231[(c)]	0.6
GS57	GS11	237	8.3	2723	1950	0.00211	235	1825	4	5.6	7.69		1.34	226	
GS11	GS32	131	8.3	1635	2061.6		70	730	1.73	6.3	7.27	7.27	3.85	235	
GS32		66	7.6	337	4073		79	2555	4	6.5	9.21		3.94	730	
GS58	GS55	69	13	655.6	186.3	0.01421	110	730	2	8	9.01		2.04	126	
GS55	GS56	97	24	1452	621**		126	6935	8.1	10	15.68		4.00	1943	
GS09	GS37	527	4.3	8178	1242	0.00191	142	4015	1.75	5	6.17	6	2.15	676	2.8
GS37		198	4.3*	967	231.5	0.01077	375	7665	3.8	5	7.66	7.78	1.84	1050	-1.5
GS41		126	19	1959	771.3	0.01818	124	5840	3.5	8	10.43	10.635	3.20	1333	-1.9
GS34		125	6	280	347.7	-0.002	452	9490	3.05	6.1	8.07		1.14	799	
GS04	GS43	25	24*	32.9	2484		368	730	0.36	8.6	8.75	8.75			
GS20		21	20	130	6.2	-0.13	64								
GS22		23	20*	172.8	67	-0.03	71								

T_R is groundwater temperature at production well or abstraction temperature reported by geothermal system users.

(a) Distance of thermal plume with 1°C temperature difference between calculated temperature and undisturbed groundwater temperature.

(b) Relative errors between estimated abstraction temperature (T_{abt}) and measured temperature.

(c) 7°C isotherm.

* Estimated major fractures thickness using the closest well information.

**Estimated transmissivity using data from Baracos et al. (1983).

2.4 Discussion

Within the City of Winnipeg, five out of eight geothermal systems injected heat between 60 to 80% of the estimated heat into the Upper Carbonate aquifer by extracting up to 100% permissible groundwater quantity. This indicated that the geothermal systems maintain the average temperature difference between EWT and LWT up to 4°C in a year. One of these geothermal systems was utilized for heating and cooling that operated with average temperature difference per year ranging from 1°C to 3.4°C. This indicated that the geothermal system mostly provided cooling than heating. Heat rejected by geothermal system creates thermal plume surrounding recharge wells causing an increase of groundwater temperature in its production well and in the neighbourhood area.

Travel time of heat from wastewater depends on the spacing between production and recharge wells, as well as the abstraction rate, transmissivity of the aquifer, and natural gradient of groundwater level at production well and recharge well (Lippmann and Tsang 1980; Clyde and Madabhushi 1983; Banks 2009). As common problem in urban area, geothermal systems within the City of Winnipeg have limited space. Majority of geothermal systems within the City of Winnipeg require peak pumping rate up to 0.05 m^3/s with distances between production and recharge well less than 200 m (Figure 2.19). Four geothermal systems separated their recharge wells less than 30 m from production wells: 25 m at GS04, 21 m at GS20, 24 m at GS21, and 23 m at GS22. These geothermal systems require peak pumping rate between 0.0008 to 0.0038 m^3/s. Based on thermal breakthrough time estimation (Table 2.1), temperature increase occurred at the production wells of GS20 and GS22 within the first three months of their operation. At GS04, thermal breakthrough occurred after a year of operation due to its low injection rate. The system started its operation in summer 2012 and the history recorded background temperature between 7

to 8.5°C (Ferguson and Woodbury 2004, 2007). This estimation is in agreement with the 2014 temperature record reported by the user which indicated varied temperature between 8.26 to 9.53°C from January to December with peak temperature in August. At GS21, although the distance between production well and recharge well is only 24 m, very little interference of heat from wastewater is expected because of elevation difference between abstraction and re-injection. At this location the casing of recharge well was extended to the depth where the open hole portion of production well was ended to create vertical separation (Sinclair 2007).

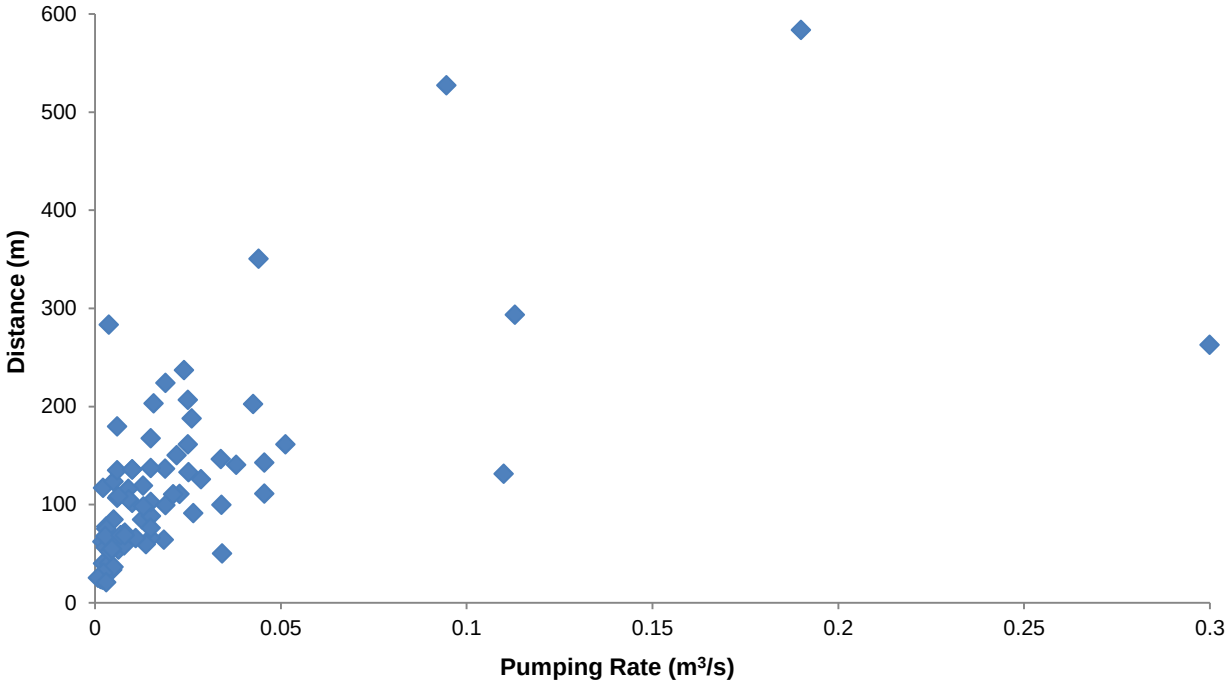

Figure 2.19 Distance between production well and recharge well.

Thermal plume size indicates how far the heat of wastewater travelled which can be identified by the increase of groundwater temperature at SD monitoring wells. Area A (Fig. 2.3) shows the concentration of geothermal systems on the western part of Winnipeg, where the majority operates for cooling purposes (Figure 2.4). In this area, maximum peak rates of groundwater extraction will occur during the summer season (Figure 2.6). Within this area,

GS01, GS19 and GS51 are permitted to divert groundwater up to 923 dam^3, 756 dam^3 and 1195 dam^3 respectively (Figure 2.5). GS51 run for cooling during spring to fall season, while GS01 and GS19 run for cooling on all seasons. From these three geothermal systems, the estimated heat injection annually is $60x10^9$ kJ, while the heat extraction during winter season from the neighbourhood geothermal systems is $6x10^9$ kJ. The injected wastewater will increase the groundwater temperature in this particular area especially in the summer season. There are three Manitoba Sustainable Development observation wells that monitor groundwater temperature in this area: one well is located on the north of GS14 (G05MJ087), one well is within GS02 property (G05MJ045), and one well is on north of GS63, GS19 and GS02 (G05MJ037).

In 2014, the average groundwater temperature at SD observation well G05MJ037 was 6.4°C. At SD observation well G05MJ087, the average groundwater temperature was 8.55°C which was within the temperature reported in 2002 and 2007 between 8 to 9°C (Ferguson and Woodbury 2004, 2007). While groundwater temperature measurement at observation well G05MJ045 indicated that the groundwater temperature was higher than the maximum temperature set by Manitoba Sustainable Development. Unlike the monitoring well across GS14, the groundwater temperature fluctuated, with higher degree during the summer season and lower degree during the winter season. This occurred because GS02 installed a well water equipment cooling system. In winter, GS02 pumped groundwater and ran the water through a heat exchanger to transfer heat to outside air, therefore lowering wastewater temperature prior injecting the water back into the aquifer. The record indicated groundwater temperature 5.5°C when GS02 started its geothermal system in 1977. Groundwater temperature increased to 8.9°C in 1985. Since GS02 was modified to include a well water cooling system, groundwater temperature dropped to 8.3°C. Despite this effort, as shown in Figure 2.13, the groundwater

temperature increased to above 13°C. This measurement was supported by GS01 groundwater use record in 2014 which stated groundwater temperature ranging from 10.5 to 11.8°C. There are 2 other buildings near by GS02 that inject massive heat into aquifer per year, GS01 and GS19 (Figure 2.14). Both buildings run their geothermal system all year for cooling purpose. The geothermal wastewater from these buildings also contributed to the increase of groundwater temperature in the area.

In southwestern Winnipeg, GS07 ran mostly for space cooling since its operation in 2012. The system ran for space heating only in December to February depending on the building load demands. Low temperature change during these months indicated that the system also ran to deliver cooling during winter. This was supported by temperature change record in December 2015 and January 2016 which indicated positive temperature change (Figure 2.17). Although the geothermal system was designed for cooling and heating, the design of building envelope and occupants affect the building heating and cooling demand when the building is in operation. Because GS07 is a newer building, the building was designed with high rating insulation. The store also accommodates many people who will generate heat in the building from their body; therefore lowering heating demand for the building. GS07 has been injecting heat into Upper Carbonate aquifer since 2013 with very little heat extraction for balancing. The Upper Carbonate aquifer beneath GS07 received heat input from thermal wastewater at an average of $10x10^9$ kJ per year since the system started which lead to groundwater temperature increased at production well from 6.7°C in January 2013 to 7.25°C in September 2017. The rapid temperature increase in 2017 could be attributed to the high volume of groundwater extraction for cooling from the previous years (Figure 2.12). The numerical modelling indicated the high groundwater

temperature occurred only on one production well (PW-3) while the other three production temperature increased up to 0.3°C (Chapter 3).

About 3 km east of GS07, observation well G05OC053 (Figure 2.13) recorded average temperature increase from below 7.02°C in 2012 to 7.2°C in 2017 with maximum temperature reached 7.3°C in July 2017. This observation well is located about 340 m north of GS41. Report of groundwater temperature at GS41 production well in 2014 indicated 10.6°C. The geothermal system has been providing industrial cooling since 1994. Groundwater temperature at production well in 1998 was reported between 8 to 9°C, and in 2000 the temperature increased between 10 to 11°C (Wiecek 2001a). Regional groundwater temperature in this area was historically between 7 to 8°C (Wiecek 2001a; Ferguson and Woodbury 2004). In 2001, the system was modified to include additional recharge well, alternate injection of wastewater between two recharge wells, and winter chilling system. Since the modification, temperature at G05OC053 was measured about 6.7°C (Ferguson and Woodbury 2007). Thermal breakthrough time for this geothermal system was estimated at 124 days. In 2014, the thermal plume was estimated at more than 1300 m downstream of its recharge well (Table 2.1).

There were no SD observation wells that recorded groundwater temperature on the east and northeast of the City of Winnipeg (Figure 2.13). Geothermal systems on this side of the city recorded temperature increases in their production wells. Temperature at production well of GS55 reached 15.9°C in December 2018 (Personal communication with Maintenance Manager of GS55 on January 2, 2019), an increase of almost 6°C from temperature recorded in 1988. The system was operated for industrial cooling with the estimated heat injection of $11x10^9$ kJ per year. The thermal front of 1°C temperature difference was estimated at almost 2 km downstream its recharge well in 2007. Downstream of GS55 is GS56 that runs for heating and cooling

(Figure 2.3 and 2.4). Driller's report for GS56, indicated groundwater temperature measurement in August 2006 was 5.6°C. However, the consultant report indicated the temperature at production well in 2007 was 8.8°C (Miller January 10, 2008). Considering the distance between the geothermal systems is about 1.5 km, the temperature increase was likely caused by the continuous pumping that extracted groundwater influenced by the thermal plume from GS55 recharge well.

On the east of GS56, GS43 provides industrial cooling for plastic and composite manufacturing since 1998 (Figure 2.3). Consulting report indicated a history of temperature increased in this location from 7.2°C in 1998 to 12.7°C in 2003 and 14°C in 2009 (Oleksiuk 2009). Hydraulic analysis indicated groundwater recirculation from recharge well to production well due to the groundwater flow direction or gradient change. When the system was started the groundwater flow was from east toward the city centre, high groundwater extraction by GS11 (Oleksiuk 2009; Bell 2009) and GS32 causing the groundwater flow towards the east (Figure 2.2). Since then the function of wells were exchanged. However, average groundwater temperature in 2013 and 2014 were recorded at 11.2 and 11.4°C. During these years, GS43 injected heat at $9.6x10^9$ and $8.3x10^9$ kJ respectively.

Close to east perimeter of the city, four geothermal systems indicated groundwater temperature increase in their production wells: GS11, GS57, GS37, and GS09 (Figure 2.13 and 2.2). GS11 reported supply water temperature in December 2013 and December 2014 at 7.05 and 7.85°C respectively, with average temperature for 2014 was 7.2°C. Groundwater temperature measured in December 2011 was 6.3°C (Burns and Sinclair 2012a). The geothermal system consists of two separate systems, the east system caters the east end of the building and the west system caters the west side of the building. The east geothermal wells consist of one production

and one recharge wells, with recharge well is located about 130 m northeast of east production well. The west geothermal wells consist of one production and two recharge wells, with recharge wells are located about 75 m north and 75 m northwest of west production well. The system runs from mid-May to September every year. Besides the geothermal wells, the building also has one well on each side of the building that is being used to extract groundwater for 365 days a year for processing which is 100% consumptive (Burns and Sinclair 2012a). The estimated peak flow of groundwater extraction for cooling was 5642 m^3/d for 4.5 months (135 days) and for processing was 2268 m^3/d for 365 days (Burns and Sinclair 2012a). Therefore, the estimated groundwater extraction for cooling was 762 dam^3 per year and for processing was 828 dam^3 per year. Assuming 5°C temperature difference between LWT and EWT, the geothermal system injects an estimated heat at $16.5x10^9$ kJ into the aquifer. Although the building extracted more groundwater for processing (heat), since it was consumptive use and the groundwater was not returned back into the aquifer, there was no cooler groundwater injected into the aquifer. The heat injected in summer was expected to dissipate through the extraction for processing outside the cooling season (Burns and Sinclair 2012a). Thermal breakthrough time for the west system was estimated at 70 days. Therefore, the increase of groundwater temperature at the production well in December when the wastewater was not injected back into the aquifer indicated that thermal wastewater from injection during cooling season already reached the production well.

Up-gradient of GS11 is GS57 which utilized geothermal system for heating and cooling of an office building and cooling for hatchery processing facility (Bell and Friesen 2008a). The estimated groundwater extraction for cooling was 994 dam^3 per year. There was no information about the groundwater quantity or rate for the heating season. Using 4°C temperature difference, the estimated thermal breakthrough time was 235 days and thermal plume size was less than 230

m after 5 years of operation ending in 2014. The distance between recharge well of GS57 and production well of GS11 is about 900 m, therefore it was unlikely that the temperature increase in GS11 production well was influenced by wastewater from GS11.

GS37 and GS09 are located north of GS11 with GS09 is located up-gradient of GS37 (Figure 2.13 and 2.2). GS09 provides industrial cooling for recycling facility by extracting and injecting groundwater up to 2985 dam^3 per year. The groundwater temperature at production well was 5°C in 2000 (Wiecek 2001b) and 6°C in 2011. The system was not extracting groundwater from 2012 to 2014. The estimated thermal breakthrough time was 142 days. The calculation also produced the estimated abstraction temperature 2.8% higher than the reported temperature. After 11 years of operation, 1°C thermal front reached 632 m downstream of GS09 recharge well.

GS37 provides industrial cooling for plastic manufacturing facility by extracting and injecting groundwater up to 353 dam^3 per year. Because there was no information about the depth of the major fracture in this location, information from GS09 was applied. The estimated thermal breakthrough for this system was 375 days. Using the average temperature difference recorded by the user, the estimated abstraction temperature in 2014 was 7.66°C which was 1.5% less than the observed temperature.

2.5 Conclusion

Seven maps of geothermal energy systems that are being utilized within the City of Winnipeg were developed to provide information and resources on the current usage and impacts of the geothermal systems. As of 2015, 87 open loop geothermal systems were registered within the City of Winnipeg and surrounding areas, 48 systems for cooling purposes and 39 systems for heating and cooling purposes. The permissible quantity of groundwater diverted for geothermal

energy was 32,650 dam^3 annually. The maximum pumping rates of groundwater that can be diverted from the aquifer were varied from 0.0008 m^3/s to 0.3 m^3/s. The casing depth of production wells were between 9.75 to 46 m from the ground surface, with open hole depths were between 24 to 160 m depth. The production wells and recharge wells were separated between 24 to 580 m. The systems were estimated to reject more than $470x10^9$ kJ heat into the aquifer and extract about $116x10^9$ kJ heat from the aquifer. The available data indicated that the geothermal systems rejected up to 80% of the estimated heat into the aquifer with groundwater extractions reached 100% of the permissible quantity. Therefore, the geothermal systems injected groundwater into the aquifer with the average temperature difference below 4°C. Injection groundwater with a positive average of temperature difference in a year increased groundwater temperature surrounding the geothermal systems. Most cases came from geothermal system for industrial cooling system and combined heating and cooling system that ran mostly for cooling.

The impact of wastewater injection on the aquifer surrounding geothermal system can be estimated using equation 2.5, 2.6, 2.8, and 2.9. Good results were obtained by applying the thickness of main water bearing fractures as the effective thickness of the aquifer. The analytical approach was able to estimate the abstraction temperatures with less than 3% relative error. Thermal plume estimation was able to identify the influence of thermal wastewater from a recharge well to the neighbour's production well. Due to the limited data available, further investigation should be performed to define the suitable analytical approach for Upper Carbonate aquifer.

Some implementations have been performed to prevent the increase of groundwater temperature such as designing newer geothermal systems as combined heating and cooling, limit

re-injection wastewater temperature between 1.5 to 12°C, limit temperature difference between abstraction and re-injection temperature to 5°C, and adding winter chilling system on the existing systems. This study showed that despite its purpose to balance heat injection during cooling season, combined heating and cooling geothermal system is still injecting more heat than extracting it because the geothermal system runs for cooling longer than heating. Although Manitoba Sustainable Development specifies the groundwater temperature management in every license issued, many users re-inject groundwater with temperature higher than 12°C or apply temperature difference more than 5°C. Many users also do not record the groundwater quantity and temperature at production well and recharge well as required, causing the monitoring more difficult. Installing a winter chilling system proves to be successful in preventing temperature increase although the system also facing limitation such as its ability to balance the heat injection due to warm winter.

Preventing the increase of groundwater temperature should be included in early stage of design to assess the sustainability of the geothermal system and its impact on the neighbour geothermal system. The activities may include: adding a winter chilling system for industrial cooling system or combined heating and cooling system that runs for cooling longer than for heating, injecting the wastewater into different elevation than the open hole depth of the production well, recording the location of major fractures in the Upper Carbonate aquifer that produce water, and performing analytical approaches to predict abstraction temperature in the production well and how far the thermal wastewater will travel downstream.

3 Modelling the effect of Open Loop Geothermal System with Multiple Wells on Upper Carbonate Aquifer

Abstract

Demand on groundwater as a source of energy has increased in recent years. The Upper Carbonate aquifer beneath the City of Winnipeg is heavily utilized for cooling and heating system causing a groundwater temperature increase in several geothermal system locations. A modeling study was conducted to investigate the impact of an open loop geothermal system with multiple wells on groundwater temperature within the Upper Carbonate aquifer beneath the City of Winnipeg, Manitoba, Canada. A 3D numerical model of the Upper Carbonate aquifer in the southwestern area of Winnipeg was developed and calibrated using the flow and heat transport code FEFLOW. Three steps of calibration were performed: a steady state fluid flow to determined initial hydraulic heads, transient fluid flow to determined hydraulic conductivities and specific storage of the Upper Carbonate aquifer, and heat transport simulation to identified thermal properties of the Upper Carbonate aquifer. Five schedules were created to find the extraction rate distribution on each production well that represent the actual distribution. The best option to deliver low entering water temperature (EWT) is by extracting the groundwater quantity required in a month from PW-1, PW-2, PW-3 and PW-4 with a distribution of 50%, 11%, 17%, and 22% respectively. Transient calibration involved adjusting thermal properties of carbonate bedrock and the extraction rate distribution on four production wells. Model performance was evaluated by comparing the simulated EWT with the observed EWT collected from the geothermal system. A period of 30 years was simulated under three difference scenarios based on the operating history of the geothermal system. Long term simulation showed that higher groundwater flow increases the thermal plume size, while high temperature creates a

higher temperature zone within the thermal plume. The model predicted groundwater temperature increase at the production well from 6.7°C to 9°C. The wastewater injection will create a thermal plume with the 7°C isotherm reaching 1,500 m downstream of the production well. Therefore, maintaining the injection temperature and the temperature difference between the leaving water temperature (LWT) and the EWT within the regulated values are important for the sustainability of the geothermal system and the groundwater environment.

3.1 Introduction

Demand on groundwater as a source of energy has increased in recent years. The Upper Carbonate aquifer beneath the City of Winnipeg is heavily utilized for cooling and heating system. A Groundwater Heat Pump (GWHP) is an open loop geothermal system that uses groundwater as the source or sink of energy. The system extracts groundwater from an aquifer; directs it to a heat exchanger and injects the wastewater back into the aquifer or directs it to a river or a sewer system. Compared to other heat pumps, the system offers greater energy efficiency and energy saving, also lower initial and operating costs (Milenić et al. 2010; Mustafa Omer 2008; Self et al. 2013). The optimum performance of an open loop geothermal system depends on hydraulics and thermal properties of the aquifer (Nam and Ooka 2010; Casasso and Sethi 2015; Park et al. 2015). Injection of thermal wastewater into the aquifer creates a warm or cool thermal plume which become a pollutant for downstream geothermal users, and exposes the system to thermal feedback (Banks 2009) causing a groundwater temperature increase in the production well. Within the City of Winnipeg, groundwater temperature increases have been reported occurring in several geothermal locations, reaching to 16°C from its ambient temperature around 6°C (Ferguson and Woodbury 2006). Groundwater temperature increase

makes the current practice unsustainable and planning to prevent the increase in temperature should be included in early development (Ferguson 2004) by performing risk assessment as proposed by (Banks 2009): assessment of distance between production and recharge well, analytical modelling of heat migration and numerical modelling.

Numerical model programs for groundwater can be used to support planning during early stage development of a geothermal energy system. A simulation of groundwater extraction and injection for certain number of years can be performed to study the impact of the system on the groundwater. Hecht-Méndez et al. (2010) compiled a review on the available programs for heat transport in porous and fractured media. However the accuracy of transport simulation depends on the reliability of subsoil data that often is scarce.

Installation of an open loop geothermal system influences the thermal budget of groundwater particularly in the aquifer beneath an urban area. Numerical models have been used to study the impact of open loop geothermal systems in urban areas. A study of cumulative impact of open loop geothermal systems in central London, UK, on the groundwater temperature of a Chalk aquifer resulted in thermal interference between geothermal systems especially in the area that utilized more geothermal systems. This condition affected the efficiency of the geothermal system in generating the energy required (Herbert et al. 2013). A study to investigate open loop geothermal system as an alternative technology for a district heating network in urban area of Turin, Italy, indicated that groundwater heat pump installations for densely populated areas will cause subsurface thermal degradation which will affect the performances of surrounding installations (Verda et al. 2012). The efficiency of a geothermal system also can be affected by thermal breakthrough at the production well. A study of thermal impact on an up-gradient production well was performed on a large scale geothermal heating and cooling system

in southeastern Washington State. The result indicated that thermal breakthrough at the production well occurred when the system was run with a higher pumping rate. Therefore, running a geothermal system under low pumping rates not only lowering operating cost but also preventing thermal breakthrough at the production well (Freedman et al. 2012). Ferguson and Woodbury (2006) developed a numerical model to study the efficiency of an individual geothermal system and the effect of neighbouring geothermal systems on each other. The analysis was performed on four adjacent buildings that require large groundwater use, in the western area of Winnipeg. The result showed interference effects among three geothermal systems due to spacing between geothermal systems which indicated the limit of geothermal systems that can be utilized in the area. (Ferguson 2004) developed a generic model for the Upper Carbonate aquifer that also can be used to determine the areal extent of thermal anomalies caused by thermal wastewater injection. He examined the situation for geothermal systems consisting of one production well and one recharge well which is known as a doublet. He concluded that spacing of the wells and their pumping rates have a greater effect than material properties in a homogeneous aquifer. He also stated the necessity to conduct analysis based on a site specific case.

An open loop geothermal system can have multiple production wells and recharge wells. The objectives of this study were to develop a numerical model of the Upper Carbonate aquifer in the southwestern area of Winnipeg, and to determine the impact of a geothermal system with multiple wells on groundwater temperature.

3.2 Methods

3.2.1 **Study Site**

The geothermal system is located in Tuxedo business area, in Winnipeg, Manitoba, Canada (Figure 3.1).

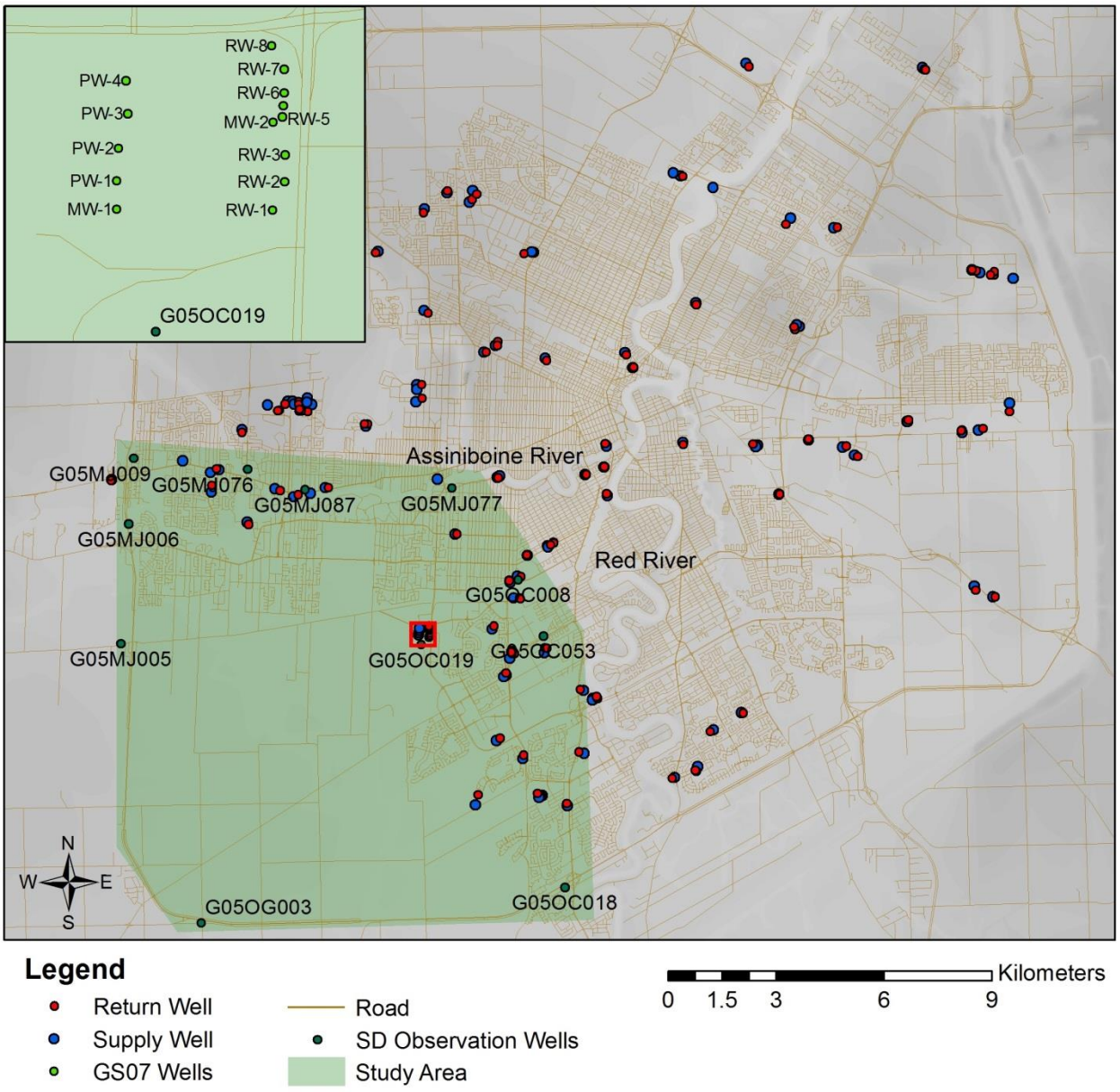

Figure 3.1 Study Area in the southwestern of Winnipeg showing the active pumping wells within the City of Winnipeg, the observation wells operated by Manitoba Sustainable Development and GS07 wells (insert).

The geothermal system was designed to generate heating and cooling for a 37,000 m^2 retailer store which opened its door for customers on November 28, 2012. The property is framed by the Assiniboine River on the north and the Red River on the east. In the provincial water well database, there are eleven observation wells that are situated within the study area. One observation well G05OC019 is located approximately 300 m from the property.

3.2.1.1 Geology and hydrogeology

Stratigraphy of the Winnipeg area consists of the surficial deposits and the carbonate bedrock (Baracos et al. 1983). The surficial deposits consist of three units: upper complex zone, glaciolacustrine silty clays, and tills. The upper complex zone thickness reaches 4.5 m in thickness. This unit consists of stratified silty clay and silt, varying amount of organic soils, man-made fill and alluvial silts and sands. Under the upper complex zone lies glaciolacustrine silty clay with thickness ranging from zero to 21 m. The upper part of this unit is weathered to a brown or mottled grey-brown colour, highly plastic with laminate structure and stiff consistency. The lower part of the unit is grey, medium to highly plastic and firm to stiff consistency. The upper part of glaciolacustrine silty clay is highly fissured which decreases in frequency in accordance with the depth. An intergranular hydraulic conductivity is in the order of $8.6x10^{-7}$ to $8.6x10^{-9}$ m/d (Baracos 1957; Mishtak 1964). The horizontal permeability of the clay is twice of the vertical. Till underlies the clay unit with thickness ranging from zero to 9 m. The upper section of the till is loose, soft and water bearing while the lower section is dense to very dense. The bottom part of the tills is highly cemented by calcium carbonate. The hairline joints in the cemented tills are the source of its permeability. Average hydraulic conductivity for the till is $2.6x10^{-3}$ m/d (Baracos et al. 1983).

The carbonate rock under the Winnipeg area is characterized by Paleozoic carbonate formations with thickness ranging from 76 to 230 m. The Upper Carbonate aquifer is the major aquifer overlaying the Winnipeg area that is located in the top 15 to 30 m of the dolomitic limestone and dolomite. The aquifer permeability is characterized by a network of fracture openings, joints and bedding planes. The joint blocks size from 0.3 to 3 m with joint openings size ranging from hairline fractures to more than 0.3 m wide; and the height of bedding planes openings usually no more than 2.5 cm. Maximum width of fractures openings occur at the bedrock surface and decreases in size in accordance with depth. The aquifer is semi confined by the glacial deposits on top and the slightly pervious carbonate rock below. The transmissivity ranges from 25 to 2500 m^2/d and the storage coefficient varies from $1x10^{-6}$ to $1x10^{-3}$ (Baracos et al. 1983).

Between depths of 60 to 90 m, the carbonate bedrock is impermeable. The Middle Carbonate aquifer has been found in western Winnipeg at 90 m depth from bedrock surface. The transmissivity is lower than the Upper Carbonate aquifer ranging from 250 to 1,250 m^2/d and storage coefficient in the range of $1x10^{-5}$ to $1x10^{-4}$. The Lower Carbonate aquifer is located at the bottom 15 m of carbonate bedrock. The transmissivity for lower carbonate aquifer is estimated at less than 62 m^2/d (Baracos et al. 1983).

The Upper Carbonate aquifer receives most of its recharge from thin till layer in the Interlake area, through coarse-grained tills and glaciofluvial sediments east of Winnipeg and through the Birds Hill glaciofluvial complex northeast of Winnipeg (Render 1970). When precipitation occurs, some of the water reaches the Upper Carbonate aquifer through fractures of clay and till layer that acts as a semi-confining layer (Ferguson 2004; Day 1978; Pach 1994).

Groundwater flow beneath Winnipeg is from East, Northwest and Southwest (Figure 3.2). Its flow is radial towards the city centre with varied water level due to the pumping (Render 2010).

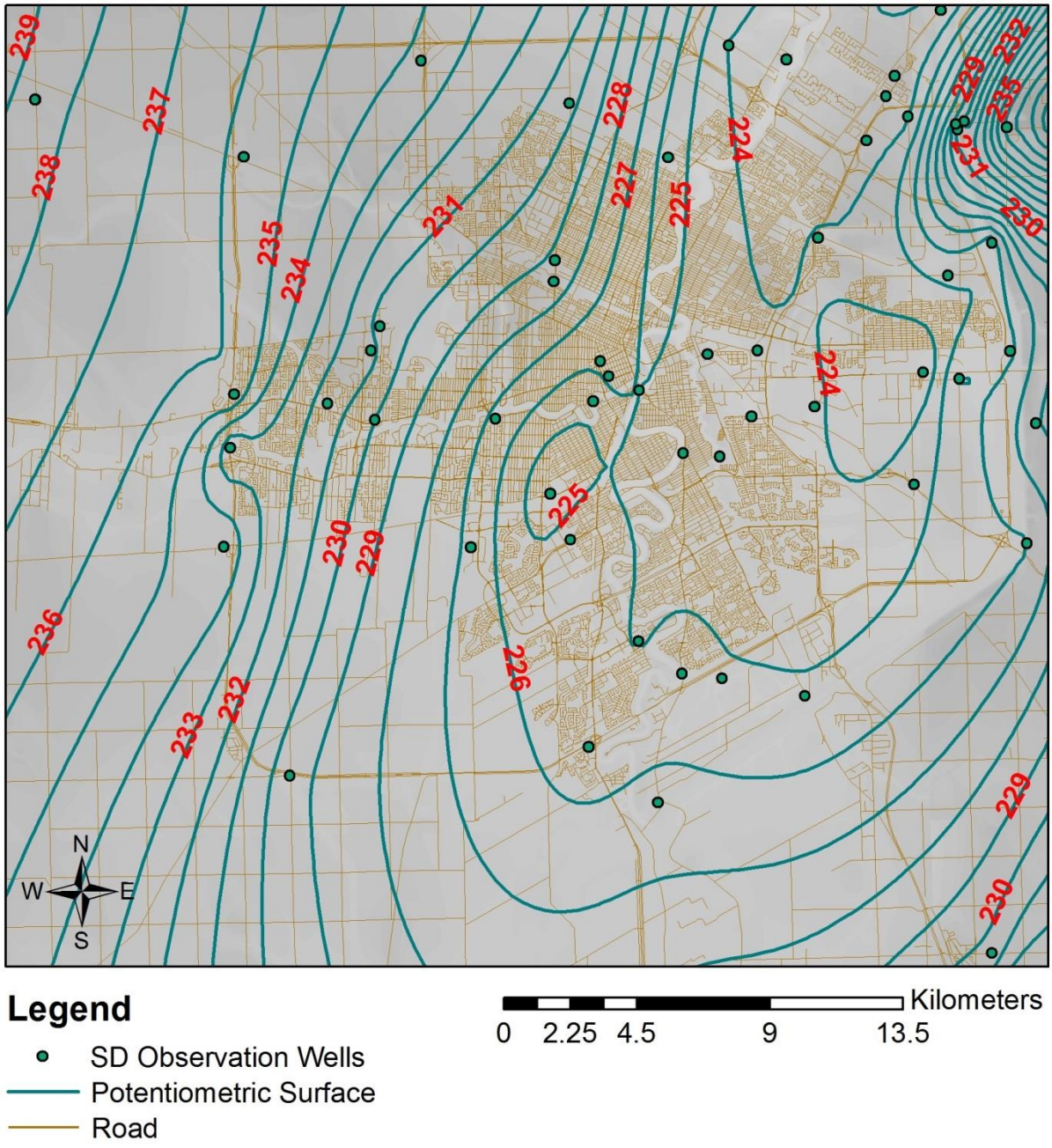

Figure 3.2 Potentiometric surface on May 11, 2012

3.2.1.2 Aquifer Testing

The geothermal system wells were installed between April 2012 and May 2012. The driller's report for the extraction wells recorded the stratigraphy beneath the study area which was clay between 0 to 15 m depth below ground surface, till between 15 to 22 m depth from ground surface and limestone at the depth between 21 to 52 m below ground surface. In this study area, the upper 15 m of bedrock contains limited water and majority of groundwater was encountered in fractures between 36.3 m and 47.3 m below ground surface (Burns and Sinclair 2012b).

Table 3.1 Location of wells, depth of well casing and depth of well hole (UTM Zone 14N)

Wells	Location (UTM Coordinates)		Casing Diameter (mm)	Casing Depth (m)	Total Depth (m)
	Easting (m)	Northing (m)			
System Supply Wells					
PW-1	628,432.00	5,522,266.20	243	30.02	51.81
PW-2	628,435.40	5,522,326.70	194	32.92	51.81
PW-3	628,451.70	5,522,390.90	194	32	51.81
PW-4	628,448.50	5,522,452.00	243	31.39	51.81
System Recharge Wells					
RW-1	628,720.50	5,522,212.60	146	21.03	51.81
RW-2	628,742.40	5,522,264.40	146	21.64	52.73
RW-3	628,743.30	5,522,314.70	146	21.03	51.81
RW-4	628,738.30	5,522,385.50	146	21.49	51.81
RW-5	628,740.20	5,522,405.50	146	21.79	51.81
RW-6	628,741.60	5,522,428.80	146	22.1	51.81
RW-7	628,742.00	5,522,472.90	146	20.73	51.81
RW-8	628,719.20	5,522,516.00	146	21.03	48.77
System Monitoring Wells					
MW-1	628,431.80	5,522,214.20	128	22.29	53.33
MW-2	628,721.40	5,522,375.30	128	21	60.96

Measurements of static water levels were performed at MW-1, PW-1, PW-3, RW-1, RW-4, RW-5, RW-6, RW-8, and G05OC019. The depths of water levels were measured from top of casing. The only information regarding top of casing was at production well PW-1 with height

between 0.58 to 0.77 m above ground surface. A four-hour pumping test was performed at production well PW-1. Transducers were installed on MW-1, PW-1, PW-3, RW-1, RW-8, and G05OC019 for hydraulic heads measurement. The first three hours of the test were performed with discharge ranging from 4,007 to 4,764 m^3/d. After three hours, pumping rate was reduced to 3,641 m^3/d for 40 minutes and then to 2,344 m^3/d to complete the four-hour pumping test. The hydraulic heads recorded during these three hours were used to calculate the transmissivity and storativity of the aquifer using graphical analytical. The transmissivity for the carbonate aquifer on this site was estimated at 1,339.2 m^2/d and the storavity was estimated at 0.00046. The estimated transmissivity was higher than the value for this area reported by (Baracos et al. 1983). The groundwater had very poor quality and was brackish. Water analysis indicated that the groundwater is corrosive and contains 5,380 mg/L total dissolved solid.

3.2.1.3 Geothermal System

The geothermal system is 100% non-consumptive, all the water is recharged back into the aquifer. Therefore, no hydraulic effect is expected on the groundwater. Although the water license requires the system to be set for maximum temperature rise and drop at 5°C, the pump was set to maintain 3°C temperature difference (Sinclair 2015). The system recharges warm water to the aquifer during summer months and cold water during winter months.

The system was designed to deliver a peak flow of 9,812 m^3/d during peak demand periods for cooling and heating. During peak demand periods, the peak flow at PW-1, PW-2, PW-3 and PW-4 are 4,906 m^3/d, 1,090 m^3/d, 1,635 m^3/d, and 2,180 m^3/d respectively. The system was expected to operate at pumping rates between 2,725 m^3/d to 7,631 m^3/d, during normal heating and cooling periods; and under 2,725 m^3/d during shoulder seasons. The information collected from the geothermal system in March 2015 indicated that the system delivered peak flow of

9,936 m^3/d at 32°C air temperature in summer, 5,616 m^3/d at -37°C in winter and the breakeven temperature was -15°C at flow rate of 1,728 m^3/d when no heating or cooling was required (Sinclair 2015).

The automated system utilizes PW-1 at all times with an operational range between 2,453 m^3/d and 4,906 m^3/d. Under the automated system, PW-1 always runs first followed by PW-2, PW-3 and PW-4 in sequence, as required to meet the heating and cooling demands. This system can be overridden manually allowing each pump to be operated individually or in combination.

The recharge well network consists of two branches; the first branch is three wells on the south, RW-1, RW-2 and RW-3 (Figure 3.1). The second branch is five wells on the north, RW-4, RW-5, RW-6, RW-7, and RW-8 (Figure 3.1). Each individual well can be turned off by closing the gate valve at the well, or closing the branch valve to close the entire branch. Closing the gate valve(s) is necessary to prevent the recharge wells system from running under vacuum due to low flow condition.

3.2.2 **Data**

The geothermal system recorded the groundwater quantity extracted from and injected back into aquifer from February 2014 to September 2017, as well as the groundwater temperature entering geothermal system (EWT) and temperature leaving the geothermal system (LWT) from January 2013 to September 2017 (Figure 2.12). For the analysis, data from March 2014 to September 2017 were used (Figure 3.3). Ground surface temperature was not available for study site, for modelling purpose monthly average soil temperature at the depth of 50 cm from the surface measured at Highway 59 was adopted. Soil temperature data recorded from March 2008 to February 2009 were used.

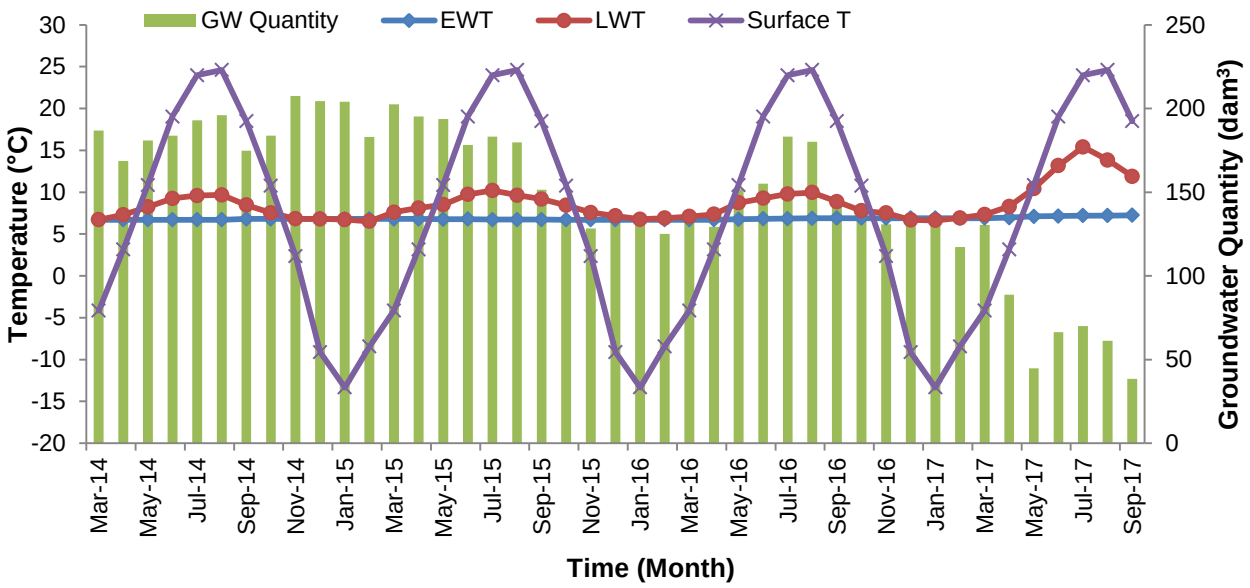

Figure 3.3 Flow and temperature data

3.2.3 **Model Development**

Analysis was performed using FEFLOW 7.0 (Diersch 2017). FEFLOW was chosen for its ability to couple groundwater flow and heat transport simulation for large numbers of production and recharge wells that required fine discretization (Herbert et al. 2013); as well as its ability to incorporate spatially variable aquifer properties, geologic layering, and screening of production well and recharge well over multiple intervals (Bridger and Allen 2014).

The model was run in steady state mode for static water level calibration and in transient mode for pumping test calibration and heat transport. Surface elevation, model boundary and wells locations were developed using ArcGIS 10.4.1 (Inc. 1999-2016). Surface elevation was obtained by importing digital elevation models of Southern Manitoba from Earth Explorer (Survey 2014) to ArcGIS (Inc. 1999-2016). The Winnipeg road map was added into the map for better identification of the location of pumping wells. The top elevation of carbonate rock was developed using supply well casing depth data (Figure 2.9), provincial observation wells information, and geological maps of Winnipeg (Baracos et al. 1983). The bottom of the aquifer

was developed using supply well depth data (Figure 2.8) and provincial observation wells information.

3.2.3.1 Model domain and boundary conditions

Assuming there was no hydraulic connection due to dense overlay clay, both the Assiniboine River and the Red River were not considered as boundaries for the model. Instead the potentiometric surface measurement on May 11, 2012 (Figure 3.2) was used to define boundary conditions such as constant head boundaries. A model with an area of approximately $16x10^7$ m^2 (Figure 3.1) was created to accommodate the hydraulic head of 236 m asl and 224 m asl in the west and east of the model (Figure 3.2). The model area covered approximately 13,300 m by 13,700 m with the maximum depth of 87 m. Triangular prisms were used to create model mesh consisting 84,980 elements (47,399 nodes) with lateral dimension range from 700 m at the outer boundary to 0.5 m adjacent to the production and supply wells. The model was discretized into ten layers, four top layers for clay and till layer, two layers in the middle for carbonate rock with limited water and four bottom layers for carbonate rock with major water bearing fractures (Figure 3.4 A and B). The thickness of carbonate rock with limited water was determined using the difference between the depth of injection wells casing and supply wells casing (Table 3.1).

Constant hydraulic head boundary conditions were applied over the entire vertical face of the model on upper west, southwest, east and northeast sides. Initially the values were set at 236 m for the upper west boundary, 230 m for the southwest boundary, 225 m for the east boundary and 224 for the northeast boundary (Figure 3.3 C and D). No flow boundaries were applied on lower west, north and south sides of the model. Assuming no recharge from clay and till layer, a no flow boundary condition was applied on the surface of the model. A no flow boundary condition also was applied on the bottom side of the model because groundwater was not found

at the depth deeper than the deepest part of supply wells (Burns and Sinclair 2012b), therefore no influx was expected from below the aquifer.

The constant temperature boundary condition at 6.7°C were applied on upper west, southwest, east and northeast boundaries. Zero flux temperature conditions were applied on the lower west, north and south and bottom boundaries. Initially, zero flux condition was also applied on the surface of the model for groundwater flow calibration purposes. For heat transport simulation, time varying constant temperature boundary condition was applied on the model surface to employ ground surface temperature. Initial temperature 6.7°C was applied on carbonate aquifer layers based on groundwater use recorded on January 2013 (Figure 2.12). The same initial temperature was applied to clay/till layer based on earlier research which indicated mean annual soil temperature between 6 to 7°C measured at 150 cm below surface (Krpan 1982).

Multi-layer well boundary conditions were used on all production and recharge wells. Using the multi-layer well feature, the flow rate on each well was automatically distributed along the length of well screen on each layer based on the material properties on each layer and the distribution of hydraulic head in each slice (Diersch 2017). Injection of warm water or cold water into the aquifer was modeled by applying time varying constant temperature boundary conditions on all layers corresponding with well screens at recharge well locations (Figure 3.5). During simulation, temperatures at the top and bottom of production well were measured to determine groundwater EWT to the heat exchanger.

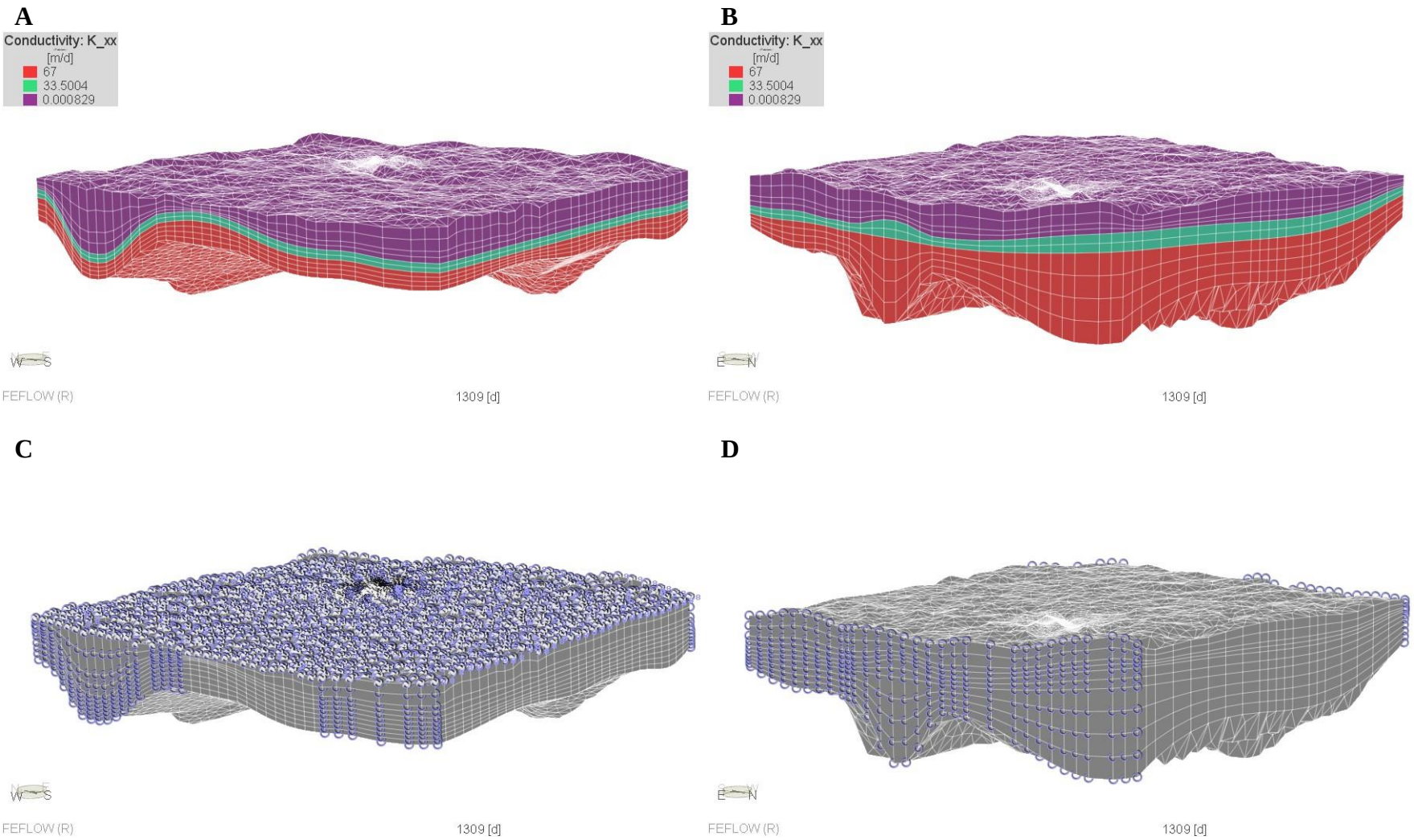

Figure 3.4 Finite-element grid: Model discretization viewed from southwest of the domain (A); Model discretization viewed from northeast of the domain (B); Model boundary conditions viewed from southwest of the domain (C); Model boundary conditions viewed from northeast of the domain (D).

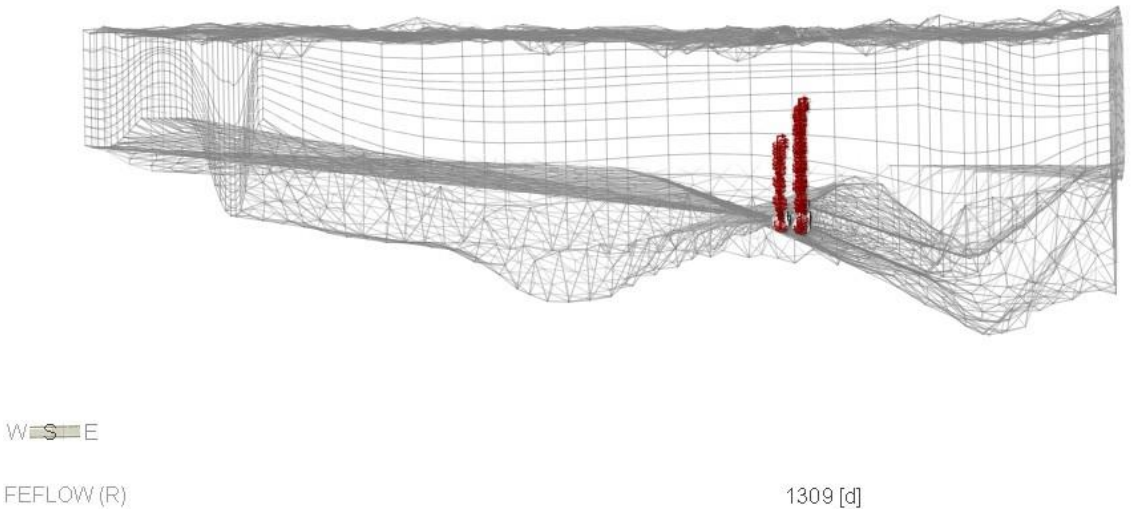

Figure 3.5 Discretization of supply wells (left) and recharge wells (right).

3.2.3.2 Model parameters

Single continuum model was chosen to represent the fractured medium as an equivalent porous medium. In this model, all layers were assumed to be homogeneous and isotropic. Assuming the groundwater flow is aligned with the *x*-axis, transient heat transport in saturated porous medium was solved using heat conservation equation in a two-phase medium, solid and liquid (Diersch 2017; Bruno et al. 2017):

$$\rho c \frac{\partial T}{\partial t} + \rho_w c_w \nu_D \frac{\partial T}{\partial x} = (\lambda + \rho_w c_w \nu_D \alpha_L) \frac{\partial^2 T}{\partial x^2} + (\lambda + \rho_w c_w \nu_D \alpha_T) \left(\frac{\partial^2 T}{\partial y^2} + \frac{\partial^2 T}{\partial z^2}\right) + H \qquad \text{Eq. 3.1}$$

Where H is the heat source/sink (W/m^3), $\rho_w c_w$ is the volumetric heat capacity of liquid phase (J/m^3.°C), ν_D is the Darcy velocity (m/s), λ is the thermal conductivity of porous medium (W/m°C), α_L is the longitudinal dispersivity (m), α_T is the transverse dispersivity (m), ρc is the volumetric heat capacity of porous medium (J/m^3.°C), and T is the temperature (°C).

The first term describes temperature variation over time which depends on the volumetric heat capacity of the porous medium (ρc):

$$\rho c = n_e \rho_w c_w + (1 - n_e)\rho_s c_s \quad \text{Eq. 3.2}$$

Where $\rho_w c_w$ is volumetric heat capacity of fluid (J/m^3.°C) and $\rho_s c_s$ is volumetric heat capacity of solid phase (J/m^3.°C); with ρ_w and ρ_s are density of fluid and solid phase (kg/m^3), while c_w and c_s are heat capacity of fluid and solid phase (J/kg.°C).

The second term of equation 3.1 describes heat transport through advection which is a function of the Darcy velocity (v_D):

$$v_D = -K\frac{\partial h}{\partial x} = -Ki \quad \text{Eq. 3.3}$$

with K as hydraulic conductivity (m/s), h as hydraulic head (m), and i as hydraulic gradient.

The third and fourth terms describe heat transport through conduction which depends on the thermal conductivity of the porous medium (λ):

$$\lambda = (1 - n_e)\lambda_s + n_e \lambda_w \quad \text{Eq. 3.4}$$

where n_e is the effective porosity, λ_s is the thermal conductivity of solid matrix (W/m°C), and λ_w is the thermal conductivity of fluid (W/m°C).

Hydraulic conductivity for clay and till combined layer was calculated using equation below assuming hydraulic conductivities for clay and till were 8.6x10^{-7} m/d and 2.6x10^{-3} m/d respectively.

$$K_c = \frac{1}{m} \times \sum_{i=0}^{n} m_i \times K_{H,i} \quad \text{Eq. 3.5}$$

The estimated hydraulic conductivity for this layer was 8.3x10^{-4} m/d. The top two layers of the Upper Carbonate aquifer represented the top part of aquifer which produced limited water, the estimated hydraulic conductivity for this layer was set to 9 m/d which was in the range of a permeable aquifer. The lower four layers of aquifer were set to 66.9 m/d hydraulic conductivity

that was obtained by dividing the measured transmissivity of 1,339.2 m^2/d with the lower aquifer thickness of 20 m. Specific storage was estimated from the storativity of 0.00046 and the lower aquifer thickness which result in $2.3x10^{-5}$ 1/m.

Thermal conductivity of groundwater was set to 0.58 W/m°C which represented the conductivity of water at 6.85°C (Incorpera et al. 2007). The volumetric heat capacity of groundwater was estimated using groundwater density (ρ_w) 1,004.2 kg/m^3 (Burns and Sinclair 2012b) and water heat capacity (c_w) 4,198 J/kg°C (Incorpera et al. 2007). For clay and till layer, volumetric heat capacity of water was set to $4,184x10^3$ J/m^3 °C.

Thermal conductivity of clay and till layer was set to 1.28 W/m°C (Bejan and Krauss 2003). The volumetric heat capacity of solid for clay and till layer was estimated using clay density of 1,450 kg/m^3 and heat capacity of clay 880 J/kg°C (Bejan and Krauss 2003). Effective porosity for these layers were set to 0.02 (Heath 1983).

Ferguson (2004) conducted research on thermal properties of carbonate bedrock beneath Winnipeg, he estimated soil samples collected at borehole W8 had thermal conductivity range from 0.87 to 3.56 W/m°C with mean value of 2.22 W/m°C, porosity range from 0.03 to 0.17 with mean value of 0.095, dry density range from 2,150 to 2,710 kg/m^3 with mean value 2,520 kg/m^3, saturated density range from 2,460 to 2,740 kg/m^3 with mean value 2,620 kg/m^3, and solid phase density range from 2,730 to 2,850 kg/m^3. Earlier research on heat capacity of limestone bedrock resulted heat capacity range from 830 to 1,200 J/kg°C (Bejan and Krauss 2003; Goranson 1942; Robertson 1988; Schön 1996).

Dispersivities are influential parameters in the propagation of thermal plume (Bruno et al. 2017). However, these parameters are often neglected in groundwater heat exchanger models due to the availability of reliable experimental data (Vandenbohede and Lebbe 2010; Gelhar et al.

1992; Ferguson 2007). Some research ignore it (Ferguson and Woodbury 2005), or use default values provided by the program (Bridger and Allen 2014; Galgaro and Cultrera 2013; Lo Russo et al. 2014), or derive the parameters from regional field studies such as dye tracer test (Epting et al. 2013) and by analytical analysis (Hidalgo et al. 2009). There is no record on heat dispersivities for the Winnipeg area, and therefore FEFLOW default values of 5 m and 0.5 m were adopted as the initial values for longitudinal dispersivity (α_L) and transverse dispersivity (α_T). These values were applied on clay/till layers and carbonate bedrock layers.

After each simulation, temperatures measured at top and bottom of a production well were averaged to represent the groundwater temperature extracted from that particular well. Assuming no heat loss from the production well to the heat exchanger, the average temperaturea at production wells were used to estimate heat exchanger EWT which is the mixing temperature of groundwater extraction from the production well(s):

$$EWT = \frac{\sum_{i=1}^{4} m_i c_i T_i}{\sum_{i=1}^{4} m_i c_i} \quad \text{Eq. 3.6}$$

where m_i is the groundwater mass (kg), c_i is the groundwater heat capacity (J/kg.°C), and T_i is the groundwater temperature (°C), i is the supply well index 1 to 4.

3.2.3.3 Calibration

Three steps of calibrations were performed. The first calibration was a steady state fluid flow to determine hydraulic head on each boundary. The calibration was performed by adjusting hydraulic head on each boundary and compared the simulated hydraulic head measured on each observation well to the observed values. Observed values of hydraulic heads were obtained from Manitoba Sustainable Development observation wells (Figure 3.1).

The second calibration was transient fluid flow to determine hydraulic conductivity and specific storage of carbonate aquifer. Transient model calibration was performed by simulating pumping test at PW-1. This well was pumped between 4,007 to 4,764 m^3/d for three hours. During the calibration process, adjustment of the horizontal hydraulic conductivity, vertical hydraulic conductivity and specific storage were made on upper and lower sections of carbonate aquifer to improve the fitting between the simulated and the observed drawdown curves at observation wells: MW-1, PW-3, RW-1, RW-8, and G05OC019. Throughout simulation the ratio of K_{xx}, K_{yy}, and K_{zz} were maintained at $K_{xx} = K_{yy}$ and $K_{zz} = 0.1\ K_{xx}$.

The third calibration was performed as part of the heat transport simulation to identify suitable thermal properties of carbonate bedrock for this model. The model was simulated using the groundwater extraction rate, EWT and LWT measured from March 2014 to September 2017. The transient calibration involved adjusting the thermal conductivity, volumetric heat capacity, effective porosity, longitudinal dispersivity and transverse dispersivity of carbonate bedrock, as well as the extraction rate distribution on four supply wells. The EWT at each simulation time was estimated using equation 3.6.

Five schedules (Figure 3.6) were created to find the extraction rate distribution on each production well that represented the actual distribution. Schedule 1 represented the extraction rate based on the comparison of flow rate on each well to flow rate of the geothermal system during the peak demands period. Using this schedule, every month PW-1 supplies groundwater at 50% of monthly pumping rate, while PW-2, PW-3, and PW-4 supply groundwater at 11%, 17%, and 22% of monthly pumping rate respectively. Schedule 2 represented the extraction rate based on the automated system where PW-1 always operates with flow rate up to 3,925 m^3/d, followed by PW-2 with flow rate up to 872 m^3/d, then PW-3 with flow rate up to 1,308 m^3/d, and

finally PW-4 for the remaining flow required. Schedule 3 represented the extraction rate with PW-4 extracts groundwater first with flow rate up to 1,744 m^3/d, followed by PW-1 with flow rate up to 3,925 m^3/d, then PW-3 with flow rate up to 1,308 m^3/d, then PW-2 for the remainder. Schedule 4 represented the distribution where PW-3 always operates first with flow rate up to 1,308 m^3/d, followed by PW-2 with flow rate up to 872 m^3/d, then PW-4 with flow rate up to 1,744 m^3/d, and PW-1 for the remaining flow. Schedule 5 was created as a combination of schedule 3 and 4 with some modification.

Variety combinations of thermal properties were applied on each schedule, the fitting between simulated and observed EWT were observed on two simulation periods: the first period from March 2014 to September 2017 (day 0 to 1309) and the second period from April 2017 to September 2017 (day 1126 to 1309). This method was adopted due to the abrupt reduction on the extraction rate and temperature increase from April 2017 to September 2017 (Figures 3.3 and 3.6).

Two performance criteria were applied on each simulations result: R^2 (R-squared) coefficient of determination, to determine how well the model fits the data; and RMSE (Root Mean Squared Error), to determine the accuracy of the model by measuring the difference between simulated and observed values. R^2 value of 1 indicates a perfect model and RMSE value of 0 indicates a perfect fit of simulated value to a data.

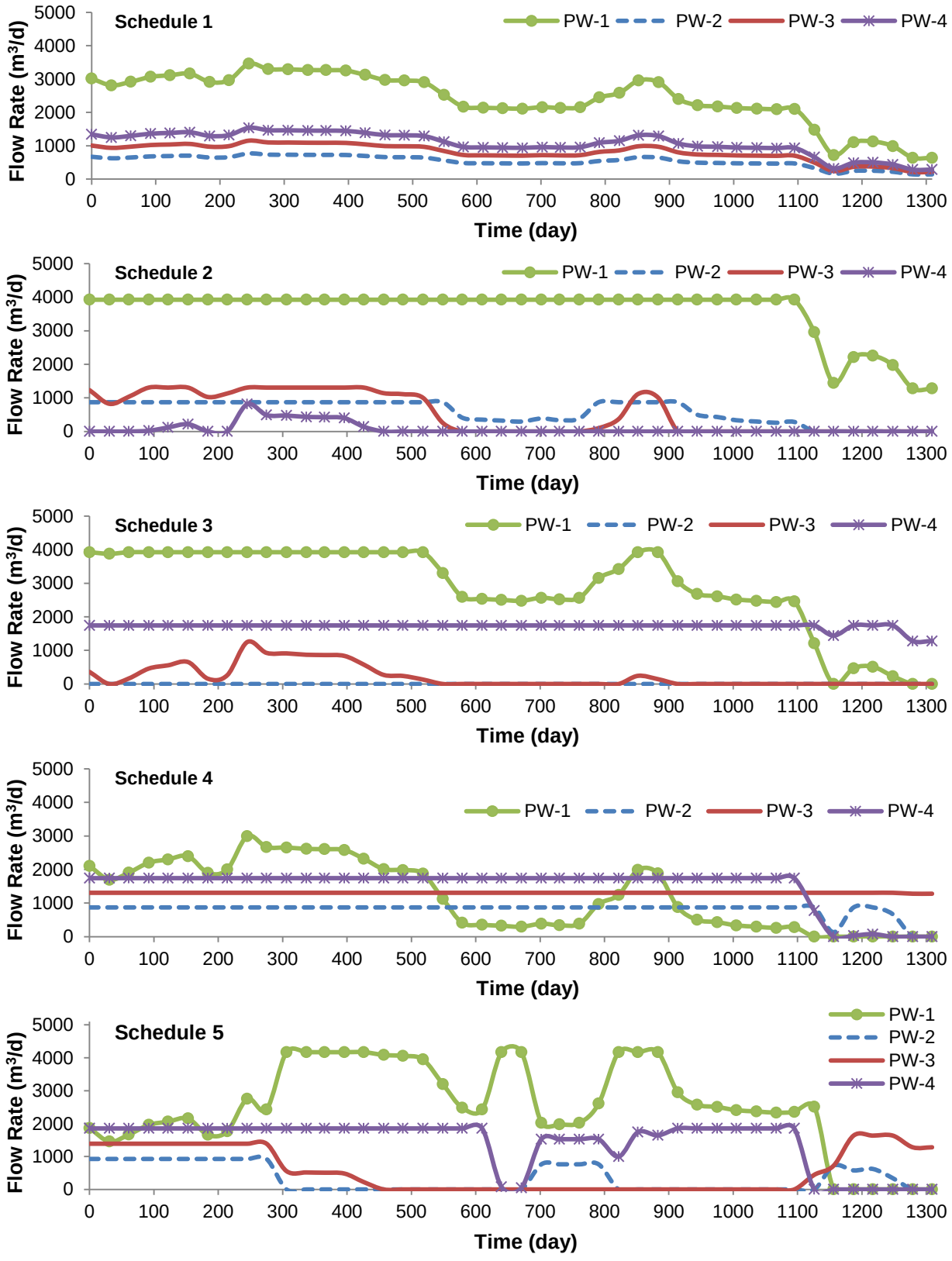

Figure 3.6 Schedule of extraction rate distribution for each supply well.

3.2.3.4 Sensitivity analysis

The purpose of the sensitivity analysis was to investigate the influence of thermal and transport properties on the EWT. The analysis was performed on groundwater extraction rate distribution to each well (schedule) and thermal properties: volumetric heat capacity of solid, thermal conductivity of solid, effective porosity, longitudinal and transverse dispersivity. The analysis involved varying the value of each property and schedule to the calibrated model.

3.2.3.5 Long-term simulation

The groundwater use licence permits the geothermal system to extract groundwater up to 1,640 dam^3 per year. As the purpose of groundwater is not for consumption, the geothermal system is required to return the groundwater back into the aquifer with condition that the injected temperature is between 1.5 to 12°C. Manitoba Sustainable Department also specifies that the temperature difference between LWT and EWT should not exceed 5°C (Matthews 2003). Groundwater usage from March 2014 to September 2017 indicated two periods when the geothermal system was operated using 138 % and 70% of the permissible flow (Figure 3.3). From October 2014 to September 2015, the system extracted 2,132 dam^3 and returned the thermal wastewater back into aquifer with all parameters within the range set by Manitoba Sustainable Development (Figure 3.3). While from October 2016 to September 2017, the geothermal system extracted 1,148 dam^3 but the recharge water temperature reached 15.4°C which indicated temperature difference of 8.2°C. Mean outside air temperature during these two periods indicated that the weather from October 2014 to September 2015 was harsher than the period from October 2016 to September 2017 (Figure 3.3).

Long term simulation (30 years) was conducted using schedule 1 which operates all supply wells at all time to deliver the required groundwater. The purpose of long term simulation was to

study the probable effect of geothermal system on the groundwater after years of operation. Simulations were conducted in three conditions (Table 3.2):

1. 130% permissible groundwater quantity with temperature difference from October 2014 to September 2015.
2. 70% permissible groundwater quantity with temperature difference from October 2016 to September 2017.
3. 80% permissible groundwater quantity with temperature difference from October 2016 to September 2017.

One year flow distribution and temperature difference (table 3.2) were applied on each year until the simulation reach 30 years.

Table 3.2 Distribution of Groundwater flow and temperature difference between EWT and LWT for long term simulation.

Simulation	1		2		3	
Month	Q (dam^3)	ΔT (°C)	Q (dam^3)	ΔT (°C)	Q (dam^3)	ΔT (°C)
October	170.56	0.72	137.2	0.87	156.8	0.87
November	191.88	0.03	130.7	0.61	149.4	0.61
December	191.88	0.01	132.1	-0.21	150.9	-0.21
January	191.88	-0.08	130.9	-0.27	149.6	-0.27
February	170.56	-0.28	117.2	0.02	133.9	0.02
March	191.88	0.8	130.5	0.41	149.1	0.41
April	191.88	1.3	88.7	1.33	101.4	1.33
May	170.56	1.73	44.7	3.34	51.1	3.34
June	170.56	2.94	66.4	6.01	75.9	6.01
July	170.56	3.48	70.0	8.21	80.0	8.21
August	170.56	2.91	61.3	6.63	70.0	6.63
September	149.24	2.46	38.4	4.64	43.9	4.64
Flow quantity	2132.0	(dam^3/year)	1148.0	(dam^3/year)	1312.0	(dam^3/year)

3.3 Results

3.3.1 **Flow Calibration**

Two fluid flow calibrations were performed to obtain the aquifer hydraulic properties suitable for this model. The first calibration was a steady state fluid flow to determine initial hydraulic head suitable for the model. Simulated hydraulic heads were compared to observed hydraulic head at the observation wells. The good result was obtained by putting different constant hydraulic head on each boundary. Constant heads on the upper west boundary were 236.9 m on the north side and 235.2 m on the south side. On the southwest boundary, the constant head was 229.51 m. The east boundary had constant heads of 225.2 m on the south side and 225.83 m on the north side. As for the northeast boundary, constant heads were 225.83 m, 222 m, 223.48 m, and 226.6 m respectively from the south side to the north side of the boundary (Figure 3.7). The calibration produced R^2 coefficient of determination between simulated and observed hydraulic head of 0.9998 and RMSE of 0.07644 m. The hydraulic head obtained from constant head calibration was then used as the static water level for drawdown calculation and the initial hydraulic head for pumping test calibration.

The next calibration was transient fluid flow using pumping test data to determine hydraulic conductivity and specific storage of the carbonate aquifer. The good fit of drawdown curves (Figure 3.8) were obtained with combination of horizontal hydraulic conductivity of 67.0 m/d and 30.0 m/d for lower and upper section of carbonate aquifer respectively, vertical hydraulic conductivity of 6.7 m/d and 3.0 m/d for lower and upper sections of aquifer, and specific storage of 8.9×10^{-6} 1/m for carbonate aquifer and clay/till layers. The calibrated hydraulic conductivity indicated transmissivity for the model matched with the result from the aquifer testing (Burns & Sinclair, 2012b). Although horizontal hydraulic conductivity of 30 m/d

for upper section of aquifer is still in a highly permeable range, this value is still less than half of hydraulic conductivity of lower section of aquifer. Specific storage 8.878×10^{-6} 1/m indicates that the confined aquifer thickness is 51.81 m which is the depth of wells from the ground surface (Table 3.1), this shows that by using a fully confined aquifer, all layers are treated as a saturated porous medium.

The model was then adjusted using the calibrated constant heads, hydraulic conductivities and specific storage to obtain the initial hydraulic head and ready for heat transport simulation.

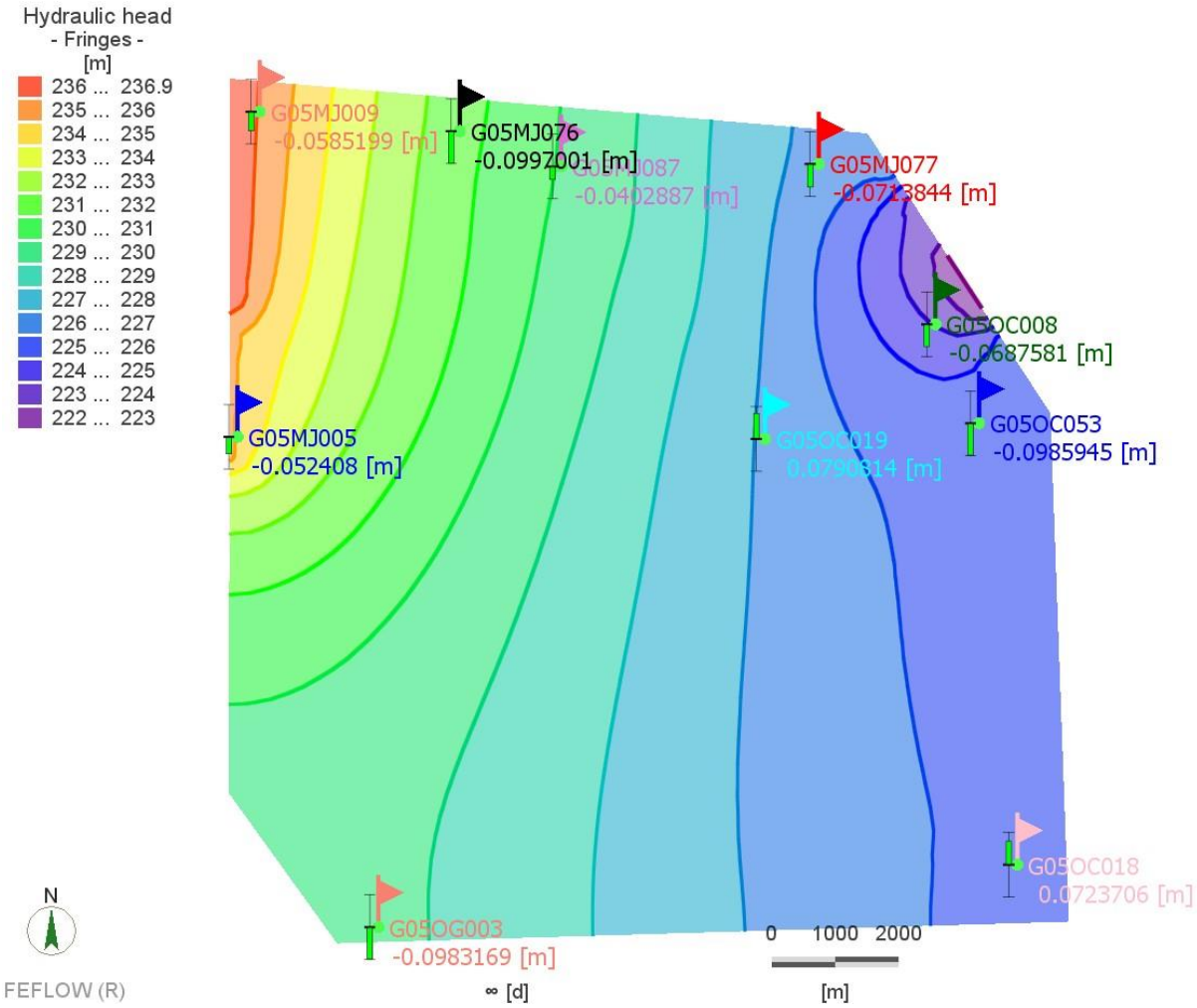

Figure 3.7 Result of constant hydraulic head calibration

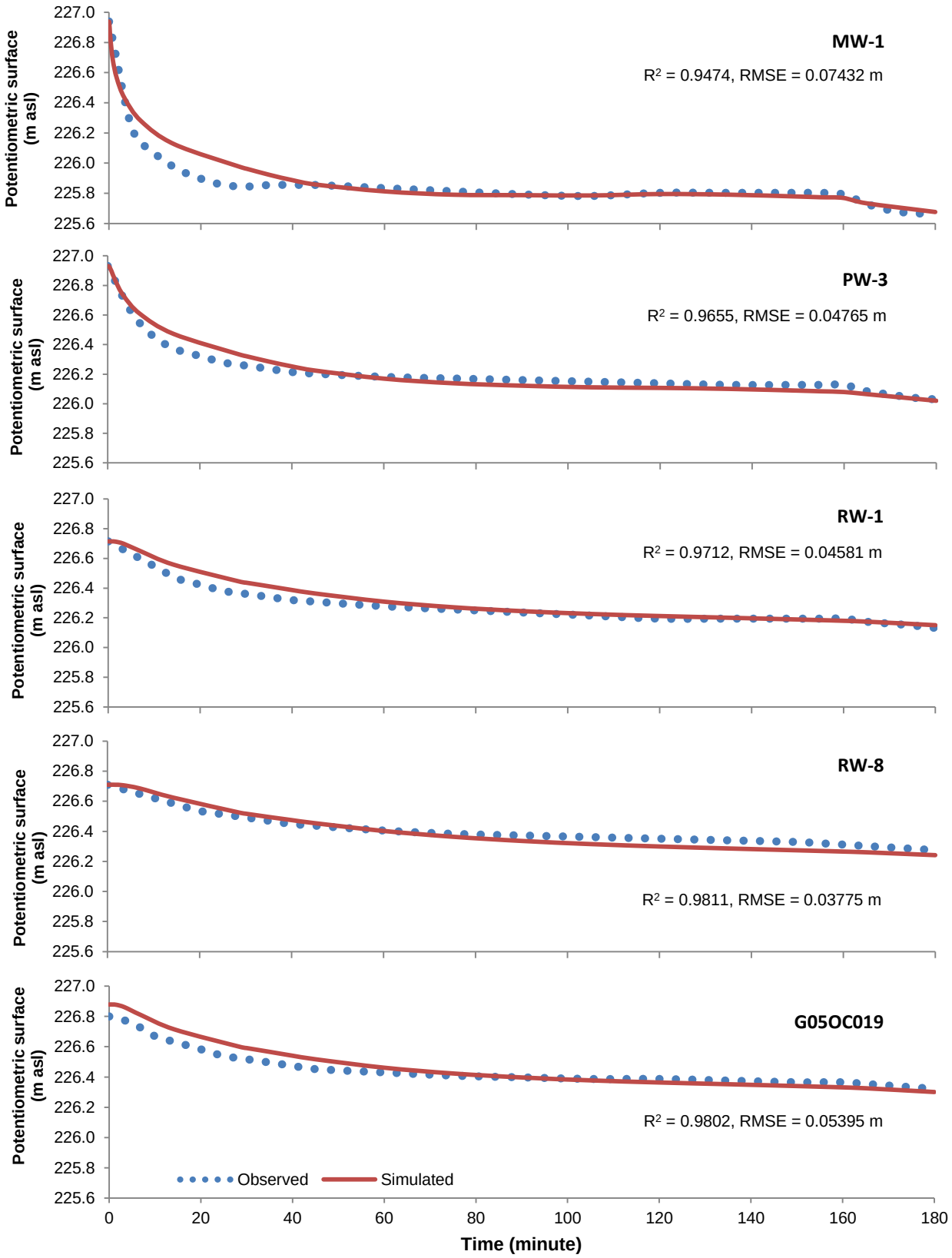

Figure 3.8 Pumping test result: simulated and observed drawdown curve at each observation well

3.3.2 **Heat Transport Simulation**

3.3.2.1 Distribution of groundwater extraction

Entering water temperature to a heat exchanger is highly influenced by the distribution of groundwater extraction. Overall, schedule 1 (Figure 3.6) produced the lowest EWT compared to the other four schedules. Using this schedule, the temperature at PW-1 and PW-4 (Figure 3.9) were always low due to high groundwater extraction, PW-1 extracted 50% and PW-4 extracted 22% of groundwater flow required by geothermal system. PW-2 extracted 11% of flow required which was less than 17% extracted by PW-3. Despite this setting, the temperature at PW-3 was always the highest; this occurred because PW-3 was the closest production well to the array of recharge wells and located on the path of groundwater extraction to PW-1, PW-2 and PW-4.

Schedule 2 produced the EWT higher than schedule 1 (Figure 3.12 A); however, groundwater temperature on each well has no significant increase (Figure 3.9). Using this schedule, temperature at PW-4 was 6.7°C most of the time due to the automatic sequence which required PW-4 to extracted water only after PW-1, PW-2 and PW-3 had reached their maximum operating capacity. Although PW-1 always operated to deliver most of groundwater flow required, the increase temperature at this well was not significant due to PW-1 location from recharge wells and toward groundwater flow. When PW-1 extracted groundwater, the extraction flow was parallel to the groundwater flow in the opposite direction.

Schedule 3 delivered the EWT slightly lower than schedule 1 except on the last three months of the simulation (Figure 3.12 A). Temperatures at PW-1 and PW-4 were always low due to the pumping, while the significant temperature increase occurred at PW-2 and PW-3 due to limited pumping (Figure 3.9). Using this schedule, the required groundwater flow for each month mostly was delivered by PW-4 and PW-1 because both wells had higher maximum operating rate

compared to PW-3 and PW-2. Although the geothermal system never extracted groundwater from PW-2, the temperature increased significantly at PW-3 due to its location from the recharge wells. Similar to schedule 1 and 2, schedule 3 was not able to provide the EWT above 6.9°C.

Schedule 4 delivered the EWT higher than the other schedules (Figure 3.12 A). By extracting groundwater from PW-3 at all time, the increase of temperature at PW-3 was hindered. Due to the maximum operating rate assigned for each pump, PW-3, PW-2 and PW-4 supplied the required groundwater until 1095 day (Figure 3.6), any extraction using PW-1 would reduce the temperature in PW-3 (Figure 3.9). Using this schedule the EWT reached above 7.25°C on day 1279.

Schedule 5 was able to deliver the EWT similar to schedule 3 from day 0 to 1126. From day 1156 to 1309, the schedule was able to deliver temperature close to the observed EWT. Similar to schedule 3, by extracting groundwater from PW-3 and PW-2, the EWT reached above 7°C beyond day 1126.

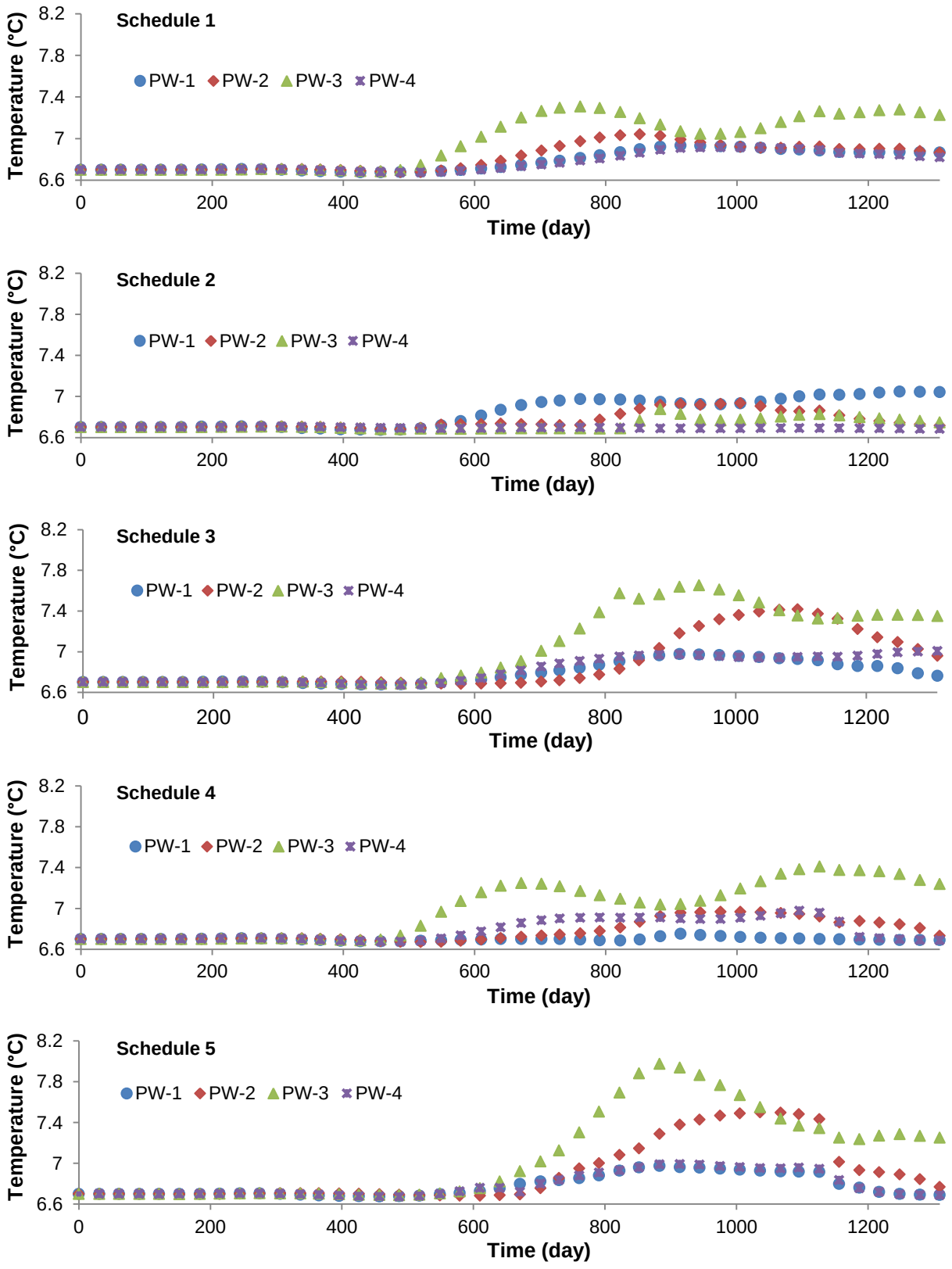

Figure 3.9 Temperature in supply wells due to groundwater extraction schedule

3.3.2.2 Thermal properties calibration

Different combinations of thermal properties were applied on each schedule of extraction rate distribution (Figure 3.6). A good fit between the simulated and observed EWT (Figure 3.10) was obtained using schedule 5 with carbonate bedrock thermal properties:

- Volumetric heat capacity of solid phase = $3200x10^3$ J/m^3 °C.
- Thermal conductivity = 2.2 W/m°C
- Effective porosity = 5%
- Longitudinal dispersivity = 1.5 m and transverse dispersivity = 0.15 m

For simulation period from day 0 to 1309, the calibration produced 0.8102 for R^2 between simulated and observed EWT and 0.07796°C for RMSE. For day 1126 to 1309, R^2 was 0.9652 and RMSE was 0.021°C.

Although the geothermal system was designed with the automatic sequence to extract groundwater using PW-1 first followed by PW-2, PW-3, and PW-4, the calibration result proved that the automatic sequence did not work. The automatic sequence failed due to the well operating condition which required maintenance mostly caused by sediment clogging the filter screens.

Volumetric heat capacity of $3200x10^3$ J/m^3 °C indicates that the carbonate bedrock beneath Winnipeg has a high heat capacity. With the solid phase density between 2,730 to 2,850 kg/m^3 (Ferguson 2004), heat capacity of the bedrock ranging from 1,123 to 1,172 W/kg°C makes the aquifer suitable as heat source and sink. Thermal conductivity of carbonate aquifer was estimated in the range of 0.87 to 3.56 W/m°C (Ferguson 2004), applying variety of these values on the model showed no impact on the EWT (Figure 3.12 C). For the calibrated model, the mean value of 2.2 W/m°C (Ferguson 2004) was applied. During calibration, the ratio of longitudinal and transverse dispersivity was maintained at 10:1. Bruno et al. (2017) suggested to use a

longitudinal dispersivity less than 2 m and a transverse dispersivity less than 0.2 m to prevent the underestimation of the thermal impact on the aquifer. Changing the longitudinal dispersivity and transverse dispersivity to 1.5 m and 0.15 m improved the value of R^2 and RMSE between simulated and observed EWT.

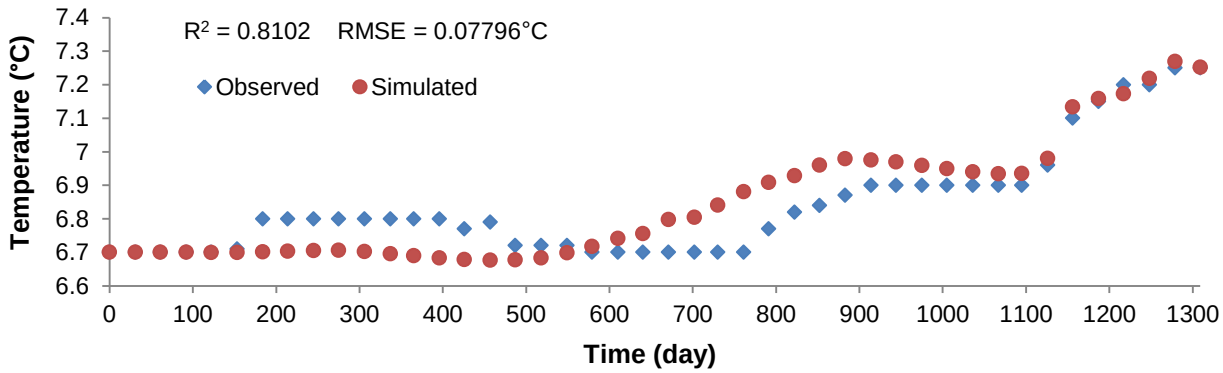

Figure 3.10 Result of thermal properties calibration showing good fit between simulated and observed EWT.

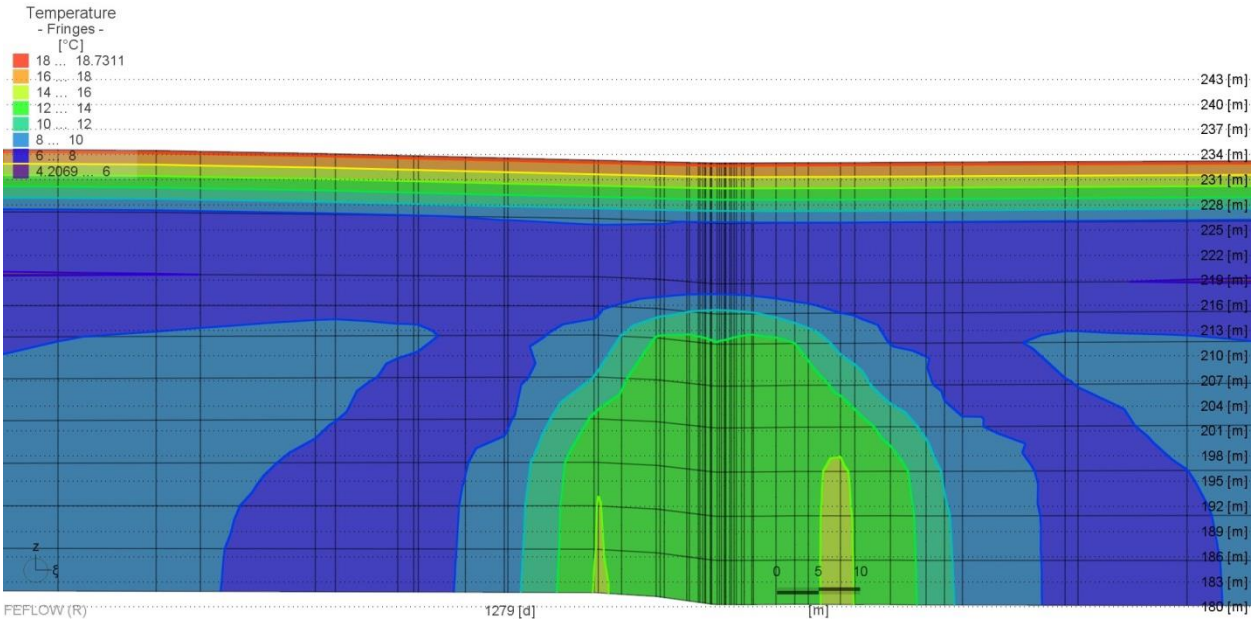

Figure 3.11 Cross section of calibrated model at recharge well for 1279 day (end of August 2017).

The cross section of the calibrated model at the end of August 2017 (early September 2017), showed a good representation of temperature profile on top 10 m of clay and till layer (Figure 3.11). Comparison was performed using temperature profile at provincial observation wells G05OJ028 and G05OJ022 (Ferguson 2004).

3.3.2.3 Sensitivity analysis

When the calibrated model was simulated by varying thermal conductivity of solid from 1.5 to 3.5 W/m °C (Figure 3.12 C), the result indicated only slight change on the EWT compared to the value of thermal conductivities. This showed thermal conductivity had very little or no influence on the EWT. Effective porosity had a slight influence on the EWT (Figure 3.12 D), smaller effective porosity increased the EWT. The influence however was not as significant as the dispersivity parameters. Generally, the increase value of dispersivity parameters increased the EWT. On all simulations, transverse dispersivity was assumed to be 10% of longitudinal dispersivity. Volumetric heat capacity of solid was highly influenced the EWT, the increase of volumetric heat capacity of solid reduced the EWT. These results were consistent with earlier research on the sensitivity of porous medium thermal properties on thermal plume size (Lo Russo et al. 2012).

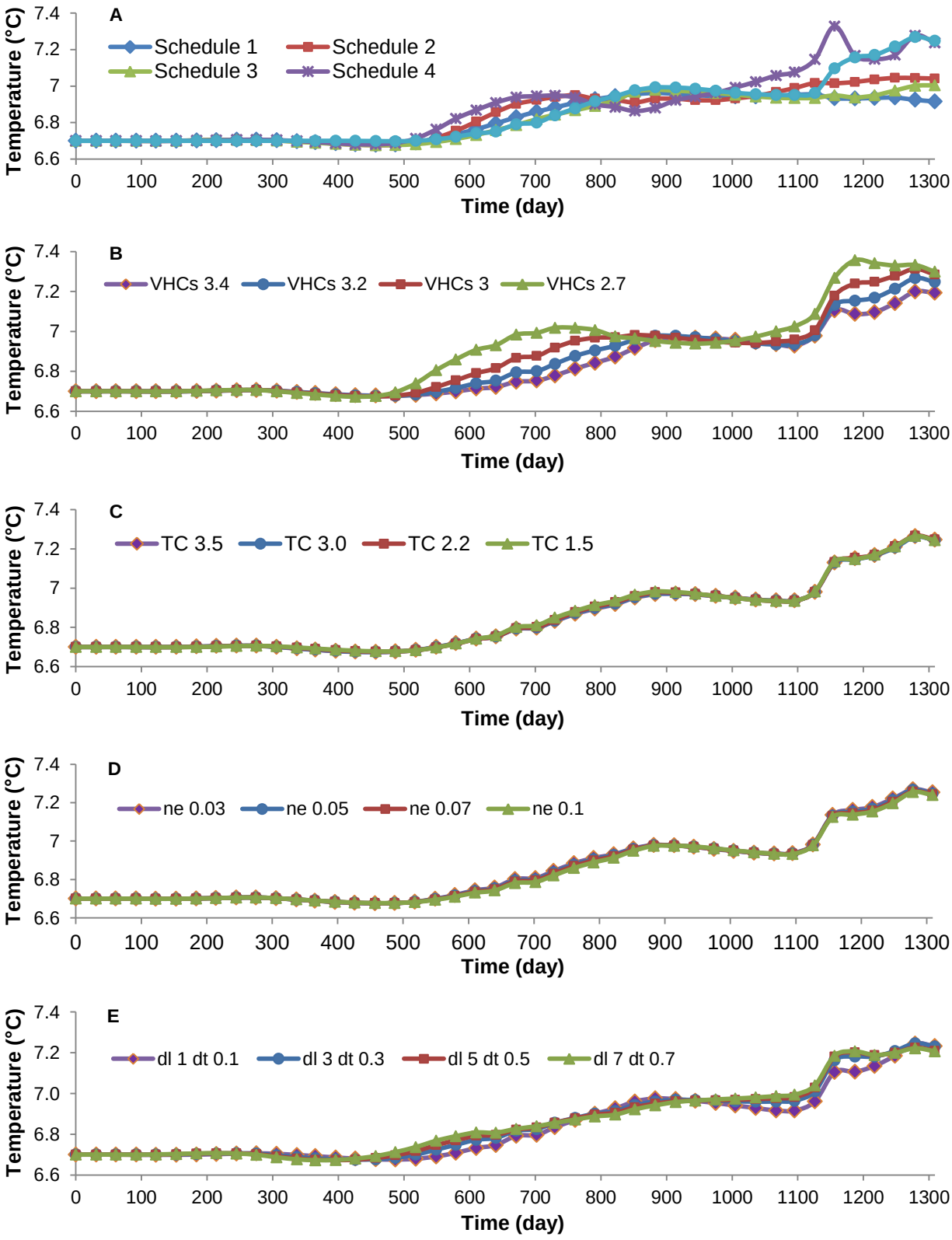

Figure 3.12 Sensitivity analysis result on: extraction rate distribution schedule (A), volumetric heat capacity of solid phase (B), thermal conductivity (C), effective porosity (D), longitudinal and transverse dispersivity (E).

3.3.2.4 Long-term simulation

Comparison between the results of simulation 1 and 2 (Figure 3.13) indicate that the EWT estimation using simulation 1 will always higher than simulation 2. The difference between simulation 1 EWT and simulation 2 EWT reached 0.45°C, beyond twenty years, the differences become smaller. After thirty years, the temperature in PW-3 reaches 8.7°C for simulation 1 and 8.54°C for simulation 2. Generally temperatures in PW-3 for simulation 1 are always higher than simulation 2. However, after 20 years there are months when temperatures in PW-3 for simulation 2 are higher than simulation 1. Assuming the geothermal system extracts groundwater only from PW-3, injection water will reach slightly over 12°C under simulation 1. While for simulation 2, the injection temperature will reach 17°C. Increasing groundwater flow rate while keeping same temperature difference (simulation 3), will increase EWT. In 15 years, EWT estimation using simulation 3 is higher than simulation 1.

Comparison between thermal plumes created by simulation 1, 2 and 3 (Figure 3.14) shows simulation 1 creates a bigger area of thermal plumes; while simulation 2 and 3 create higher temperature zones inside the plumes. Plume length is measured from PW-1 to the farthest side of isoline, parallel to the direction of groundwater flow. Plume width is measured on the widest part of the plume perpendicular to the arbitrary length of the plume. After 10 years, simulation 1 develops the 9°C isotherm only on surrounding recharge wells; simulation 2 develops similar isotherm with wider dimension; while simulation 3 develops the 9°C isotherm almost reaching supply wells with temperature at PW-3 beyond 8°C. After 20 years, the 9°C isotherm in simulation 1 is moving closer to supply wells but the area covered is smaller than simulation 2; and simulation 3 develops the biggest 9°C isotherm area with the 10°C isotherm approaching supply wells. Temperature breakthrough of 8°C occurs in PW-3 for both simulation 1 and 2. After 30 years, while simulation 1 only develops plume with the 7°C, 8°C, and 9°C isotherms;

simulation 2 develops the 10°C isotherm downstream the recharge wells approximately 160 m in the direction of groundwater flow; and simulation 3 develops the 10°C isotherm area approximately 887 m long by 806 m wide with the temperature in PW-3 above 9°C. Despite having a higher temperature zone within its thermal plume, for thirty years span, simulation 2 always deliver a lower EWT because the groundwater rate is lower than simulation 1.

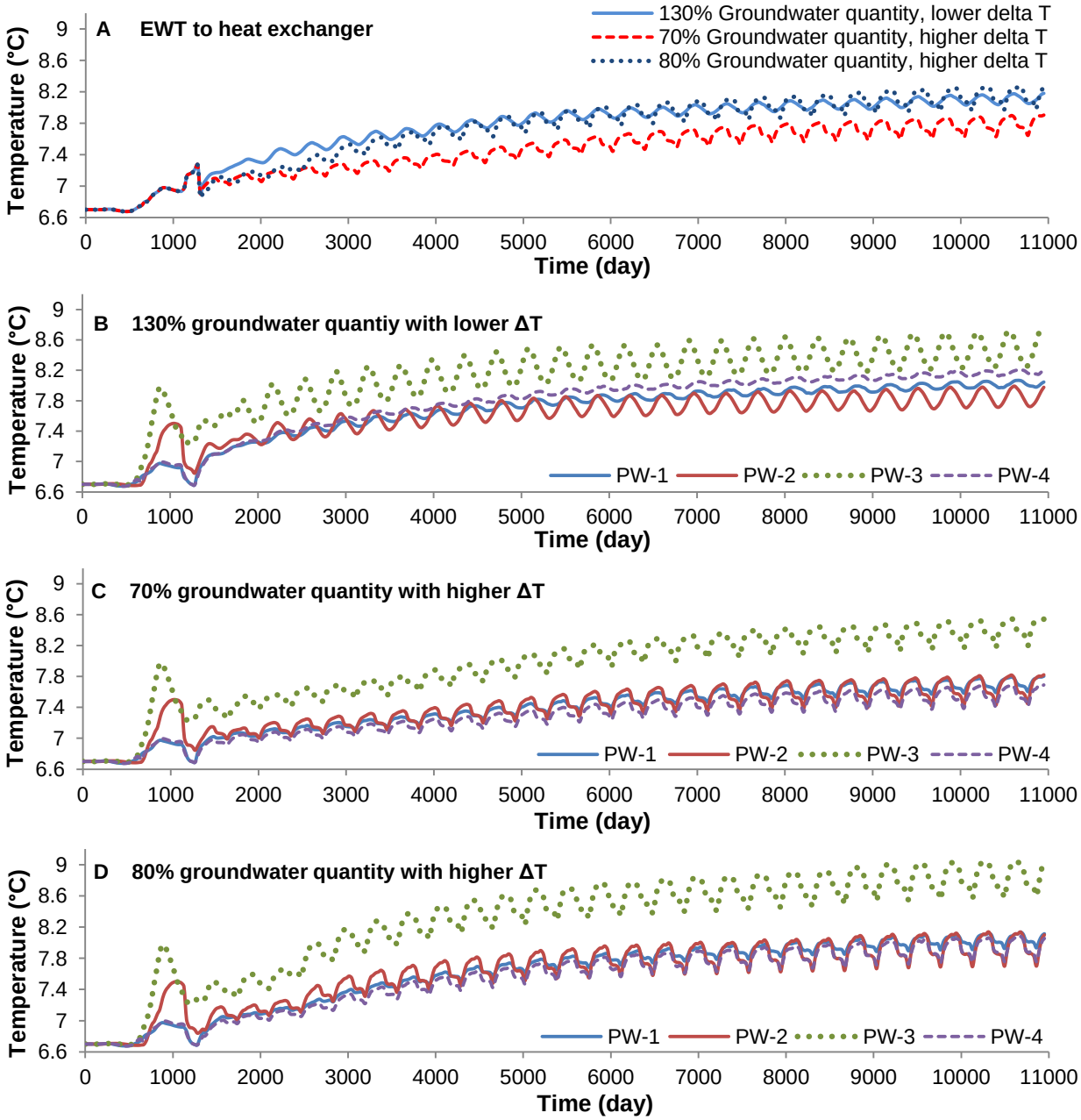

Figure 3.13 Long term simulation result: EWT to heat exchanger (A); Groundwater temperature on each supply well for simulation 1 (B), simulation 2 (C), and simulation 3 (D).

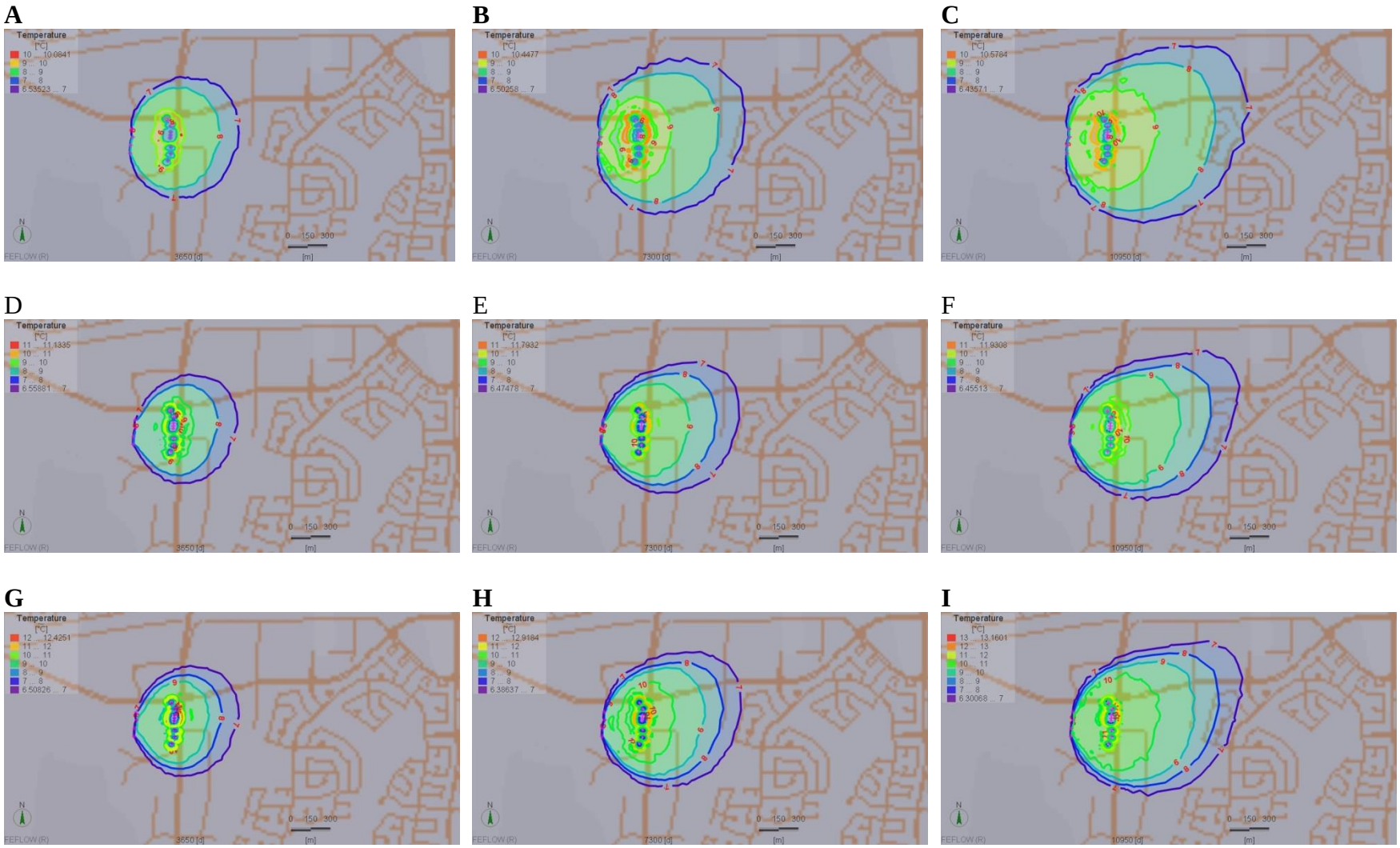

Figure 3.14 Thermal plume: 10 years simulation 1 (A), 20 years simulation 1 (B), 30 years simulation 1 (C), 10 years simulation 2 (D), 20 years simulation 2 (E), 30 years simulation 2 (F), 10 years simulation 3 (G), 20 years simulation 3 (H), and 30 years simulation 3 (I).

Table 3.3 Estimated thermal plume size for each simulation

Simulation 1

Temperature	7°C		8°C		9°C		10°C	
Time (d)	L (m)	W (m)	L (m)	W (m)	L (m)	W (m)	L (m)	W (m)
3650	900	900	805	793				
7300	1230	1146	1050	990	725	750		
10950	1490	1282	1260	1100	870	884		

Simulation 2

Temperature	7°C		8°C		9°C		10°C	
Time (d)	L (m)	W (m)	L (m)	W (m)	L (m)	W (m)	L (m)	W (m)
3650	890	830	740	690	75			
7300	1145	953	970	838	806	725		
10950	1418	1100	1190	930	975	825	160	

Simulation 3

Temperature	7°C		8°C		9°C		10°C	
Time (d)	L (m)	W (m)	L (m)	W (m)	L (m)	W (m)	L (m)	W (m)
3650	890	830	750	708	670	640		
7300	1145	990	1050	900	925	825	723	675
10950	1435	1142	1255	1000	1140	950	887	806

3.4 Discussion

Applying the schedule 1 groundwater extraction distribution on a long term simulation shows the EWT reduction from 7.25°C to 6.9°C at simulation day 1309 (Figure 3.13 A). The reduction occurs because of low temperature in PW-1, PW-2, and PW-4. Using simulation 2, the geothermal system extracts groundwater with temperature up to 0.45°C (day 4441) lower than simulation 1 and creates a thermal plume with the 7°C isotherm covering area approximately 80% of thermal plume created using simulation 1. At the end of 30 years, simulation 2 creates the 10°C isotherm area downstream of the recharge wells and the gap between EWTs is closer.

This condition indicates that in a longer term simulation 2 will create the 10°C isotherm bigger than simulation 1 which will increase temperature in supply wells that may surpass simulation 1. After 30 years, the maximum temperature of 9°C occurs in PW-3 (simulation 3), an increase about 2.3°C from ambient temperature. This increase may still be acceptable for the geothermal system; however, the 10°C thermal plume will affect the neighbouring area.

Although running the geothermal system with high temperature injection and low groundwater extraction will deliver a lower EWT and develop a smaller thermal plume size, the system may need more groundwater to meet the requirement in harsher weather. Increasing groundwater flow not only will increase the size of thermal plume and temperature within the plume but also increase the temperature in supply wells. In reality, maintaining groundwater extraction using PW-1 at all time is not possible, as shown by schedule 5; the main supply well could also be PW-2, PW-3 or PW-4. If this condition occurs, the EWT will be higher than using schedule 1. Looking at the operating history (Figure 3.3), the geothermal system mostly operates to deliver cooling. Although the groundwater quantities for heating season are higher than for cooling season, the temperature differences between EWT and LWT are always within 0.2 to 1°C (Figure 3.3), hence the geothermal system will never be able to balance the heat injection during cooling season, as shown by the long term simulation (Figures 3.13 and 3.14).

Earlier research indicated that running geothermal system under low pumping rates will lower operating cost and prevent thermal breakthrough at the production well (Freedman et al. 2012; Banks 2009). However, the long term simulation shows the important of maintaining injection temperature within the regulation set by Manitoba Sustainable Development. The regulation of injection temperature between 1.5 to 12°C and temperature difference up to 5°C were defined to prevent impact on the groundwater ecosystem (Brielmann et al. 2011).

Maintaining the condition that meet the regulation will require good management in operating the geothermal system. Kavanaugh and Rafferty (2014) described a design procedure for open loop geothermal system that can be used to aid the management of groundwater extraction flow and injection temperature. Based on the simulation, there are options that may prevent the temperature increase such as:

- Ensure the total groundwater quantity use in a year is no more than the amount listed in the water use license.
- During the cooling season: maintain the temperature difference between LWT and EWT up to 5°C, and injection groundwater temperature up to 12°C. By doing this, the system will require higher groundwater pumping rate (Rafferty 2001) compared to 8°C temperature difference. Extract groundwater using PW-1 first, follow by PW-2; and inject wastewater into the second branch of recharge wells (RW-4, RW-5, RW-6, RW-7, and RW-8). Should the geothermal system requires groundwater extraction in excess of PW-1 and PW-2 combined maximum flow rate, use schedule 1 and distribute waste water into all recharge wells.
- During the heating and shoulder seasons: increase the temperature difference between EWT and LWT up to 5°C and lower the LWT but it should not be below 1.5°C. By increasing the temperature difference, the geothermal system will require less flow rate (Rafferty 2001) compared to 0.3°C temperature difference. Use PW-4 first to extract groundwater, then PW-3; and inject waste water into first branch of recharge wells (RW-1, RW-2, and RW-3).
- Install a winter chilling system that has proven to hinder groundwater temperature increase in the aquifer (Lindell and Mann 2015). During winter season, the extracted groundwater is directed to winter chilling system before returning it to the aquifer. The system will lower the groundwater temperature using cold winter air and thermally balance the heat load from

summer season. Installing a winter chilling system increases the groundwater extraction in a year. The system also requires monitoring to ensure its purpose is achieved.

3.5 Conclusion

Three-dimensional model was developed for southwestern part of Winnipeg using hydrogeological map, provincial observation wells, geothermal system wells, and earlier research on carbonate rock aquifer. Three steps of calibration were performed: constant hydraulic head calibration, pumping test calibration and heat transport calibration. Sensitivity analysis was performed to study the influence of thermal properties of carbonate rock beneath the City of Winnipeg on groundwater temperature in supply wells.

Groundwater extraction distribution plays important role in groundwater temperature entering heat exchanger. The geothermal system was designed with automatic setting which assigns PW-1 first, to supply groundwater volume required by the system until it reaches the maximum operating rate. The remaining groundwater will be fulfilled by PW-2, PW-3, and PW-4, in the same manner as PW-1. Sensitivity analysis showed that automatic distribution setting was able to maintain low temperature in each supply well. However, in reality the automatic setting did not work due to sediment clogging on the filter screen. The best option to deliver low EWT is by distributing the groundwater required in a month to all supply wells with PW-1 supply 50%, PW-2 supply 11%, PW-3 supply 17%, and PW-4 supply 22% of the required groundwater quantity.

Since its operation, the geothermal system has applied two different conditions which do not meet groundwater use licence requirements: extracting higher groundwater quantity and injecting high temperature wastewater. Three long term simulations were performed to study the impact of these conditions. Results showed that higher groundwater flow increased thermal

plume size, while high temperature created a higher temperature zone within the thermal plume. Therefore, good management in maintaining groundwater extraction within the permissible quantity and injection temperature within the regulated value is important for the sustainability of the geothermal system, and groundwater environment.

Despite the purpose of geothermal system to deliver heating and cooling, the system operates mostly for cooling. Generally, in a year the system will deliver heating for 2 months, cooling for 8 months and 2 months are shoulder seasons. The increase of groundwater temperature can be delayed by always assigning PW-1 to extract more groundwater required in a month or assigning a different combination of supply wells and recharge wells for different seasons. The other option is installing winter chilling system which is already proven to hinder groundwater temperature increase.

4 Recommendation for future research

1. Geothermal energy maps developed in this study could be used to provide aid in the early design stage of a geothermal system. Updating the maps regularly is necessary to provide the latest information on open loop geothermal systems within the City of Winnipeg. Obtaining groundwater flow and temperature from each user is necessary for a better result on the heat balance calculation.
2. Develop a map that shows the depth of water bearing fractures. This map will provide useful information in the early stage development of geothermal systems.
3. Further study on thermal plume analytical approaches to find the proper technique which suitable for Upper Carbonate aquifer.
4. Optimize the numerical model developed in this study by adding more layers, obtaining the distribution of groundwater extraction data on daily basis, recording the distribution of groundwater injection on daily basis, and recording the temperature in each supply well.
5. Three dimensional model in this study can be used for analyzing different geothermal system in southwestern part of Winnipeg by modifying hydraulic properties using the pumping test data performed at the location of the geothermal system. The model also can be used to study the impact of multiple geothermal systems in southwestern Winnipeg. Applying multiple systems will require pumping test data from each system.

Reference

Abesser, C. 2010. Open-loop ground source heat pumps and the groundwater systems: A literature review of current applications, regulations and problems. Keyworth, Nottingham: British Geological Survey.

Arning, E., M. Kölling, H.D. Schulz, B. Panteleit, and J. Reichling. 2006. Effect of nearsurface thermal extraction on geochemical processes in aquifers. *Grundwasser* 11 no. 1: 27-39.

Banks, D. 2009. Thermogeological assessment of open-loop well-doublet schemes: a review and synthesis of analytical approaches. *Hydrogeology Journal* 17 no. 5: 1149-1155.

Baracos, A. 1957. The Foundation Failure of the Transcona Grain Elevator. *The Engineering Journal* no. July 1957: 973-977.

Baracos, A., D.H. Shields, and B. Kjartanson. 1983. Geological Engineering Maps and Report for Urban Development of Winnipeg., ed. D. H. Shields. Department of Geological Engineering, University of Manitoba, Winnipeg, Manitoba.: Cantext Publications.

Bauer, M., D. Bendel, A. Eppinger, W. Franßen, M. Heinz, B. Keim, D. Mahler, N. Milkowski, U. Pasler, K.M. Rolland, R. Schölch-Ighodaro, U. Stein, M. Vöröshazi, and M. Wingering. 2009. Umweltministerium Baden-Württemberg, Arbeitshilfe zum Leitfaden zur Nutzung von Erdw€arme mit Grundwasserw€armepumpen. U. Baden- Würrtemberg, Stuttgart.

Bejan, A., and A.D. Krauss. 2003. *Heat Transfer Handbook*. New Jersey: John Wiley & Sons, Inc.

Bell, J.J. 2004. Well Condition Assessment – Central Park Lodge – 70 Poseidon Bay, Winnipeg,
Manitoba. Wardrop Engineering Inc.

Bell, J.J. 2009. Evaluation of Rising Intake Groundwater Temperature – Well to Well Cooling System Melet Plastics Inc – 34 De Baetes St. Friesen Drillers Ltd.

Bell, J.J. 2011. Hydrogeological Investigation for Groundwater Cooling - Villa Tache (Winnipeg Condominium Corp No. 346), 400 Rue Des Meurons - City of Winnipeg, Manitoba. Friesen Drillers Ltd.

Bell, J.J. 2012a. Hydrogeological Investigation for Groundwater Heating and Cooling, Proposed Assiniboine Credit Union (6169385 Manitoba Limited) Building, 3217 Portage Avenue (RL 111-Parish of St. Charles), City of Winnipeg, Manitoba. Friesen Drillers Ltd.

Bell, J.J. 2012b. Replacement of (2) Return Wells and Supply Well Condition Assessment - Holy Rosary Church, 510 River Avenue - City of Winnipeg, Manitoba. Friesen Drillers Ltd.

Bell, J.J. 2014. Installation of Replacement Return Well – Golden Links Lodge site-2280 St. Mary's Road, Winnipeg, Manitoba. Friesen Drillers Ltd.

Bell, J.J., and J.M. Friesen. 2008a. Hydrogeological/Geothermal Investigation - Well to Well Cooling System Granny's Poultry Co-operative Limited, Winnipeg, Manitoba. Friesen Drillers.

Bell, J.J., and J.M. Friesen. 2008b. Hydrogeological/Geothermal Investigation – Proposed Personal Care Home. Southeast Resource Development Corporation (SERDC) – RL 1-2 Parish of St. Vital – City of Winnipeg, Manitoba. Friesen Drillers Ltd.

Bell, J.J., and J.M. Friesen. 2011. Hydrogeological Investigation for Groundwater Geothermal Use – MHRC Facility, 125 Carriage Road (Lot 1 Block 6 Plan 10281 WLTO in RL 7 to 10 – Parish of St. James), City of Winnipeg, Manitoba. Friesen Drillers Ltd.

Betcher, R. 1995. *Groundwater in Manitoba : hydrogeology, quality concerns, management*. Saskatoon, Sask: Environment Canada, National Hydrology Research Institute, Environmental Sciences Division.

Bielus, L. 2005. Winpak Ltd. 100 Saulteaux Crescent, Relocation of Supply Wells for an Existing Groundwater Cooling System Hydrogeologic Report. UMA.

Bonte, M., P.J. Stuyfzand, G.A. Berg, and W.A.M. Hijnen. 2011. Effects of aquifer thermal energy storage on groundwater quality and the consequences for drinking water production: a case study from the Netherlands. *Water Science & Technology* 63: 1922-1931.

Bridger, D.W., and D.M. Allen. 2014. Influence of geologic layering on heat transport and storage in an aquifer thermal energy storage system.(Report). *Hydrogeology Journal* 22 no. 1: 233.

Brielmann, H., T. Lueders, K. Schreglmann, F. Ferraro, M. Avramov, V. Hammerl, P. Blum, P. Bayer, and C. Griebler. 2011. Shallow geothermal energy usage and its potential impacts on groundwater ecosystems. *Grundwasser* 16 no. 2: 77-91.

Brons, H.J., J. Griffioen, C.A.J. Appelo, and A.J.B. Zehnder. 1991. (Bio)geochemical reactions in aquifer material from a thermal energy storage site. *Water Research* 25 no. 6: 729-736.

Bruno, P., C. Alessandro, P. Francesca, G. Alberto, and S. Rajandrea. 2017. Thermal Impact Assessment of Groundwater Heat Pumps (GWHPs): Rigorous vs. Simplified Models. *Energies* 10 no. 9: 1385.

Burns, J., and J. Mann. 2006. Manitoba Hydro Dorsey Converter Station Groundwater Cooling April 2005 – January 2006 Monitoring Report. KGS Group.

Burns, J., and R.D. Sinclair. 2012a. Information for Water Right License Application, Proposed Malteurop Canada Inc. Geothermal System, 3001 Dugald Road, Winnipeg, Manitoba. KGS Group.

Burns, J., and R.D. Sinclair. 2012b. Information for Water Rights License Application, IKEA Properties Ltd., 1135 Kenaston Boulevard, Winnipeg, Manitoba. KGS Group.

Casasso, A., and R. Sethi. 2015. Modelling thermal recycling occurring in groundwater heat pumps (GWHPs). *Renewable Energy* 77 no. C: 86-93.

Clyde, C.G., and G.V. Madabhushi. 1983. Spacing of Wells for Heat Pumps. *Journal of Water Resources Planning and Management* 109 no. 3: 203-212.

Danielopol, D.L., C. Griebler, A. Gunatilaka, and J. Notenboom. 2003. Present state and future prospects for groundwater ecosystems. *Environmental Conservation* 30 no. 2: 104-130.

Day, M.J. 1978. Movement and hydrochemistry of groundwater in fractures clayey deposits in the Winnipeg area., University of Waterloo, Waterloo, Ontario.

Diersch, H.J.G. 2017. FEFLOW 7.0 –User's Manual. DHI-WASY GmbH, Berlin, Germany.

Domenico, P.A., and G.A. Robbins. 1985. A New Method of Contaminant Plume Analysis. *Ground Water* 23 no. 4: 476-485.

Epting, J., A. García-Gil, P. Huggenberger, E. Vázquez-Suñe, and M.H. Mueller. 2017. Development of concepts for the management of thermal resources in urban areas – Assessment of transferability from the Basel (Switzerland) and Zaragoza (Spain) case studies. *Journal of Hydrology* 548: 697-715.

Epting, J., F. Händel, and P. Huggenberger. 2013. Thermal management of an unconsolidated shallow urban groundwater body. *Hydrology and Earth System Sciences* 17 no. 5: 1851.

Epting, J., M.H. Müller, D. Genske, and P. Huggenberger. 2018. Relating groundwater heat-potential to city-scale heat-demand: A theoretical consideration for urban groundwater resource management. *Applied Energy* 228: 1499-1505.

Ferguson, G. 2007. Heterogeneity and Thermal Modeling of Ground Water. *Ground Water* 45 no. 4: 485-490.

Ferguson, G., and A. Woodbury. 2006. Observed thermal pollution and post-development simulations of low-temperature geothermal systems in Winnipeg, Canada. *Hydrogeology Journal* 14 no. 7: 1206-1215.

Ferguson, G., and A.D. Woodbury. 2004. Subsurface heat flow in an urban environment. *Journal of Geophysical Research: Solid Earth* 109 no. B2: n/a-n/a.

Ferguson, G., and A.D. Woodbury. 2005. Thermal sustainability of groundwater-source cooling in Winnipeg, Manitoba. *Canadian Geotechnical Journal* 42 no. 5: 1290-1301.

Ferguson, G., and A.D. Woodbury. 2007. Urban heat island in the subsurface. *Geophysical Research Letters* 34 no. 23: n/a-n/a.

Ferguson, G.A.G. 2004. Groundwater and heat flow in southeastern Manitoba : implications to water supply and thermal energy, Thesis (Ph.D.)--University of Manitoba, Fall 2004.

Freedman, V.L., S.R. Waichler, R.D. Mackley, and J.A. Horner. 2012. Assessing the Thermal Environmental Impacts of an Groundwater Heat Pump in Southeastern Washington State. *Geothermics* 42.

Fry, V.A. 2009. Lessons from London: regulation of open-loop ground source heat pumps in central London. *Quarterly Journal Of Engineering Geology And Hydrogeology* 42: 325-334.

Galgaro, A., and M. Cultrera. 2013. Thermal short circuit on groundwater heat pump. *Applied Thermal Engineering* 57 no. 1-2: 107-115.

Gelhar, L., C. Welty, and K. Rehfeldt. 1992. A critical review of data on field-scale dispersion in aquifers. *Water Resources Research, Washington, DC* 28 no. 7: 1955-1974.

Gelhar, L.W., and M.A. Collins. 1971. General Analysis of Longitudinal Dispersion in Nonuniform Flow. *Water Resources Research* 7 no. 6: 1511-1521.

Goranson, R.W. 1942. Heat capacity of rocks. In *Handbook of physical constants*, ed. F. Birch, 235-236.

Guimerá, J., F. Ortuño, E. Ruiz, A. Delos, and A. Pérez-Paricio. 2007. Influence of Ground-source Heat Pump on groundwater. In *European Geothermal Congress*. Unterhaching, Germany.

Hähnlein, S., P. Bayer, and P. Blum. 2010. International legal status of the use of shallow geothermal energy. *Renewable and Sustainable Energy Reviews* 14 no. 9: 2611-2625.

Hähnlein, S., P. Bayer, G. Ferguson, and P. Blum. 2013. Sustainability and policy for the thermal use of shallow geothermal energy. *Energy Policy* 59 no. C: 914-925.

Hähnlein, S., N. Molina-Giraldo, P. Blum, P. Bayer, and P. Grathwohl. 2010. Cold plumes in groundwater for ground source heat pump systems. *Grundwasser* 15 no. 2: 123-133.

Hancock, P., R. Hunt, and A. Boulton. 2009. Preface: hydrogeoecology, the interdisciplinary study of groundwater dependent ecosystems. *Hydrogeology Journal* 17 no. 1: 1-3.

Heath, R.C. 1983. Basic Groundwater Hydrology. US Geological Survey, Denver, Colorado.

Hecht-Méndez, J., N. Molina-Giraldo, P. Blum, and P. Bayer. 2010. Evaluating MT3DMS for Heat Transport Simulation of Closed Geothermal Systems. *Ground Water* 48 no. 5: 741-756.

Herbert, A., S. Arthur, and G. Chillingworth. 2013. Thermal modelling of large scale exploitation of ground source energy in urban aquifers as a resource management tool. *Applied Energy* 109 no. C: 94-103.

Hidalgo, J.J., J.s. Carrera, and M. Dentz. 2009. Steady state heat transport in 3D heterogeneous porous media. *Advances in water resources* 32: 1206-1212.

ESRI Inc. 2016. ArcGIS 1999-2016.

Incropera, F.P., D.P. Dewitt, T.L. Bergman, and A. Larine. 2007. *Fundamentals of heat and mass transfer*. 6th ed. Hoboken, NJ: John Wiley.

Kavanaugh, S. 2008. A 12-Step method for closed-loop ground-source heat-pump design. *ASHRAE Transactions* 114 no. 2: 328.

Kavanaugh, S.P., and K. Rafferty. 2014. *Geothermal Heating and Cooling: Design of Ground-Source heat Pump Systems*: ASHRAE. Atlanta, GA.

Kazmann, R.G., and W.R. Whitehead. 1980. The spacing of heat pump supply and discharge wells. *Groundwater Heat Pump Journal* Summer: 28-31.

Kinzelbach, W. 1992. *Numerische Methoden zur Modellierung des Transports von Schadstoffen im Grundwasser,* . 2 ed: Oldenbourg, München.

Krpan, J.D.B. 1982. The characterization and estimation of soil temperatures in Manitoba, Thesis (M.A.)--University of Manitoba, Spring 1982.

Lear, T.J. 1987. Letter to Minister of Natural Resources Re: Winpak Limited. MCW Consultants Ltd.

Lindell, P., and J. Mann. 2015. Dorsey Station Well Water Cooling System Environmental Monitoring (2011 - 2014) 2014 Annual Monitoring Report. KGS Group.

Lippmann, M.J., and C.F. Tsang. 1980. GROUND WATER USE FOR COOLING: ASSOCIATED AQUIFER TEMPERATURE CHANGES. *Ground Water* 18 no. 5.

Lo Russo, S., L. Gnavi, E. Roccia, G. Taddia, and V. Verda. 2014. Groundwater Heat Pump (GWHP) system modeling and Thermal Affected Zone (TAZ) prediction reliability: Influence of temporal variations in flow discharge and injection temperature. *Geothermics* 51: 103-112.

Lo Russo, S., G. Taddia, and V. Verda. 2012. Development of the thermally affected zone (TAZ) around a groundwater heat pump (GWHP) system: A sensitivity analysis. *Geothermics* 43: 66-74.

Lucas, J. 1994. Performance of the WINPAK Aquifer Heating and Cooling Project. MCW Consultants Ltd.

Lund, J.W., and T.L. Boyd. 2016. Direct utilization of geothermal energy 2015 worldwide review. *Geothermics* 60 no. C: 66-93.

Manitoba Hydro. 2016. Power Smart for Business: Commercial Geothermal Program Guide.

Manitoba Sustainable Development. 2003. Well Information Report: Sun Valley School. 25 November 2003.

Manitoba Sustainable Development. 2009. Well Information Report : X-Potential. 14 October 2009.

Manitoba Sustainable Development. 2012. Well Information Report: Guertin Bros. 14 March 2012.

Manitoba Sustainable Development. 2017. Constructing and Sealing Wells in Manitoba: Information for Well Drillers and Well Sealers.

Mann, J. 2008. Manitoba Hydro Dorsey Station Groundwater Cooling Annual Monitoring Report. KGS Group.

Matthews, R. 2003. Regulatory Framework and Examples of Ground-Source Heating/Cooling Technology in the Winnipeg Area. In *56th Canadian Geotechnical Conference – 4th Joint IAH-CNC/CGS Conference – 2003 NAGS Conference*. Winnipeg, Manitoba.

Milenić, D., P. Vasiljević, and A. Vranješ. 2010. Criteria for use of groundwater as renewable energy source in geothermal heat pump systems for building heating/cooling purposes. *Energy & Buildings* 42 no. 5: 649-657.

Miller, R. January 10, 2008. Correspondence to Manitoba Sustainable Development.

Mishtak, J. 1964. Soil Mechanics aspects of the Red River Floodway. *Canadian Geotechnical Journal* 1 no. 3: 133-146.

Muela Maya, S., A. García-Gil, E. Garrido Schneider, M. Mejías Moreno, J. Epting, E. Vázquez-Suñé, M.Á. Marazuela, and J.Á. Sánchez-Navarro. 2018. An upscaling procedure for the optimal implementation of open-loop geothermal energy systems into hydrogeological models. *Journal of Hydrology* 563: 155-166.

Mustafa Omer, A. 2008. Ground-source heat pumps systems and applications. *Renewable and Sustainable Energy Reviews* 12 no. 2: 344-371.

Nam, Y., and R. Ooka. 2010. Numerical simulation of ground heat and water transfer for groundwater heat pump system based on real-scale experiment. *Energy & Buildings* 42 no. 1: 69-75.

Oleksiuk, D. 2009. Melet Plastics Geothermal Industrial Cooling System – Discharge of Groundwater to Surface. D. Oleksiuk & Associates Inc.

Pach, J.A. 1994. Hydraulic and solute transport characteristics of a fractured glacio-lacustrine clay; Winnipeg, Manitoba., University of Waterloo , Waterloo, Ontario.

Palmer, C., D. Blowes, E. Frind, and J. Molson. 1992. Thermal energy storage in an unconfined aquifer: 1. Field injection experiment. *Water Resources Research* 28 no. 10: 2845-2856.

Park, B.-H., G.-O. Bae, and K.-K. Lee. 2015. Importance of thermal dispersivity in designing groundwater heat pump (GWHP) system: Field and numerical study. *Renewable Energy* 83: 270-279.

Park, B.-H., B.-H. Lee, and K.-K. Lee. 2018. Experimental investigation of the thermal dispersion coefficient under forced groundwater flow for designing an optimal groundwater heat pump (GWHP) system. *Journal of Hydrology* 562: 385-396.

Pophillat, W., G. Attard, P. Bayer, J. Hecht-Méndez, and P. Blum. 2018. Analytical solutions for predicting thermal plumes of groundwater heat pump systems. *Renewable Energy*.

Render, F. 2010. Winnipeg Carbonate Aquifer Water Elevation. The Association of Professional Engineers and Geoscientists of the Province of Manitoba (APEGM).

Render, F.W. 1970. Geohydrology of the metropolitan Winnipeg area as related to groundwater supply and construction. *Canadian Geotechnical Journal* 7 no. 3: 243-274.

Render, F.W. 1981. Hydrogeologic aspects of supply well – recharge well air conditioning in the Birchwood Area of Winnipeg, 44. Manitoba Department of Natural Resources, Water Resources Branch, Winnipeg, Manitoba.

Render, F.W. 1983. Hydrogeology of the Winnipeg Area. In *Geologic Engineering Maps & Report for Urban Development of Winnipeg*, ed. D. H. S. a. B. K. A. Baracos, 29-40. Winnipeg, Manitoba: Cantext Publications.

Risser, D.W. 2010. Factors Affecting Specific-Capacity Tests and their Application - A Study of Six Low-Yielding Wells in Fractured-Bedrock Aquifers in Pennsylvania. USGS Scientific Investigations Series 2010–5212.

Robertson, E.C. 1988. Thermal Properties of Rocks. US Geological Survey, Reston, Virginia.

Schön, J.H. 1996. *Physical properties of rocks : fundamentals and principles of petrophysics*. New York: Pergamon.
Self, S.J., B.V. Reddy, and M.A. Rosen. 2013. Geothermal heat pump systems: Status review and comparison with other heating options. *Applied energy* 101: 341-348.
Sinclair, R.D. 2003. Final Report: Dorsey Converter Station Groundwater Cooling Feasibility Study. KGS Group.
Sinclair, R.D. 2006. Water Right License Application Supporting Information, Mark Brandt Trucking Ltd., 65 Eagle Drive, Winnipeg, Manitoba. KGS Group.
Sinclair, R.D. 2007. Water Rights License Application Supporting Information: Centre for Natural Medicine, 1218 Lorette Avenue, Winnipeg, Manitoba. KGS Group.
Sinclair, R.D. 2008. Final Report: Hydrogeological Assessment Report in Support of Groundwater Licensing for 1025 and 1055 Grant Avenue. KGS Group.
Sinclair, R.D. 2009. Final Report: Hydrogeological Water Supply Assessment and Construction of a 300 mm (12 inch) Diameter PVC Cased Replacement Well and Well Water Pipeline at Freshwater Fish Marketing Coorporation, 1199 Plessis Road, Winnipeg, Manitoba. KGS Group.
Sinclair, R.D. 2015. IKEA heat/water flow data. Email dated March 11, 2015.
Tamburi, A.J., G.K. Bell, and E.A. Wolowich. 1987. Problem Investigation and Solution International Inn Groundwater Cooling System. E. J. Faraci and Associates.
Thiessen, K., and J. Mann. 2010. Manitoba Hydro Dorsey Station Groundwater Cooling System 2009 Annual Monitoring Report. KGS Group.
Thiessen, K., J. Mann, and R. Sinclair. 2011. Manitoba Hydro Dorsey Station Well Water Cooling System Environmental Monitoring (2009-2012) 2010 Annual Monitoring Report, vol. KGS Group.
U.S. Environmental Prptection Agency. 1999. Heat Pump and Air Conditioning Return Flow Wells. In *The Class V Underground Injection Control Study*, vol. 19. EPA/816-R-99-014s.
U.S. Geological Survey. 2014. Earth Explorer, vol. 2015.
Vandenbohede, A., and L. Lebbe. 2010. Parameter estimation based on vertical heat transport in the surficial zone. *Hydrogeology Journal* 18 no. 4: 931-943.
Verda, V., G. Baccino, A. Sciacovelli, and S. Lo Russo. 2012. Impact of district heating and groundwater heat pump systems on the primary energy needs in urban areas. *Applied Thermal Engineering* 40 no. C: 18-26.
Waedt, G. 1988. Boeing of Canada Supply Well Investigation E.J. Faraci & Associates Ltd.
Wiecek, S. 2001a. Inovatech Groundwater Cooling System – 70 Irene Street: Hydrogeologic Assessment of Proposed Expansion. UMA Engineering Ltd.
Wiecek, S. 2001b. XPotential Products Inc. – 999 Redonda Rd.: Hydrogeologic Assessment of Proposed Expansion. UMA Engineering Ltd.
Wiecek, S. 2004. Winnipeg Regional Health Authority Laundry Facility, 1725 Inkster Boulevard, Winnipeg, Manitoba, Proposed Groundwater Cooling System, Preliminary Stage II Groundwater Exploration Result and Recommendations. UMA Engineering Ltd.
Wolowich, E. 1990. Village West Condominiums – Cooling System Return Well Installation WARDROP Engineering Inc.
Wolowich, E.A. 1999. Assessment of Groundwater Cooling System International Inn – 1808 Wellington Ave. – Winnipeg, Manitoba. WARDROP Engineering Inc.

Wolowich, E.A., G.K. Bell, and A.J. Tamburi. 1987a. Van Walleghem School Groundwater Investigation. E.J. Faraci & Associates.
Wolowich, E.A., G.K. Bell, and A.J. Tamburi. 1987b. St. Germaine Immersion School Groundwater Investigation. E. J. Faraci & Associates.
Wolowich, E.A., G.K. Bell, and A.J. Tamburi. 1987c. Birds Hill School Groundwater Investigation and Well System Design. E.J. Faraci & Associates.
Wolowich, E.A., and A.J. Tamburi. 1987. Boeing of Canada Murray Park Plant Groundwater Heating and Cooling System Expansion. E.J. Faraci & Associates.
Wolowich, E.A., G.K. Waedt, and A.J. Tamburi. 1987. Samuel Burland School Groundwater Investigation. E. J. Faraci & Associates.